ROLE OF ALPHA B-CRYSTALLIN AND IT'S PHOSPHOMIMICS IN ANGIOGENESIS

M. Sc. Thesis
2017

Submitted to

CENTRAL DEPARTMENT OF BIOTECHNOLOGY (CDBT)
Tribhuvan University, Nepal

In partial fulfillment of the requirements for the degree of

2 years M. Sc in Biotechnology

By
PUSKAR THAPA

Supervisor

Prof. Dr. Tilak R. Shrestha

Central Department of Biotechnology
Tribhuvan University

External Supervisor

Dr. B. Kiran Kumar

Scientist
Centre for Cellular and Molecular Biology

RECOMMENDATION

This is to certify that Mr. Puskar Thapa has successfully completed his dissertation work entitled "**ROLE OF ALPHA B-CRYSTALLIN AND IT'S PHOSPHOMIMICS IN GIOGENESIS"** under my supervision.

This dissertation work was performed for the partial fulfillment for award of Master of Science in Biotechnology under the course code BT 621. The result presented here is his original findings. I, hereby, recommend this thesis for final evaluation.

…..……

Prof. Tilak R. Shrestha, PhD
(Supervisor)

Central Department of Biotechnology
Tribhuvan University
Kirtipur, Nepal

CERTIFICATE OF EVALUATION

This is to certify that this thesis entitled "**ROLE OF ALPHA B-CRYSTALLIN AND IT'S PHOSPHOMIMICS IN GIOGENESIS"** presented to evaluation committee by **Mr. Puskar Thapa** is found satisfactory for the partial fulfillment of Master of Science in Biotechnology.

.....

.....

सी सी एम बी CCMB
सीएसआईआर-कोशिकीय एवं आणविक जीव विज्ञान केन्द्र
CSIR-CENTRE FOR CELLULAR AND MOLECULAR BIOLOGY
उप्पल, रोड, हैदराबाद तेलंगाणा - 500 007. भारत
Uppal Road, Hyderabad, Telangana - 500 007. India.

Dr. Bokara Kiran Kumar

Scientist, CCMB

22nd August 2016

TO WHOMSOEVER IT MAY CONCERN

This is to certify that Mr. Puskar Thapa, 2nd year 4th Semester, M.Sc, Biotechnology, Central Department of Biotechnology (CDBT), Tribhuvan University, Kirtipur, Nepal, has successfully completed his summer training in my lab on the project entitled "**Role of alpha B-crystallin and it's phosphomimics in angiogenesis**" under my guidance from June 4th January 2016 to 15th August 2016 at "Centre for Cellular and Molecular Biology", Medical Biotechnology Complex, Hyderabad.

(B.Kiran Kumar)

CSIR- Centre for Cellular and Molecular Biology,
ANNEX-2. Clinical Research Facility Medical Biotechnology (CRF-MB),
Uppal Road, Uppal, Hyderabad-500 007, India,
Tel : +91 (040) 2719-5547 (office),
Fax :+91(040)-27160591/27160311,
Email : bokarakiran@ccmb.res.in
:+91-9177874028 (Cell No)

Dr. B. KIRAN KUMAR
Scientist
CSIR-Centre For Cellular And Molecular Biology
Hyderabad-500 007, India.

ACKNOWLEGEMENTS

I would first like to thank Prof**. Dr. Tilak R. Shrestha**, Molecular Biology Unit, Central Department of Biotechnology for overall supervision of the present dissertatio research work for me at CCMB. It is because of his collaborative effort with Dr. K. K. Bokara at CCMB that made me possible to do this work on αB-crystallin protein and its mutants on angiogenesis.

I would like to thanks **Prof. Rajani Malla,** former HOD **of** Central Department of Biotechnology, Tribhuvan University, Nepal for allowing me to do dissertation project.

I would like to thank **Dr. Kiran Kumar Bokara** whose door to office was always open whenever I ran into a trouble spot or had a question about my work. I thank him for giving me opportunity to work in his lab and for daily supervision of experiments.

With profound sense of gratitude, I am grateful to **Dr. Ch. Mohan Rao**, former Director, CCMB and the present Director **Dr. Rakesh K Mishra** for giving me an opportunity to work in an esteemed organization. I sincerely thank **Dr. T. Ramakrishna Murti, Dr. B. Raman, Dr. V Srinivas, Dr. K. Sridhar Rao** and **Dr. Amit Asthana** for their constant support and valuable advice.

I would like to thank **Mr. Kranthi Kiran Akula** for mentoring me throughout the project tirelessly and fixing every situation I was struck in. I would be always thankful to him for teaching me in all aspects. He had been great companion for me during the stay.

I sincerely thank to **Susheel Kumar N** from IICT (Indian Institute of Chemical Technology) for training me in CAM assay. I express my gratitude to **Mr. Chakravarthy** for installing and setting up the microscope required for CAM assay. I am also thankful to the Director of Poultry Research Centre for providing us with eggs for CAM assays.

It is great pleasure in showing my gratitude to **Mrs. Vani Voora, Mr. Gopisuresh, Ms. Sushma, Dr. Sunitha Kundur and Dr. Naveen Kumar** who really helped me to develop good lab practices and had been a great company for my entire stay.

I would like to thank my friends **Ms. Kushboo Tyagi** and **Ms. Shivangi Paradkar** for making my stay comfortable and all the moral support.

I would like to thank **Mrs. Vijaya** aunty and **Hanumanthu Ji** for constant help in the laboratory.

Last but not least, I take pleasure in thanking my family for their concern and continuous support throughout my stay in Hyderabad for my thesis work.

ABBREVIATIONS

AAA	αB-S19A-S45A-S59A
AAE	αB-S59E
AEA	αB- S45E
AEE	αB -S45E-S59E
AMD	Age Related Macular Degenerative Disease
Amp	Ampicillin antibiotic
CAM Assay	Chick Chorioallantoic Membrane Assay
DMSO	Dimethyl sulfoxide
DIC	Differential interference contrast
EAA	αB-S19E
EAE	αB-S19E-S59E
EEA	αB-S19E-S45E
EEE	αB-S19E-S45E-S59E
EDTA	Ethylenediaminetetraacetic acid
ERK	Extracellular signal–regulated kinase
FPLC	Fast protein liquid chromatography
FITC	Fluorescein Isothiocyanate
HCl	Hydrochloric Acid
HNSCC	Head and Neck Squamous Cell Carcinoma
HRMVEC	Human Retinal Micro Vascular Endothelial primary cell line
IGRP	Intra Genic reverse primer
IGFP	Intra Genic forward primer
IPTG	Isopropyl β-D-1-thiogalactopyranoside
i-TRAQ	Isobaric Tags for Relative and Absolute Quantitation
LB	Luria Bertani

Mg	Milligram
MQ	Milli-Q water
MAPK 1	Mitogen activated protein kinase 1
MAPKAPK2	Mitogen-activated protein kinase-activated protein kinase 2
MAPKAP	Mitogen activated protein kinase
µl	Micro liter
NaCl	Sodium Chloride
NaOH	Sodium hydroxide
Ng	Nanogram
NCBI	National center for biotechnology information
O.D	Optical Density
PBS	Phosphate Buffered Saline
PMSF	Phenylmethylsulfonylfluoride
REC	Retinal Endothelial cell
rpm	rotation per minute
RPE	Retinal Pigmented Epithelium
SDMS	Site-directed mutagenesis
SDS-PAGE	Sodium dodecyl sulfate polyacrylamide gel electrophoresis
S	Sedimentation coefficient
TE buffer	Tris EDTA
VEGF	Vascular Endothelial Growth Factor
WT	Wild Type

Table of content

Chapters

Page no.

Titles

List of figures

List of tables

CHAPTER 1.0: INTRODUCTION

Angiogenesis is an important physiological process by which new blood vessels form from pre-existing vessels. The process of angiogenesis occurs throughout the life in both healthy and diseased conditions. When metabolic activities change, angiogenesis changes proportionally, leading to proportional changes in capillarity. The role of oxygen is inevitable in the regulation of angiogenesis, and it varies according to health conditions. In the case of diseases like peripheral arterial disease or wound healing, increasing the angiogenesis can prove helpful, while in cases of cancer, rheumatoid arthritis, retinopathy, premature-retinopathy, age-related macular degenerative disease, etc., inhibition of angiogenesis gives therapeutic results. Thus, capillaries grow or regress in the tissues according to the functional demands of the body.

Going back to the first recorded evidence of angiogenesis, Scottish anatomist, and surgeon, John Hunter laid out the insights in this field, when he summarized his beliefs regarding the proportionality between vascularity and metabolic requirements (Hunter, 1840). He was the first one to link the "Basic Law of Nature" with the regulation of angiogenesis. However, the more recent history dates back to 1971, when Judah Folkman hypothesized that the growth of tumor depends on angiogenesis (Folkman, 1971). Angiogenesis is the *de novo* generation of blood vessels. Vasculogenesis occurs in both extra- and intra-embryonic tissues of the embryos (Risau, 1997; Schmidt *et al.,* 2007). It is a dynamic process which involves Cell-cell and Cell-extracellular matrix interactions. These interactions are spatially and temporally directed by growth factors and morphogens (Schmidt *et al.,* 2007; Pinter *et al.,* 1997).

Types of angiogenesis:

1. Sprouting Angiogenesis: Requires the formation of new blood vessels to overcome the condition of hypoxia and to fulfill its metabolic requirements.
2. Intussusceptive Angiogenesis: Takes place by extension of vessel wall into the lumen, which causes a single vessel to split into two.

Angiogenesis is one of the critical processes for regulating various diseases. For example, inhibiting angiogenesis in the case of tumorogenesis or promoting angiogenesis in ischemia could be a potential therapeutic strategy for controlling the disease progression.

1.1 αB-crystallin protein

The super family small heat shock protein (sHSP) includes αB-crystallin protein. Despite difference in shape and size of αB-crystallin protein (12-43kDa), it shares common feature with the sHSP (Kappe *et al*., 2002). The shared featured are highly conserved domain, a small molecular mass, dynamic quaternary structure, induction by stress and chaperone activity (Horwitz, 2003). The Kannan *et al* studied recently, the novel function of αB-crystallin protein in ocular lens has been identified in the retina and in retinal pigmented epithelium (RPE) in 2012. The gene of αB-crystallin protein has 4,649 bases (FASTA format given in appendix 3.1) including 5'UTR and 3'UTR and has three exons and two introns.

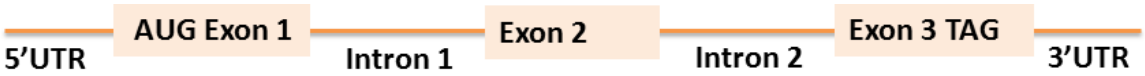

Figure 1: The diagrammatic view of αB-crystalline protein gene

1.2 αB-crystallin protein and its role in various diseases

One of the two gene products involved in the assembly of the major eye lens protein, α-crystallin, is αB-crystallin protein. Its structural function is to assist in maintaining a proper refractive index and thus the transparency of the eye lens (Horwitz, 1992, and Horwitz, 2000). It is a multimeric protein (monomeric mass – 20 kDa) and has diverse biological roles (BBA review). A member of the small heat-shock protein (sHSP) family, αB-crystallin protein exhibits chaperone activity in preventing aggregation of denatured proteins *in vitro* and plays a role in many different cellular processes such as cellular growth, transcription, differentiation, migration, and development. It has been shown to protect cells from various stress factors, prevent the aggregation or facilitate renaturation of proteins and to protect cytoskeletal elements against ischemia, injury or depolymerizing agents.

αB-crystallin protein is also widely expressed in other tissues such as heart (Bhat *et al.,*1991), skeletal muscles and the brain (Srinivasan *et al.,* 1992). It appears to be involved in transduction pathways activated during growth, differentiation and also in response to various forms of stress (Mehlen *et al.,* 1995). In the heart, αB-crystallin protein and heat-shock protein 27 are involved in stress tolerance (Verschuure *et al.,* 2002). A subsequent study showed that selective expression of αB-crystallin protein at an early stage of differentiation occurred in myoblasts resistant to differentiation-induced apoptosis. αB-crystallin protein can inhibit apoptosis at various stages by interacting with other proteins involved in the apoptotic pathways. The role of αB-crystallin protein in apoptosis suggests an important role for the protein both in development and in cancer. In autoimmune diseases such as multiple sclerosis, antibodies against αB-crystallin protein were reported. Therefore, it serves as a molecular marker for multiple sclerosis; the details of its role in autoimmune diseases are unknown (van Noort *et al.,* 2015).

The amino acid sequence of αB-crystallin protein is as shown below:

Amino acid sequence of αB-crystallin protein:

MDIAIHHPWIRRPFFPFHSPSRLFDQFFGEHLLESDLFPTSTSLSPFYLRPPSFLRAPSWFDTGLSEMRLEK
DRFSVNLDVKHFSPEELKVKVLGDVIEVHGKHEERQDEHGFISREFHRKYRIPADVDPLTITSSLSSDGVLT
VNGPRKQVSGPERTIPITREEKPAVTAAPKK

αA- and αB-crystallin protein are known to modulate the redox state, inhibit apoptosis, and regulate membrane fluidity. They can also modulate the structure and dynamics of cytoskeletal elements such as actin, tubulin, and intermediate filaments during development and differentiation. It is believed that various post-translational modifications (like deamidation, truncation, phosphorylation, oxidation, Cys-methylation, acetylation, carbamylation, and glycation) occur during aging of α-crystallin result in its functional loss and onset of cataract, in which eye lens loses its transparency. αB-crystallin protein regulates secretion of VEGF (Vascular Endothelial Growth Factor) during the postnatal neoangiogenesis. Therefore, in pathologic neovascularisation, the secretion of VEGF can be inhibited by the manipulation of αB crystallin expression.

1.3 Phosphorylation of αB-crystallin protein

αB-crystallin protein is phosphorylated at three serine residues-19, 45 and 59 (Ito *et al.,* 2001 and Eaton *et al.,* 2001). S19 phosphorylation occurs in an age-dependent manner; S59 is phosphorylated under heat stress, whereas S45 is phosphorylated in the mitotic phase of the cell cycle. In mitotic cells, phosphorylation is enhanced at Ser-19 and especially at Ser-45, whereas phosphorylation at Ser-59 is reduced. Phosphorylation at Ser-59 is associated with the localization of αB-crystallin protein in the centrosomes, cytoplasm, and midbodies of dividing cells. At least two pathways are implicated in the αB-crystallin protein phosphorylation: the p38 MAPK1 / MAPKAPK2 pathway is involved in phosphorylation of serine 59, while serine45 phosphorylation appears to be under the control of p42/44 ERK MAPK with localization in nucleus and co-localization with SC35 speckles. The kinase responsible for the phosphorylation of serine 19 is still unknown, but it is known to localize in the nucleus. Phosphorylation is presumably used to modulate the cellular role of this protein, the details of which remain unclear. The cellular function of αB-crystallin protein has been highlighted by the identification of an inherited mutation R120G that is associated with desmin-related myopathy (Vicart *et al.,* 1998). It has been shown that the R120G mutant is hyper phosphorylated at all the three serine residues and this hampers the transport of αB-crystallin protein into the nucleus (Ahmad *et al*., 2008). The exact role of hyper phosphorylated R120G αB-crystallin protein in desmin-related myopathy is yet to be understood. In the lens, αB-crystallin protein phosphorylation by cAMP-dependent kinase is age-related and is induced in response to stress (Wang *et al.,* 2000 and Ueda *et al.,* 2002).

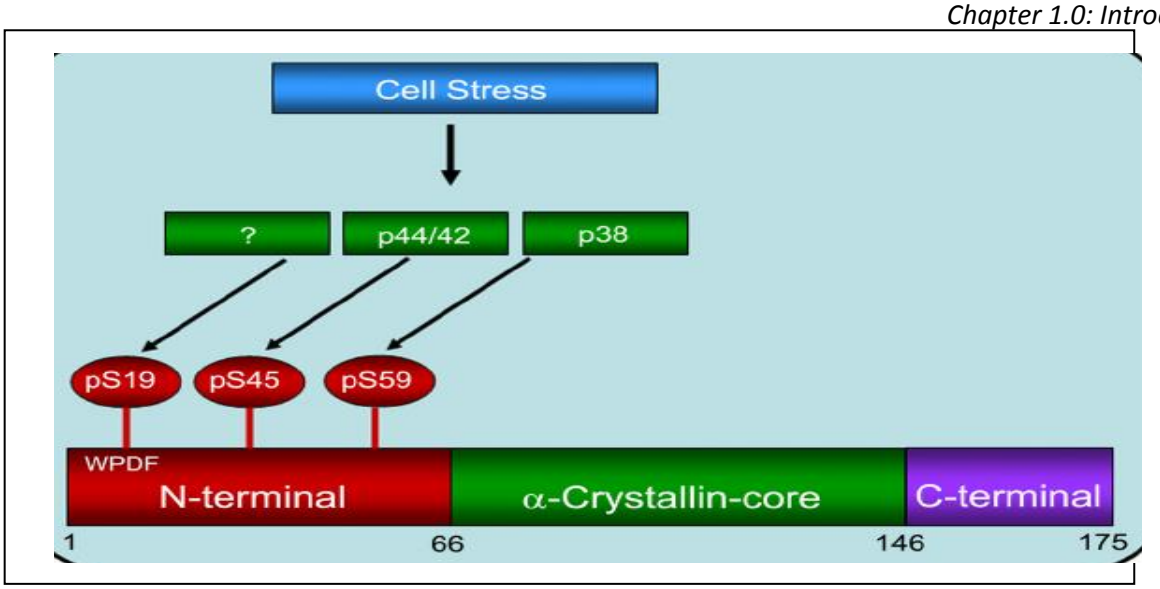

Figure 2: Structural organization of αB-crystallin protein. αB-crystallins have a crystallin core domain flanked by variable N-terminal domain and C-terminal extension. Three known phosphorylation sites on αB-crystallin are located in the N-terminal domain and two of them can be activated by p44/42 and p38 MAP kinases as well as other yet to be determined pathways. And the at 19th position still cause of activation is unknown.
(Source: Kannan *et al*., 2012**)**

αB-crystallin protein negatively regulates apoptosis and is involved in cell division, cell differentiation, etc. Reports regarding the role of phosphorylation in the chaperone function of αB-crystallin protein are debatable. Studies on phosphorylation-mimicking mutants of αB-crystallin protein (αB-3D, S19D, S45D & S59D) showed a reduction in the oligomeric size and reduction in its chaperone-like activity (Ito *et al.,* 2001). Another study showed that the single phosphorylation mimic (S19D) did not affect the chaperone-like activity of αB-crystallin protein, but the double mutant (S19D/S45D) had significantly reduced activity (Aquilina *et al.,* 2004). However, a study from our laboratory (Ahmad *et al.,* 2008) as well as that from another laboratory (Ecroyd *et al.*, 2007), showed that 3D αB-crystallin protein, a protein mimicking phosphorylation at all the three serine, exhibited significantly higher chaperone-like activity against amorphous as well as amyloid aggregation of proteins.

1.4 αB crystallin protein in angiogenesis process

Angiogenesis (neovascularization) is an important phenomenon that promotes tumor growth and is also responsible for compromised vision in retinopathy of prematurity,

diabetic retinopathy, and age-related macular degeneration. An earlier study suggests that αB-crystallin protein and VEGF share a feedback loop, as αB-crystallin protein may stabilize and chaperone misfolded VEGF (Ghosh *et al.,* 2007). Supporting these findings, Kase *et al.,* demonstrated that in αB-crystallin protein-deficient mice, the expression of VEGF was decreased. VEGF and αB-crystallin protein have been shown to co-localize in the Endoplasmic Reticulum, which is hypothesized to stimulate VEGF secretion, leading to angiogenesis. Further, the absence of αB-crystallin protein chaperone activity results in degradation of VEGF. Thus, the stabilization of VEGF by αB-crystallin protein might contribute to the development of retinopathies.

Stimulation of angiogenesis by VEGF is a well-established phenomenon (Ferrara, 1999, 2001), but recent studies have shown that some alterations in vasculogenesis might also be involved in the condition of diabetic retinopathy (Asahara *et al.,* 1997; Guthrie *et al.,* 2005; Kelly *et al.,* 2005; Lee *et al.,* 2006a). In diabetic condition, the survival of endothelial cells is compromised, which is evident by the increased number of apoptotic RECs and formation of acellular capillaries (Duh and Aiello, 1999; Mizutani *et al.,* 1996). Though the expression of VEGF is increased in diabetic retinopathy, the cell survival is compromised; this indicates that the VEGF prosurvival signaling pathway is altered in retinal endothelial cells (RECs) in the case of diabetes.

Resnikoff *et al.,* in 2004, reported that age-related macular dystrophy (AMD) is one of the leading causes of vision loss. RPE apoptosis induced by oxidative stress can be protected by αB-crystallin protein (Yaung *et al.,* 2007). With ageing, the chaperone activity of αB-crystallin decreases which can lead to accumulation of misfolded proteins. Accumulation of misfolded protein called Drusen accumulates on the Bruch's membrane, right behind the macular region. Eventually, it breaks the Bruch's membrane, and sets a stage for the entry of vasculature into the retina and the vitreous humor. Secreted VEGF induces the formation of blood vessels in the retina and slowly progresses into the vitreous humor. Studies in αB-crystallin protein null mice showed an increase in endothelial apoptosis and decreased intraocular angiogenesis (Kase *et al.,* 2010). αB-crystallin protein is ubiquitously present in different tissues, but the maximum level is observed in lens (Bhat and Nagineni, 1989; de

Jong *et al.,* 1993; Horwitz *et al.,* 1999; Inaguma *et al.,* 1995; Iwaki *et al.,* 1990, 1989; Lowe *et al.,* 1992). During pathological conditions like AMD (De *et al.,* 2007; Nakata *et al.,* 2005), diabetes (Kandpal *et al.,* 2012; Kumar *et al.,* 2005) and multiple sclerosis (Ousman *et al.,* 2007; Rothbard *et al.,* 2012), the expression of αB-crystallin protein has been shown to be regulated (Robinson and Overbeek, 1996). The expression of αB-crystallin protein is also upregulated by temperature and this increase in αB-crystallin protein is dependent on the heat shock factors (Kato *et al.,* 1999). The role of αB-crystallin protein in the pathogenesis of AMD is not very clear. The expression of αB-crystallin protein showed a drastic increase in the Retinal Pigment Epithelium (RPE) of pathologic samples of patients with both "dry" and "wet" AMD when compared to that of the control samples (De *et al.,* 2007). The RPE associated with drusen shows an increase in αB-crystallin protein expression, and it is also confirmed that αB-crystallin protein is a component of drusen (Crabb *et al.,* 2002; De *et al.,* 2007; Nakata *et al.,* 2005). αBcrystallin has a critical role in the quality control of proteins due to its ability to degrade or renature the damaged proteins in stress conditions. In neurodegenerative diseases like AMD, the expression of αB-crystallin protein is increased (Crabb *et al.,* 2002; De *et al.,* 2007; Nakata *et al.,* 2005). The formation of drusen is also hypothesized to be an outcome of increased autophagy and exocytic activities in aged RPE (Wang *et al.,* 2009a). Experimental evidence has also shown that RPE cells release αB-crystallin protein through the exosomal route (Sreekumar *et al.,* 2010). RPE barrier breaks down in severe oxidative stress, which leads to accumulation of αB-crystallin protein exosomes in basolateral side of the RPE. This indicates that the exosomes may be a source of αB-crystallin protein accumulation in drusen (Sreekumar *et al.,* 2010). The studies and recent developments regarding the role of αB-crystallin protein in AMD suggest that the increased expression of αB-crystallin protein in RPE may serve as a biomarker of AMD (De *et al.,* 2007).

Earlier studies suggest that in retinal diseases such as proliferative diabetic retinopathy and proliferative vitreoretinopathy, the expression of crystallins (αA-crystallin and αB-crystallin protein) in the vitreous humor were downregulated (Yu *et al.,* 2008, 2014; Wang, 2012, 2013). The proteomics profiling and i-TRAQ quantitation of retina obtained from oxygen-induced retinopathy mice showed the levels of isoform 1 of α crystallinA chain, isoform 2 of

α crystallin A chain, α crystallin B chain, γ crystallin D and β-A3/A1 crystallin were down-regulated (Zhou *et al.,* 2011). Contrary to this, other studies have shown that expression of αA- and αB-crystallin protein is up-regulated in the retinas of patients with proliferative diabetic retinopathy (Fort *et al.,* 2009; VanGuilder, 2011). Interestingly, in a knock-out mouse model of αB-crystallin protein, endothelial cell tubular morphogenesis and severity of oxygen-induced retinopathy was attenuated (Kase *et al.,* 2011). It has also been shown to suppress endothelial cell apoptosis during tumor angiogenesis (Dimberg *et al.,* 2008). These studies indicate that αB-crystallin protein promotes angiogenesis.

Thus, upon taking into account the various studies on retinopathies and AMD, the role of αB-crystallin protein in angiogenesis is not clear.

1.5 Chick Chorioallantoic Membrane Assay (CAM assay) as a model to study angiogenesis

Chick embryo chorioallantoic membrane (CAM) assays have been widely used to study angiogenesis (Richardson and Singh, 2003). It has many advantages- highly vascularized nature of CAM promotes the efficacy of the experiment, it is reproducible, has a short observation period (days), is inexpensive, closed system, naturally immunodeficient (Cimpean, Ribatti and Raica, 2008). Multiple tests per individual CAM are possible, and allows large scale screening (Tufan and Satiroglu-Tufan, 2005), biology and physiology are well known, availability of *in vivo* imaging (Deryugina and Quigley, 2015), allows direct visualization (Valdes, Kreutzer and Moussy, 2002).

Chorioallantoic membrane (CAM) is an extraembryonic membrane which serves more than one function during embryo development. The embryo is covered by three layers; amnion, chorion, and allantois. CAM is the site of exchange of respiratory gases, calcium transport from the eggshell, acid-base homeostasis in the embryo, and ion and water re-absorption from the allantoic fluid.

The CAM model has also been used in pre-clinical screening to assess the efficacy of drugs and inhibitors on tumor growth. Hagedorn *et al.*, reported that treatment of human glioma cells with receptor tyrosine kinase inhibitors inhibited tumor growth in a CAM model in

2005. However, a major drawback of the CAM assay is that it is labor-intensive due to the large number of eggs that are required to obtain consistent results. It should also be noted that this is a non-mammalian system, and this fact needs to be taken into consideration when interpreting results.

1.6 Objectives of the study

1.6.1 General objectives

To investigate the role of wild type αB-crystallin protein and its phosphor-mimicking mutants in angiogenesis.

1.6.2 Specific objectives

i. To make the phosphorylation-mimicking mutants (single, double and triple) mutation in the coding region of αB-crystallin protein coding gene.
ii. To isolate pure mutated αB-crystallin protein including wild-type αB-crystallin.
iii. To investigates the effect of wild type αB-crystallin protein and mutated protein on angiogenesis using the Chick Chorioallantoic Membrane (CAM) assay.
iv. To study the effect of αB-crystallin protein and the phosphorylation-mimicking mutants on tubular morphogenesis, migration, and proliferation of human retinal micro vascular endothelial cells (HRMVECs).

1.7 Research hypothesis

1.7.1 Null hypothesis

There is no role of wild type αB-crystallin protein and its phosphor-mimicking triple (EEE, AAA), double (EEA, EAE, & AEE) and single (AAE, AEA & EAA) mutants in angiogenesis.

1.7.2 Alternative hypothesis

i. Wild type αB-crystallin protein and its phosphor-mimicking triple (EEE, AAA), double (EEA, EAE, & AEE) and single (AAE, AEA & EAA) mutants have suppressing role in angiogenesis.

ii. Wild type αB-crystallin protein and its phosphor-mimicking triple (EEE, AAA), double (EEA, EAE, & AEE) and single (AAE, AEA & EAA) mutants have inducing role in angiogenesis

CHAPTER 2.0: LITERATURE REVIEW

Small Heat shock proteins (sHsps) are 12-43 kDa proteins that are ubiquitously present in the cytosol of all cells and tissues even in the absence of stress conditions (Jakob *et al.,* 1993). The mammalian small heat shock proteins are present as oligomers and act as molecular chaperones. sHsps are characterized by a variable N-terminal region, a conserved $\sim$ 90-residue α-crystallin domain, and a variable C-terminal extension. The α-crystallin domain is fairly conserved across species: the sequence similarity ranges from 19% to 60%. In structures determined so far, the α-crystallin domain adopts a seven-stranded β-sandwich fold (Kim *et al.,* 1998). The "α-crystallin domain" has a critical role in the chaperone function (delaying aggregation of damaged proteins and the onset of opacity in the fiber cells that lack the machineries necessary for protein turnover) and the N-terminal is believed to help in the assembly of functional and high molecular mass oligomers. Ten sHsps have been identified in the human genome (Kappe *et al.,* 2003). The α-crystallin of the vertebrate lens is one of the sHsps which plays a critical role in the acquisition and maintenance of lens optical properties.

2.1 Crystallin protein

The name crystallin was first coined by Berzelius in 1830 to describe the gelatinous substances that could be isolated from the crystalline lens (Augusteyn, 2004). These heterogeneous proteins were classified into alpha, beta, and gamma families, defined mainly by the sizes of oligomers they form, charge and immunological properties which occur in all vertebrate classes; whereas, delta crystallins occur only in reptiles and birds (Tardieu & Delaye, 1988; Delaye, 1983; Jaenicke & Slingsby, 2001).

2.2 α-Crystallin protein

The α-Crystallin is the major protein of the mammalian lens, accounting for about half of the total protein in most species. Eye lens α-crystallin is a polydisperse mixture of large aggregates assembled from two types of polypeptides, the αA-crystallin and αB-crystallin protein (CRYAA and CRYAB), which are located on different chromosomes and with

molecular weights around 20kDa. In human, the αA-crystallin gene is located on chromosome 21 and encodes a polypeptide of 173 amino acid residues, whereas αB-crystallin protein gene is located on chromosome 11 and encodes for 175 amino acid residues. The individual polypeptide chains of αA-crystallin and αB-crystallin protein are held together by non-covalent interactions. Sequence comparisons reveal that they belong to the small heat shock proteins (sHsps) family, having four structural and functional features: (i) a small monomeric molecular mass between 12 and 43 kDa; (ii) the formation of large oligomeric complexes; (iii) the presence of a moderately conserved central region called the "α-crystallin domain"; characterized by a stretch of 80-100 conserved amino acid residues" (Horwitz*,* 1992; Horwitz*,* 1993, Horwitz *et al.,* 1998) and (iv) molecular chaperone activity. The "alpha crystallin domain" is flanked by a non-conserved, largely hydrophobic N-terminal domain and a small, unstructured C-terminal extension which vary in length and sequence. Due to the presence of "alpha crystallin domain", α-crystallin functions as a molecular chaperone. This domain is preceded by an N-terminal region of variable length and considerable sequence diversity. In most cases, a short C-terminal tail extends downstream of the α-crystallin domain. The "α-crystallin domain" plays a critical role in chaperone activity and the N-terminal is believed to help in the assembly of functional higher molecular mass oligomers.

2.3 αB-crystallin protein

One of the two gene products in the α-crystallin assembly is αB-crystallin protein. Its structural function is to assist in maintaining a proper refractive index and thus the transparency of the eye lens (Horwitz, 1992, Horwitz, 2000; Cobb *et al.,* 2002). It is a multimeric protein (monomeric mass – 20kDa) and has diverse biological roles. As a chaperone belonging to the small heat-shock protein (sHsp) family, αB-crystallin protein has been shown to prevent aggregation of denatured proteins *in vitro* and plays a role in many different cellular processes such as cellular growth, transcription, migration, differentiation and development. It has been shown to protect cells from various stress factors, prevent the aggregation or facilitate renaturation of proteins and to protect cytoskeletal elements against ischemia, injury or depolymerizing agents.

αB-crystallin protein is also widely expressed in other tissues such as cardiac (Bhat *et al.,*1991), skeletal muscles and the brain (Srinivasan *et al.,* 1992; Klemenz *et al.,* 1993), where it appears to be involved in transduction pathways activated during growth and differentiation and in response to various forms of stress (Mehlen *et al.,* 1995). In the heart, αB-crystallin protein and heat-shock protein 27 are involved in stress tolerance (Verschuure *et al.,* 2002). A subsequent study showed that selective expression of αB-crystallin protein at an early stage of differentiation occurred in myoblasts resistant to differentiation-induced apoptosis. αB-crystallin protein can inhibit apoptosis at various stages by interacting with other proteins involved in the apoptotic pathways. The role of αB-crystallin protein in apoptosis suggests an important role for the protein both in development and in cancer.

2.4 Phosphorylation of αB-crystallin

Phosphorylation appears to be one of the modulators of chaperone functions of small heat shock proteins.αB-crystallin protein is known to get phosphorylated at three different serine residues, S19, S45 and S59 *in vivo*, during ischemia and in response to cytotoxic signals and mitogenic and inflammatory agents (Ito *et al.,* 2001; Eaton *et al.,* 2001). Both phosphorylated and unphosphorylated forms exist in the eye lens as well as in other tissues.

Phosphorylation occurs in age dependent manner, S59 is phosphorylated under heat stress, whereas S45 is phosphorylated in the mitotic phase of the cell cycle. In mitotic cells, phosphorylation is enhanced at Ser-19 and especially at Ser-45, whereas phosphorylation at Ser-59 is reduced. Phosphorylation at Ser-59 is associated with the localization of αB-crystallin protein in the centrosomes of dividing cells. At least two pathways are implicated in the αB-crystallin protein phosphorylation: the p38 MAPK1 / MAPKAPK2 pathway is responsible for the phosphorylation of serine-59, while serine-45 phosphorylation appears to be under the control of p42/44 ERK MAPK. The kinase responsible for the phosphorylation of serine 19 is still unknown. Phosphorylation is presumably used to modulate the cellular role of these proteins, the details of which remain unclear. The importance of this role has been highlighted by the identification of an inherited mutation in αB-crystallin protein that is associated with desmin-related myopathy (Vicart *et al.,*

1998). In the lens, αB-crystallin protein phosphorylation by cAMP-dependent kinase is age-related and is induced in response to stress (Wang *et al.,* 2000; Ueda *et al.,* 2002). αB-crystallin protein negatively regulates apoptosis and is involved in cell division, cell differentiation, etc. Reports regarding the role of phosphorylation in the chaperone function of α-crystallin are debatable.

Studies on phosphorylation mimicking mutations of αB-crystallin protein (αB-3D, S19D, S45D & S59D) showed reduction in the oligomeric size and reduction in its chaperone-like activity (Ito *et al.,* 2001). While the single phosphorylation mimic (S19D) did not affect the chaperone-like activity the double mutant (S19D/S45D) had significantly reduced activity (Aquilina *et al.,* 2004). On the other hand, an increase in the extent of binding of the phosphorylation mimics of αB-crystallin protein to destabilized mutants of T4 lysozyme than wild type αB-crystallin protein was reported, suggesting that phosphorylation leads to enhancement in its chaperone function (Koteiche *et al.,* 2003). A comprehensive investigation is therefore required to have a conclusive understanding on the role of phosphorylation in the chaperone-like activity of α-crystallins. Phosphorylation modulates the functioning of αB-crystallin protein as a molecular chaperone. Inhibition of nuclear export demonstrated that phosphorylation of αB-crystallin protein is required for import into the nucleus. As revealed by mutant analysis, phosphorylation at Ser-59 is crucial for nuclear import, and phosphorylation at Ser-45 is required for speckle localization (den Engelsman *et al.,* 2005). Co-immuno precipitation experiments suggested that the import of αB-crystallin protein is possibly regulated by its phosphorylation-dependent interaction with the survival motor neuron (SMN) protein, an important factor in small nuclear ribonucleoprotein nuclear import and assembly (den Engelsman *et al.,* 2005). This interaction was supported by co-localization of endogenous phosphorylated αB-crystallin protein with SMN in nuclear structures.

Serine phosphorylation at the 59^{th} position in αB-crystallin protein has been shown to confer increased protection to the cells exposed to apoptotic insults (Ito *et al.,* 2001; Hoover *et al.,* 2000; van den Issel *et al.,* 1998). In the heart, oxidative stress can lead to the activation of p38 and MAPKAPK-2 and in cardiac myocytes, stress increases p38-mediated

MAPKAPK-2, the latter of which phosphorylates αB-crystallin protein on Ser-59 (Maulik *et al.,* 1998; Nakano *et al.,* 2000). Moreover, blocking p38-mediated MAPKAPK-2 activation inhibits αB-crystallin protein phosphorylation on Ser-59 and enhances apoptotic myocyte death (Hoover *et al.,* 2000). These results are consistent with a role for phosphorylation of αB-crystallin protein on Ser-59 in mediating the cytoprotective actions of this small heat shock protein (sHsp). Mimicking phosphorylation of αB-crystallin protein on serine-59 is necessary and sufficient to provide maximal protection of cardiac myocytes from apoptosis (Morrison *et al.,* 2003). Serine-59 phosphorylation of αB-crystallin protein down-regulates its anti-apoptotic function by binding and sequestering Bcl-2 in breast cancer cells.

2.5 Angiogenesis by factors VEGF-A, αB-crystallin protein and its phosphorylation

In complex multicellular animals such as humans the diffusion of oxygen in the tissues is limited to 100 to 200 µm, which makes an extremely developed vascular system absolutely essential. A blood capillary is lined endothelial cells which form tight junctions, surrounded by the basement membrane and are generally supported by the connective tissue and extracellular matrix. Formation of new blood vessels is not just important during the development, but also during wound healing, formation of placenta, during menstruation and during organ regeneration. In order to maintain the vascular system, a process of development of new blood vessels from the existing blood vessels called angiogenesis is required. This process is strictly regulated by pro-angiogenic and anti-angiogenic factors. The balance between these two factors is very strictly controlled and often, the balance is aberrant in disease conditions such as tumor growth, diabetic retinopathy and rheumatoid arthritis. Vascular Endothelial Growth factor (VEGF) is one of important pro-angiogenic factors (Roskoski 2007). It is involved in physiological angiogenesis.

As per the current literature the VEGF family comprises of seven members which have the core VEGF homology domain viz., VEGF-A, VEGF-B, VEGF-C, VEGF-D, VEGF-E, VEGF-F and PlGF (Hoeben *et al.,* 2004). VEGF-A is a dimeric glycoprotein protein with molecular weights 34 to 42 kDa. It has seven isoforms. All of the isoforms exist as homodimer, whereas the monomers of each isoforms consist of 121, 145,148, 165, 183 or 206 amino acids. All

isoforms are coded by a single VEGF-A gene with eight exons (Ortega *et al.,* 1999) where, amino acids coded by exon-1 to exon-5 are common to all isoforms. Amino acids coded by exon1-5 are conserved in all isoforms apart from isoform VEGF-A_{148}. Exons -6 and -7 code for heparin-binding domains, whose presence determines the bioavailability of the protein. Isoforms VEGF-A_{145}, VEGF-A_{189} and VEGF-A_{206} have heparin-binding domains which are coded by both exon-6 and exon-7 and therefore are tightly bound to heparin proteoglycans in the extracellular matrix. Isoform VEGF-A_{121}, does not contain any heparin-binding domain and is the most diffusible isoform of VEGF-A. Isoform VEGF-A_{165} has one heparin-binding domain coded by exon-6 and is moderately diffusible. Plasmin are proteases which are known to degrade the extracellular matrix, thereby releasing the heparin-bound VEGF-A. VEGF-B is found abundantly in skeletal muscle and pancreas, whereas VEGF-C and VEGF-D are excessively found in heart, colon, placenta and small intestines. VEGF-E is virus-encoded VEGF. Out of all the VEGF members VEGF-A is most studied for its angiogenic effects. Both VEGF-A_{121} and VEGF-A_{165} have high angiogenic effects. However, VEGF-A_{165} is the common isoform which is found in pathological conditions in adults. Hitherto, in this report VEGF-A refers to VEGF-A_{165} unless mentioned otherwise. VEGF-A is a potent mitogen, an important permeability inducer in endothelial cells and has an important role in maturation of new blood vessels, and known to promote anti-apoptotic signaling in endothelial cells (Nishijima *et al., 2007;* Sheikpranbabu *et al.,* 2009). VEGF-A is expressed in various other human tissues such as hair follicles, glomerular epithelium of kidney and epithelium of choroid plexus in brain where it does not cause angiogenesis showing its specificity as mitogen towards the endothelial cells (Witmer *et al.,* 2003). It is observed that hypoxic conditions in the tumor microenvironments causes increased expression in VEGF-A to meet with the oxygen requirements. The role of VEGF in tumor survival through excessive angiogenesis was first hypothesized in 1922 (Lewis, 1922; Ide *et al.,* 1939). The growth of tumor was greatly dependent on the angiogenesis around the tumor which helps to maintain the necessary microenvironment and nutrition for tumor cells (Folkman, 1971). It was later confirmed that VEGF-A could induce fenestrated neovascular endothelium, increase the permeability and decrease the selectivity of the endothelial junctions (Hobbs *et al.,* 1998; Monsky *et al.,* 1999). Retinal Pigment Epithelial (RPE) cells are known to secrete VEGF-A

which is essential for the development of the capillaries in the choroid region of eye. It is also known that loss of RPE cells or reduced production of VEGF-A by RPE cells cause atrophy in the choroid capillaries. Loss of feedback mechanisms for the expression of VEGF-A might lead to pathological conditions of eye such as Age-related Macular Degeneration (AMD), Diabetic Retinopathy (DR) and Retinopathy of Prematurity (ROP) (Ferrara, 2010; Michaelson, 1948). In retinal ischemia VEGF-A could induce neovascular response, and increased levels of VEGF-A were found in vitreous fluid and retina of patients suffering from DR and ROP where choroid neovascualrization sets in as the secondary effect (Patel *et al.,* 2006; Adamis *et al.,* 1994). Significantly high levels of VEGF-A have been found in frozen sections of neovascular membranes where high level of vasculature was also observed (Matsuoka *et al.,* 2004). In patients suffering with AMD, both blood samples and drusens show high levels of VEGF-A signifying the important role of VEGF-A in both physiological and pathological process of angiogenesis (Rudolf *et al.,* 2005). Since VEGF-A is a secreted protein; anti-VEGF-A therapies for AMD have shown considerable halt in the progression of disease (Michels *et al.,* 2006). As mentioned previously αB-crystallin protein is known to have a key role in angiogenesis and choroid neovascularization. The role of αB-crystallin protein in retinal neovascularization was emphasized by Kase and his associates in the year 2010. An increase in endothelial apoptosis and decrease in intraocular angiogenesis was seen in retinas of αB-crystallin protein null mouse mutants which were subjected to Oxygen-Induced Retinopathy (OIR) and laser-induced choroid neovascularization (CNV). In 2007, Ghosh and his associates have identified through protein pin array assay peptides 7-HPWIRRPF-14, 49-LRPPSFLR-56, 91-VKVLGDVI-98, 117-EFHRKYRI-124, 143-LTVNGPRK-150 and 157-RTIPITRE-164 of αB-crystallin protein that are interactive with VEGF-A Most of the above mentioned peptides which interact with VEGF-A belong to NTE or ACD of αB-crystallin protein, which are known to be involved in chaperone activity of the protein (Bhaktisaran *et al*, 2015) through which an interesting speculation stating chaperone-like activity of αB-crystallin protein towards VEGF-A can be made. This speculation can be supported by results from experiments done by Kase *et al* (2010) where it has been shown that decreased levels of VEGF-A in αB-crystallin protein-deficient mouse is not due to decrease in mRNA expression but rather due to altered protein secretion and ubiquitination

(Kase *et al.,* 2010), suggesting that αB-crystallin protein is a VEGF chaperone. Increase in phosphorylation levels of αB-crystallin protein (S-59) was observed in OIR and CNV injured samples. αB-crystallin protein and its phosphorylated form (S-59) were co-localized in endoplasmic reticulum (ER) suggesting a mechanism where phosphorylated αB-crystallin protein might bind to VEGF-A in cytoplasm, transport it into ER and ensure proper folding of VEGF-A in ER and its secretion into extracellular matrix.

In an another independent study siRNA-mediated knockdown of unfolded protein response (UPR) proteins ATF6 and inositol-requiring kinase1 led to decreased expression of αB-crystallin protein in endothelial cells and decreased the endogenous levels of VEGF, where UPR is responsible for maintaining intracrine VEGF levels in endothelial cells. Subsequently, conclusions were also drawn on the lines of αB-crystallin protein protecting VEGF against proteosomal degradation as inhibition of 26S proteosomal complex increased the levels of VEGF-A in αB-crystallin protein deficient mice (Kase *et al.,* 2010). Boelens and his associates in 2013 have established that knockdown of αB-crystallin protein decreases the migration rate of HNSCC cells, along with the decreased production of VEGF-A up to 1.9 – 2.1 fold in normoxia and up to 1.9 – 2.2 fold in hypoxic conditions respectively (Van de Schootbrugge *et al.,* 2013).Therefore, this interesting regulation of VEGF folding, secretion and degradation by αB-crystallin protein plays a very important role in choroid neovascularization which is the major problem in many retinopathies. Current therapeutic methods concentrate on anti-VEGF-A drugs as mentioned above, however stabilization of phosphorylated form of αB-crystallin protein in endothelial cells may decrease the effect of the treatment by conferring protection to VEGF-A. Targeting this interaction between αB-crystallin protein and VEGF-A might give rise to better therapeutic methods in cases like AMD where reduction in VEGF levels might induce hypoxic environment and worsen the condition even further. The current report concentrates on effect of phosphorylation on angiogenic effects of αB-crystallin protein.

2.6 Chick chorioallantoic membrane (CAM) assay a model to study angiogenesis

The chick chorioallantoic membrane (CAM) begins to develop after fertilization and gestation period is 21 days. The CAM is naturally immunodeficient and highly vascularized, making it an ideal system for testing angiogenesis and anti-angiogenesis (Pathak *et al.,* 2015). The growth of new blood vessels from pre-existing vascular network is called angiogenesis and involves coordinated signals to the adhesion, migration and proliferation of endothelial cell. The CAM is a useful tool to studying angiogenesis because it is relatively rapid adapted to study angiogenesis dependent process such as tumor growth (O'Reilly *et al.,* 1997). Three extraembryonic membranes are formed during development: the yolk sac membrane, the amnion, and the chorioallantoic membrane (CAM). The CAM is formed on day 3–4 of incubation by the fusion of the chorion and the allantois and it consists of three layers, ectoderm (from the chorion), mesoderm, and endoderm (from the allantois) (Romanoff, 1960). The CAM has a rich vascular system that develops within the mesodermal layer and is served by paired allantoic arteries and paired allantoic veins. By 16 days of incubation, the CAM has become so large that it covers most yolk sac, and become closely pressed against the shell membranes, which enable it to act as a gas-exchange organ receiving oxygen and eliminating carbon dioxide through the pores in the shell (Romanoff, 1960).

Being naturally immune deficient, the chick embryo accepts transplantation from various tissues and species without immune response. Chickens are protected by a dual immune system composed of B and T cells, controlling the antibody and cell mediated immunity, respectively. The B cells are differentiated in the bursa of Fabricius, whereas T cells are differentiated in the thymus (Davison, 2003; Funk and Thomson, 1996). The chick immune system does not begin to develop to function until about 2 weeks into its development (Jankovic *et al.,* 1975; Weber and Mausner, 1975). The presence of T cells can be first detected at day 11 and of B cells at day 12 (Janse and Jeurissen, 1991), and by day 18 chicken embryos become immune competent (Jankovic *et al.,* 1975). By day 10 and, respectively by day 12, monocytes and macrophages are found in the yolk sac, spleen,

bursa, gut, thymus, and in the liver (Janse and Jeurissen, 1991). The two major inflammatory cell types present in day 10–15 embryos are heterophils and monocytes. Heterophils are an avian analog of mammalian neutrophils and represent a main source of matrix metalloproteinase-9 (MMP-9) in the chick embryo, and could be identified by staining with an anti-chicken MMP-9 antibody (Zijlstra *et al.,* 2006). On the other hand, monocytes/macrophages are the major source of MMP-13 in the chick embryo and could be identified by immunostaining with an anti-MMP-13 antibody (Zijlstra *et al.,* 2004).

CHAPTER 3.0: MATERIALS AND METHODS

3.1 Expression and purification of αB-crystallin protein and its phosphorylation-mimicking mutants (singles, doubles and triples)

3.1.1 αB-crystallin protein and it's phospho-mimicking mutant clones

The clones of αB-crystallin protein and it's phosphorylation-mimic mutants and all the clones of protein in pET21a(+) vector between the restriction sites NdeI and HindIII were already available prepared in the lab. For example, the αB-crystallin protein gene has three serine(S) residues at 19th, 45th, and 59th position (Figure 2).

Serine to glutamic acid or aspartic acid mutants acts like phosphorylated protein because of the negative charge imparted by the replaced amino acids. Similarly, if Serine is replaced by a neutral amino acid like Alanine, it acts as a non-phosphorylatable mutant.

The triplet codon for serine can be replaced with another triplet codon coding for another amino acid. This is achieved by Site Directed Mutagenesis using Overlapping PCR strategy. If a serine residue is replaced by Glutamic acid (E) at 19th position and the serine at 45 and 59 are replaced by Alanine (A), then the resultant product is termed as EAA, similarly AEA, and AAE can be generated by replacing 45th and 59th position of Serine by either Glutamic acid (E) or Alanine(A). If two positions are replaced by Glutamic acid, the resultant mutant is termed as EEA, AEE, and EAE. If all the serine residues are replaced by Glutamic acid (E), the resultant mutant will be termed as EEE. Similarly, if all the serine residues are replaced with Alanine, it makes AAA which is a fully non-phosphorylatable mutant.

During this experiments, αB-crystallin protein clone and all the clones of phosphorylation-mimicking mutants clones were used. All the proteins were expressed and purified for the studies as described below.

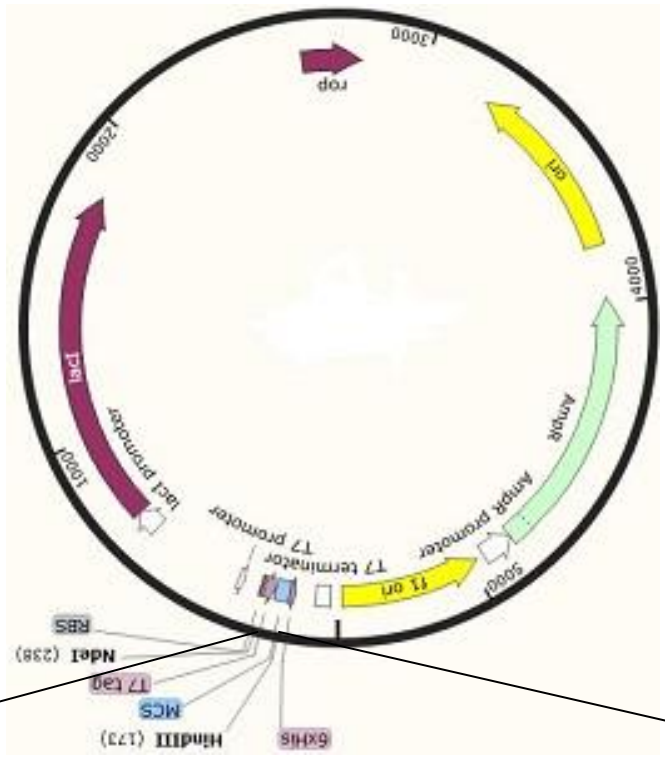

ATGGACATCGCCATCCACCACCCCTGGATCCGCCGCCCCTTCTTTCCTT**TCC**ACTCCCCC
AGCCGCCTCTTTGACCAGTTCTTCGGAGAGCACCTGTTGGAGTCTGATCTTTTCCCGACG
TCTACTTCCCTG**AGT**CCCTTCTACCTTCGGCCACCCTCCTTCCTGCGGGCACCC**AGC**TGG
TTTGACACTGGACTCTCAGAGATGCGCCTGGAGAAGGACAGGTTCTCTGTCAACCTGGAT
GTGAAGCACTTCTCCCCAGAGGAACTCAAAGTTAAGGTGTTGGGAGATGTGATTGAGGTG
CATGGAAAACATGAAGAGCGCCAGGATGAACATGGTTTCATCTCCAGGGAGTTCCACAGG
AAATACCGGATCCCAGCTGATGTAGACCCTCTCACCATTACTTCATCCCTGTCATCTGATG
GGGTCCTCACTGTGAATGGACCAAGGAAACAGGTCTCTGGCCCTGAGCGCACCATTCCC
ATCACCCGTGAAGAGAAGCCTGCTGTCACCGCAGCCCCCAAGAAATAG

Figure 3: Schematic diagram of gene construct for WT-αB crystallin protein coding gene in pET21a expression vector. The triplet codens shown in red colors were three serine coding nucleotides. The crystalline domain is shown in blue color.

Similarly, all three single phosphomimicking mutatants (AAE, AEA & EAA), three double phosphomimicking mutants (AEE, EAE & EEA) and three phosphomimicking mutants (AAA & EEE) were prepared.

Figure 4: Schematic diagrams (A-D) of gene construct for mutants WT-αB crystallin protein coding gene in pET21a expression vector cloned in NdeI and HindIII site. Site of mutation and crystallin domain are shown in red and blue color respectively.

Figure 5: Schematic diagrams (A-D) of gene construct for mutants WT-αB crystallin protein coding gene in pET21a expression vector cloned in NdeI and Hind III site. Site of mutation and crystallin domain are shown in red and blue color respectively.

The translated protein codes were as follows; the red and blue color signifies replaceable amino acid (serine (S) and glutamic acid (E)) in 19th, 45th & 59th position and crystalline domain respectively.

Translation WT- αB in 19, 45 and 59 amino acid positions (175 aa):

MDIAIHHPWIRRPFFPFHSPSRLFDQFFGEHLLESDLFPTSTSLSPFYLRPPSFLRAPSWFDTGLSEMRLEK
DRFSVNLDVKHFSPEELKVKVLGDVIEVHGKHEERQDEHGFISREFHRKYRIPADVDPLTITSSLSSDGVLT
VNGPRKQVSGPERTIPITREEKPAVTAAPKK

Translation mutated αB-AAE in 19, 45 and 59 amino acid positions (175 aa):

MDIAIHHPWIRRPFFPFHAPSRLFDQFFGEHLLESDLFPTSTSLAPFYLRPPSFLRAPEWFDTGLSEMRL
EKDRFSVNLDVKHFSPEELKVKVLGDVIEVHGKHEERQDEHGFISREFHRKYRIPADVDPLTITSSLSSD
GVLTVNGPRKQVSGPERTIPITREEKPAVTAAPKK

Translation mutated αB-AEA (175 aa):

MDIAIHHPWIRRPFFPFHAPSRLFDQFFGEHLLESDLFPTSTSLEPFYLRPPSFLRAPAWFDTGLSEMRL
EKDRFSVNLDVKHFSPEELKVKVLGDVIEVHGKHEERQDEHGFISREFHRKYRIPADVDPLTITSSLSSD
GVLTVNGPRKQVSGPERTIPITREEKPAVTAAPKK

Translation mutated αB-EAA (175 aa):

MDIAIHHPWIRRPFFPFHEPSRLFDQFFGEHLLESDLFPTSTSLAPFYLRPPSFLRAPAWFDTGLSEMRLEK
DRFSVNLDVKHFSPEELKVKVLGDVIEVHGKHEERQDEHGFISREFHRKYRIPADVDPLTITSSLSSDGVLT
VNGPRKQVSGPERTIPITREEKPAVTAAPKK

Translation mutated αB-AEE (175 aa):

MDIAIHHPWIRRPFFPFHAPSRLFDQFFGEHLLESDLFPTSTSLEPFYLRPPSFLRAPEWFDTGLSEMRL
EKDRFSVNLDVKHFSPEELKVKVLGDVIEVHGKHEERQDEHGFISREFHRKYRIPADVDPLTITSSLSSD
GVLTVNGPRKQVSGPERTIPITREEKPAVTAAPKK

Translation αB-EEA (175 aa):

MDIAIHHPWIRRPFFPFHEPSRLFDQFFGEHLLESDLFPTSTSLEPFYLRPPSFLRAPAWFDTGLSEMRLEK
DRFSVNLDVKHFSPEELKVKVLGDVIEVHGKHEERQDEHGFISREFHRKYRIPADVDPLTITSSLSSDGVLT
VNGPRKQVSGPERTIPITREEKPAVTAAPKK

Translation αB-EAE (175 aa)

MDIAIHHPWIRRPFFPFHEPSRLFDQFFGEHLLESDLFPTSTSLAPFYLRPPSFLRAPEWFDTGLSEMRLEK
DRFSVNLDVKHFSPEELKVKVLGDVIEVHGKHEERQDEHGFISREFHRKYRIPADVDPLTITSSLSSDGVLT
VNGPRKQVSGPERTIPITREEKPAVTAAPKK

Translation αB-AAA (175 aa):

MDIAIHHPWIRRPFFPFHAPSRLFDQFFGEHLLESDLFPTSTSLAPFYLRPPSFLRAPAWFDTGLSEMRLEK
DRFSVNLDVKHFSPEELKVKVLGDVIEVHGKHEERQDEHGFISREFHRKYRIPADVDPLTITSSLSSDGVLT
VNGPRKQVSGPERTIPITREEKPAVTAAPKK

Translation αB-EEE (175 aa):

MDIAIHHPWIRRPFFPFHEPSRLFDQFFGEHLLESDLFPTSTSLEPFYLRPPSFLRAPEWFDTGLSEMRLEK
DRFSVNLDVKHFSPEELKVKVLGDVIEVHGKHEERQDEHGFISREFHRKYRIPADVDPLTITSSLSSDGVLT
VNGPRKQVSGPERTIPITREEKPAVTAAPKK

3.1.2 Bacterial Transformation with clones of αB-crystallin protein and its phosphomimics

Competent BL21 (DE3) (Stratagene, La Jolla, CA, USA) cells were incubated separately with a plasmid (pET21a) (containing αB-crystallin protein gene insert (pET21a-αBWT) or any of the phosphorylation-mimicking mutant gene insert on ice for 10 minutes, followed by heat shock at 42 ^{o}C for 90 seconds. The mixture was then kept on ice for 10 minutes, and 1000 µl of LB medium was added and incubated at 37ºC for 1hr. The cells were then pelleted down at 3000rpm for 3min and resuspended in 50µl of media. The resuspended cells were spread on an LB agar plate (Tryptone 10g, yeast extract 5g, NaCl 10g, pH 7.3 and agar 1.5%) containing 100µg/ml ampicillin. The plate was incubated for 12 hrs at 37ºC to get isolated transformed colonies.

3.1.3 Primary culture

Autoclave-sterilized 10ml LB media was taken in autoclave-sterilized tube, and 10 µl of Ampicillin was added (100mg/ml) and mixed thoroughly. About 3-4 isolated colonies were taken from the transformed plate and inoculated into the LB medium and is plugged with a cotton plug. The tubes were labeled and incubated overnight at 220rpm at 37ºC.

3.1.4 Secondary culture/Large scale culture

For the over-expression of αB-crystallin protein and its mutants, the overnight primary culture was inoculated in 1L of LB medium containing 0.1 mg/ml of ampicillin and incubated at 37ºC with vigorous shaking (220rpm) for 2hrs till the O.D. at 600nm reached 0.6. Protein expression was then induced by the addition of 1ml of 1 M IPTG (appendix: 2.8)

which induces the expression of the crystallin gene present downstream of the lac promoter in the plasmid. The culture was again incubated at 37^{o}C with vigorous shaking (220 rpm) for 4hrs.

After 4hrs, the cultured samples were centrifuged in Centrifuge bottles i.e Nalgene bottle (Appendix 4: Fig.4.1 (c)) at 10,000 rpm for 10 min at 4ºC in Beckman Coulter^{TM} (Avanti centrifuge J-30I, Appendix 4: Fig.4.1 (a)) using a JLA-16.250 (Appendix: Fig: 4.1(b)) rotor to get the cell pellets. Each bottle contained cell pellet from 500ml bacterial culture.

Cell pellet from one Nalgene bottle was resuspended in 5ml of 1XTNE (Appendix: 1.3) with 1mM EDTA buffer (Tris-NaCl EDTA) and 300µl PMSF (100mM). PMSF is a protease inhibitor and was essential for the stability of the proteins. Then, 15µl Lysozyme (100mg/1ml) or 150µl Lysozyme (10mg/1ml) was added, and the volume was made up to 5 ml with 1XTNE. The mixture was then incubated on ice for 30min. Lysozyme is an enzyme that breakdown the peptidoglycan backbone of the bacterial cell wall. The whole mixture was sonicated by an Ultrasonifier for 15min (pulse time=5sec, and pulse relapse=10sec). Sonication works on the principle of cavitation. Cavitations are the formation of vapor cavities in a liquid, which is the consequence of sound waves acting upon the liquid. When the probe produces cavities in the solution, it becomes intensely agitated. During this process, care has to be taken to optimize the condition for sonication, otherwise, it may not break the DNA strands effectively, and DNA will be a probable contaminant downstream. The cell lysate was centrifuged at high speed (20,000 rpm) for 30 minutes in Beckman Coulter^{TM} centrifuge using a JA-30.5Ti rotor. The supernatant was collected in a fresh tube.

3.1.5 Salting out

Ammonium Sulfate (calculated by using encorbio.com site) was added to 30% saturation to the cell lysate in a step-wise manner. The 30% ammonium sulfate saturation eliminates most of the bacterial proteins. With increased addition of the salt, different proteins will salt out at different ammonium sulfate saturation. The lysate which is 30% saturated with ammonium sulfate is incubated on ice for 30min and then centrifuged in Beckman Coulter Centrifuge (Avanti) using a JLA-16.250Ti rotor. After centrifugation, the supernatant was

taken, and now the ammonium sulfate saturation is gradually increased to 60% saturation. This time, our desired protein αB-crystallin protein along with some contaminant proteins also salts out of the solution. This is followed by incubation on ice for 30 min. The lysate that is now 60% ammonium sulfate saturated was liquated in 1.5mL microcentrifuge tubes and the tubes were centrifuged (5810R, F45-30-11 rotor) at 14,000 rpm for 20min at 4^{o}C. After centrifugation, the cell pellets were stored at -20^{o}C for further use.

3.1.6 Gel filtration

Ammonium sulfate pellets obtained from 1000ml bacterial culture was taken and resuspended in 1-1.5ml of 1XTNE and then filtered through 0.22µm syringe filter, and the volume was adjusted to 2mL. The filtrate was loaded on to a gel filtration column (HiprepTM 26/60, SephacrylTM S-300 HR) attached to an FPLC system (Bio-rad). The column has a bed volume of 320 ml. Flow rate was maintained at 1ml/min and the fraction size was 3 ml/tube. By looking at the gel filtration chart, we identified that the fraction tube numbers 32-52 have considerable absorbance indicating the presence of protein. 12% SDS-PAGE was run with the samples containing higher absorbance values, and the bands were visualized under UV- Transilluminator detector by quick staining the gel with chloroform and then coomassie blue. Bands which had less contamination were noted, and the fractions were pooled in to a fresh centrifuge tube.

3.1.7 Ion-Exchange Chromatography

Q-Sepharose beads (GE health care) were used to pack an Ion-exchange column of bed volume 20ml. The pooled fractions sample from gel filtration was centrifuged at 20,000rpm in Beckman CoulterTM centrifuge using a JA-30.5Ti rotor, the supernatant was collected in a fresh tube and passed through the column. The first 5 ml fraction was collected in one tube to let the void volume out and the rest of the flow through is collected in another fresh tube. The purity of αB-crystallin protein and phospho-mimics was checked by SDS-PAGE. The protein bands were quickly visualized in a UV-Transilluminator with chloroform and then stained with Coomassie brilliant blue G-250.Then, the protein solution was

concentrated using Amicon ultra-filtration unit fitted with 30 kDa membrane filters. The concentrated protein samples were stored at 4^{o}C after passing it through a 0.22 µm filter.

3.2 Desalting/Buffer exchange

1X TNE buffer was exchanged with phosphate buffer using HiprepTM 26/10 Desalting column attached to an FPLC system (AKTA purifier, GE Healthcare). Bed volume of the column is 53ml. Flow rate was maintained at 4ml/min. After the column is equilibrated, the concentrated protein in 1XTNE was injected, and the eluent was collected by noting the increased absorbance on the FPLC chart.

3.3 Protein estimation

The protein was diluted in 1:10 ratio to the total volume, 10M urea is added such that the final concentration of urea in the solution is 8M. Triplicates were made, and the tubes are incubated for at least 30 minutes at room temperature. The O.D. of the samples was recorded at 280nm, and the concentration of the protein was calculated using Beer-Lamberts law, Absorbance (A) = εcl, where ε is the extinction coefficient of the protein (0.693 ml/mg), c is the concentration of the protein and l is the path length of the cuvette (1 cm).

3.4. Labeling of proteins with FITC (Fluorescein Isothiocyanate)

The FITC stock solution of 1mg/ml was made in DMSO. 50 µl of the FITC stock solution (10 µl each time with 1min time interval) was added in 1mg of protein solution. The protein solution containing FITC was incubated at 4^{o}C overnight on a rotating disc. After incubation, the solution was loaded onto HiPrepTM 26/10 Desalting column (AKTA purifier, GE Healthcare) with fresh phosphate buffer and the fractions of 1mL were collected; OD was measured at 280nm(protein) and 495nm (FITC) in a UV spectrophotometer. The fractions containing the highest OD values at 280 nm were pooled, and a final OD was measured. And the protein was estimated using "Beer Lambert's law."

3.5 Biophysical-characterization of proteins

3.5.1 Dynamic Light Scattering (DLS)

Dynamic light scattering (DLS) measures time-dependent fluctuations in the scattering intensity arising from particles undergoing random Brownian motion. Brownian motion causes Diffusion coefficient, and particle size information can be obtained from the analysis of these fluctuations. More specifically, the method provides the ability to measure size characteristics of the material in a liquid medium. Proteins consist of polypeptide chains that are sensitive to a wide range of parameters such as temperature and chemical environment. Preparation method, storage conditions, and/or buffer choice can all influence the size (oligomeric size) and quality of proteins in a sample. Photocor-FC dynamic light scattering (DLS) at a scattering angle of 90^{o}, equipped with a 633 nm laser was used for recording the scatter, and the Photocor software calculates the autocorrelation function. DynaLS software was used to analyze the data.

The protocol for DLS as follows;

1. The computer was turned on, and subsequently, the laser, PMT controller, and the Temperature controller units were turned on.
2. A DLS cuvette is washed with Milli-Q water followed by a buffer rinse. Then, 400µl of protein sample whose particle size has to be measured was transferred into the cuvette, and the mouth of the cuvette was sealed with parafilm. The cuvette is then loaded on to a cuvette holder or slot.
3. The software (Photocor) was opened in the computer and required parameters were set. Later, “File setup” was opened and a path is given such that the results will be saved in a text format in a destined folder. Click on macro and choose new and open the macro file which is an algorithm that contains the details of the program regarding the number of cycles and duration of the cycle for which the correlation reading should be measured.

4. The macro file program is used to collect the data. A series of files were saved in the chosen folder. After the data collection was complete, the data was analyzed using software called DynaLS.
5. The files that were to be analyzed could be opened in DynaLS software. DynaLS shows the autocorrelation vs. channel graph and a histogram showing the intensity (%) vs. the particle size. A report is generated and is saved. The average of all mean values will be the approximate Hydrodynamic radius of that particular protein oligomer.

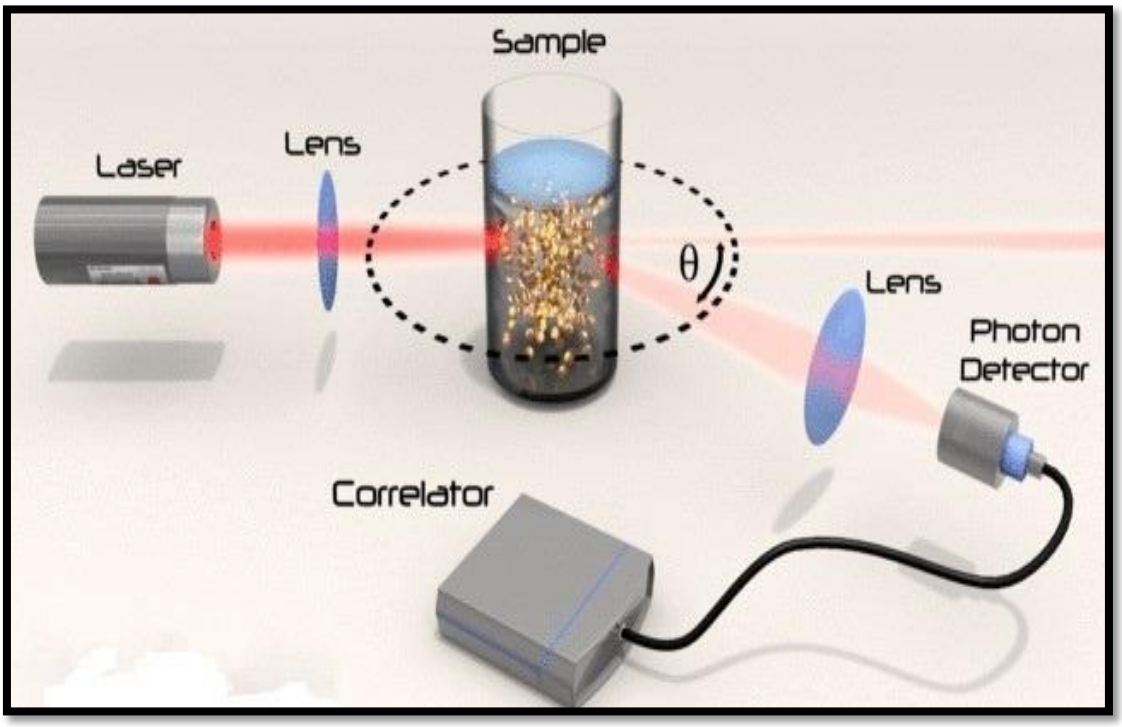

Figure 6: Schematic diagram of Dynamic light scattering (DLS) working principle.

The laser (633nm) passes through a collimator lens and then hits the cell with the solution. The light is scattered and detected by a photomultiplier that transforms a variation of intensity into a variation of voltage.

3.5.2 Analytical ultracentrifugation (AUC)

Analytical ultracentrifugation (AUC) measures the rate at which molecules move in response to centrifugal force generated in a centrifuge. This provides information about both molecular mass and shape of molecules. It is also useful for comparing different

engineered variants of the same protein/peptide, detecting aggregates in the protein sample, verifying whether a sample is entirely homogeneous in mass and conformation, establishing the native state of protein or polypeptide, detecting changes in protein conformation such as partially folded or transition to "molten globule state". Sedimentation velocity method is used to study samples over a fairly wide range of pH and ionic strength and temperatures (4 to 40^{o}C), and protein concentration 0.1 – 2 mg/ml. The volume required is ~0.45 ml.

Sedimentation velocity experiments were carried out using Proteome Lab XL-I Beckman Coulter Protein Characterization System. The AUC cells are assembled according to the protocol and the proteins (1mg/mL), and reference buffers (PBS) were loaded, and the cells were sealed. These cells were then loaded on to the rotor along with the counter balance. Then, the monochromator was fixed in place, and the centrifuge lid was closed. The vacuum pump was turned on and it took a while for the temperature to reach 20^{o}C. Then, the Proteome Lab software was used to run the program. The protein sample was spun at a speed of 28000 rpm. The concentration distribution across the cell at various times during the experiment was measured while the sample was spinning, by measuring absorbance at 280 nm.

The data was analyzed using Sedfit software. Sedfit gives us the values for sedimentation coefficients, which in turn gives the values for molecular weight of the compound based on the distribution of sedimentation coefficients.

4.6. Chorio-allantoic membrane assay (CAM) to study angiogenesis

The chick embryo chorioallantoic membrane assay has been a model for studying neovascularization (Ribatti, 2008). The CAM assay is quick, technically simple, and inexpensive. However, a major drawback is that it is labor intensive due to the large number of eggs that are required to obtain consistent results. The investigator should note that this is a non-mammalian system which should be taken into consideration when interpreting results.

The CAM assay protocol was used as follows;

1. Fertilized eggs were procured from Directorate of Poultry Research, Rajendranagar, Hyderabad. The eggs were incubated by laying them vertically in a hatchery incubator maintained at 80-82% of humidity at a temperature ranging 99-101^{o} F.
2. After three days incubation, eggs were removed from the incubator. Note: The eggs are incubated only for three days because - according to our experiments, earlier development stages had significantly lower survival rates. At the incubation period of 3days, the yolk sack which is not yet covered by the chorio-allantoic membrane (CAM) becomes thinner and tends to adhere. Egg morphology appears like a meta-ellipse, with a relatively broader side and a pointed one, and the air sac is usually located on the broader side right behind the shell where the embryo resides.

3. After disinfection of the shell center outside the air sac with 70% Ethyl alcohol, a hole is gently made over the air sac with a pointed forceps and slightly broadened such that the vascular zone is easy to be identified.

4. By gently applying pressure to the meridian running through the crack, the chorionic membrane is carefully separated using fine-pointed forceps. After that to avoid drying cover open area with sterile flexible packing film.

5. 1µg of the desired protein is loaded directly onto a tiny vascular zone with the help of a micropipette. Similarly, for positive control, VEGF (20ng) was used. For control, phosphate buffer saline (2µl) is used.

6. 0 hr pictures camera. "Capture OEM software (http://www.webopedia.com/TERM/O/OEM.html)" was used to capture the images with desired parameters. Nikon Fiber Illuminator was used as a light source was taken with the help of Stereomicroscope (SMZ745T) attached with NIKON.

7. After sealing the openings with sterile flexible packing film, the eggs were further incubated for 4hrs.

8. The Same vascular zone was again captured using same parameters by considering the previous images at 0 hr as a reference.

9. Contrast pictures were processed to get numerical data using Angioquant v1.3 (2005) softwarev (http://www.cs.tut.fi/sgn/csb/angioquant/).

10. Histograms were plotted based on lengths, sizes, and junctions using GraphPad Prism v5.01 (California US-2007) software (http://www.graphpad.com).

3.7 Protein uptake studies using human retinal micro vascular endothelial cells (HRMVECs)

The primary Human retinal micro vascular endothelial cells (HRMVECs) were obtained from cell systems Inc USA (ACBRI 181). The revival and expansion of HRMVECs was done according to the protocol recommended by the manufacturer.

3.7.1 Revival of HRMVE Cells

1. The cell culture media (CSC media) containing culture boost (growth factors), and attachment factor supplied by the manufacturer were kept for thawing in water maintained at 37^{o} C.

2. The cryo-vials were retrieved from liquid nitrogen containers and were thawed at room temperature. The vials were taken into Laminar Air Flow Hood and then the exterior of the vials were flushed with 70% alcohol.

3. The cryo-vials were carefully transferred into a sterile centrifuge tube containing 2ml of media. These tubes were now subjected to centrifugation at 1000 rpm for 5 minutes.

4. The supernatant was discarded, and the pellet was gently tapped to loosen the cell pellet. The cells were resuspended in 500 µl media.

5. Appropriate cell culture flasks (T75 or T25 flask) were coated with attachment factor. Attachment factor was added to the culture flask and swirled to form a uniform layer. The excess unbound attachment factor was removed, and cell growth medium was added (5ml in a T25 flask, 10ml in a T75 flask).

6. Now, the suspended cells were transferred into the flasks coated with attachment factor containing the complete medium. The vial was capped and incubated in a 37^{o} C

incubator with 5% CO2. The cultures were maintained until the cells reach 80-90% confluence.

3.7.2 Sub-culturing of HRMVECs

Once cells reached 90% confluency, spent media was aspirated from the culture flask. The cells were gently washed with 1X phosphate buffer, followed by a gentle treatment with Passage Reagent Group (PRG) solution as per the instructions. Approximately 1.5 X 106 cells were seeded as start-up culture in a T75 flask coated with attachment factor and labeled for the passage.

3.7.3 Uptake of FITC labeled αB–crystallin and its phosphorylation-mimicking mutant proteins in Human Retinal Microvascular Endothelial Cells (HRMVECs)

The protocol of uptake of FITC tagged protein to MRMVECs as follows;

1. HRMVE cells (~60% confluent) were harvested from a T75 flask and seeded on attachment factor coated coverslips placed in a 6 well plate. After an hour, the cells attach. CSC complete cell media (2ml) was added to each well. The 6 well plates were placed in a 37^{o}C incubator with 5% CO2.

2. The spent medium was aspirated, and fresh CSC complete medium was added with FITC conjugated αB–crystallin and its phospho-mimicking proteins at a concentration of 100µg/mL. The plates were incubated for 4 hours.

3. The spent media is removed, and a PBS wash is given. Cells were then stained with 10µg/ml Hoechst 33342 (nuclear stain) diluted in PBS for 20 minutes in the incubator. The excess stain was washed with phosphate buffer five times.

4. The cells are fixed using 10% formaldehyde solution for 12 minutes, followed by PBS washes to remove formaldehyde.

5. A small drop of mounting solution (Slow Fade Anti Fade by Molecular Probes) was added on to a grease free glass slide. Then, the cover slip having the cells was mounted

on the glass slide in an inverted position such that the cells come in contact with the mounting medium without forming any air bubbles.

6. Nail polish was added on the edges of the coverslip to seal the coverslip with mounting media.

7. When slide was ready, the images were taken using Fluorescence microscope and also using a confocal microscope.

CHAPTER 4.0: RESULTS

4.1 Site-directed mutation of human αB-crystallin gene

Artificially done specific mutation is called site-directed mutation. Several techniques designed to introduce specific mutations into a gene through oligo-mediated mutagenesis have been described (Smith, 1985; Botstein and Shortle, 1985; Wu and Grossman, 1987). Here, the method to create mutants of WT- αB crystallins single (AAE, AEA, EAA), double (EEA, EAE, AEE) and triple (EEE, AAA) mutants (appendix 3.2) is site-directed mutations and for this employed the overlapping PCR in a coding gene (Saiki et al., 1985; Mullis and Faloona, 1987) which used two different synthetic oligos as primers to amplify WT- αB crystallin (appendix 5.2).

These primers anneal at either end of the targeted nucleotide sequence and were oriented in opposite directions. Exponential amplification of the target sequence had occurred over the course of multiple rounds of denaturation, annealing and 3' extension by DNA polymerase (Mullis and Faloona, 1987).

4.1 Wild type and phosphomimicking αB-crystallin Protein purification

The ammonium sulfate pellets of αB-crystallin protein or its phosphorylation-mimicking mutants from a one-liter bacterial culture were re-suspended in 1XTNE and filtered to remove particulate matter. The volume was made up to 2 mL and was subjected to gel-filtration chromatography on a pre-packed S-300 column (HiPrep^{TM} 26/60, Sephacryl^{TM}S-300 HR) connected to an FPLC system (Bio-rad).

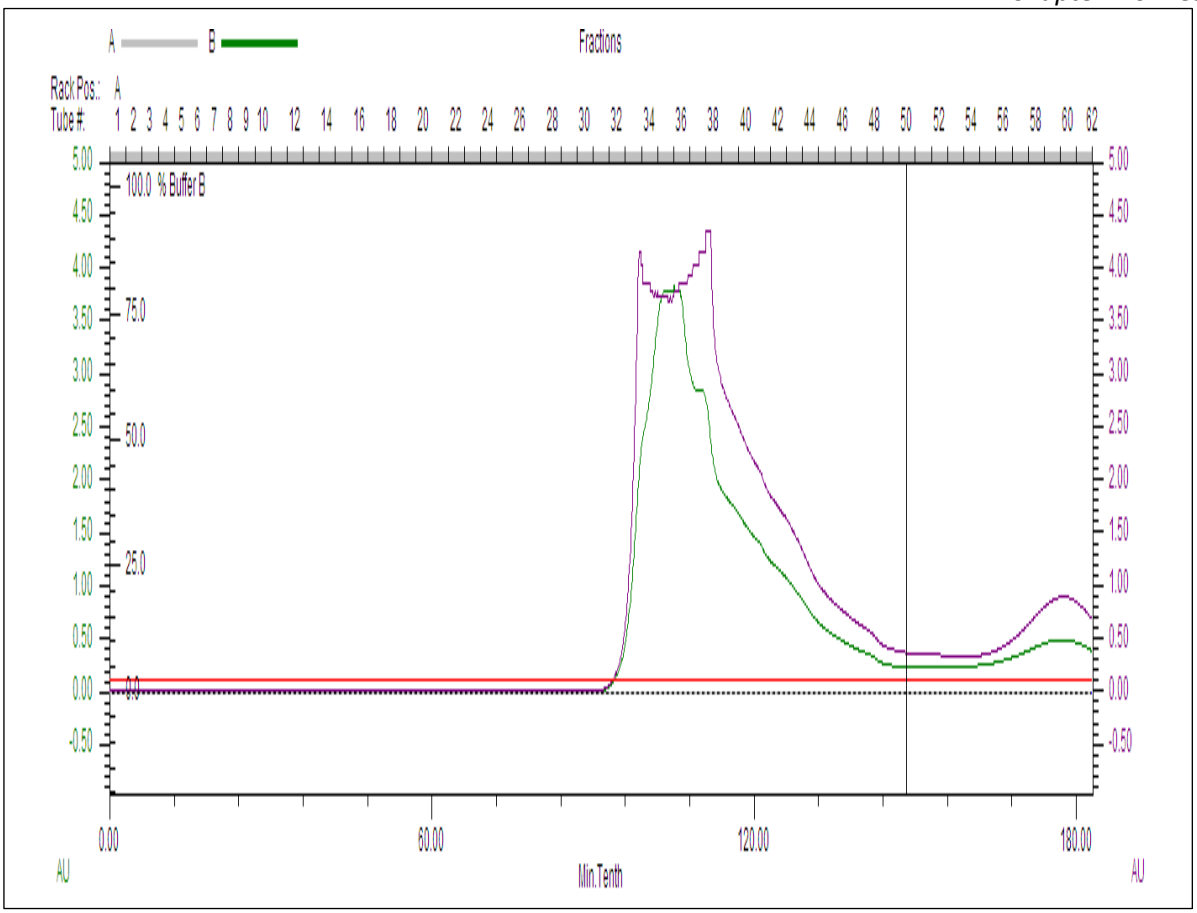

Figure 7: Screenshot image of gel-filtration chromatography of αB-crystallin protein protein. Sample run on (HiprepTM 26/60, SephacrylTM S-300 HR) connected to an FPLC system (Bio-rad). The green profile shows the absorbance of protein fractions measured at 280nm. Above are the numbers correlating to the various fractions collected after crud sample protein injection.

Fractions (3ml) were collected using a fraction collector as mentioned in the materials and methods section. To detect the fractions containing αB-crystallin protein or its phosphorylation-mimicking mutant proteins, readings of absorbance at 280nm on the FPLC run chart were noted and the fractions having the highest absorbance (Fig 7) were loaded onto a 12% SDS-polyacrylamide gel and subjected to electrophoresis at a constant current of 30mA.

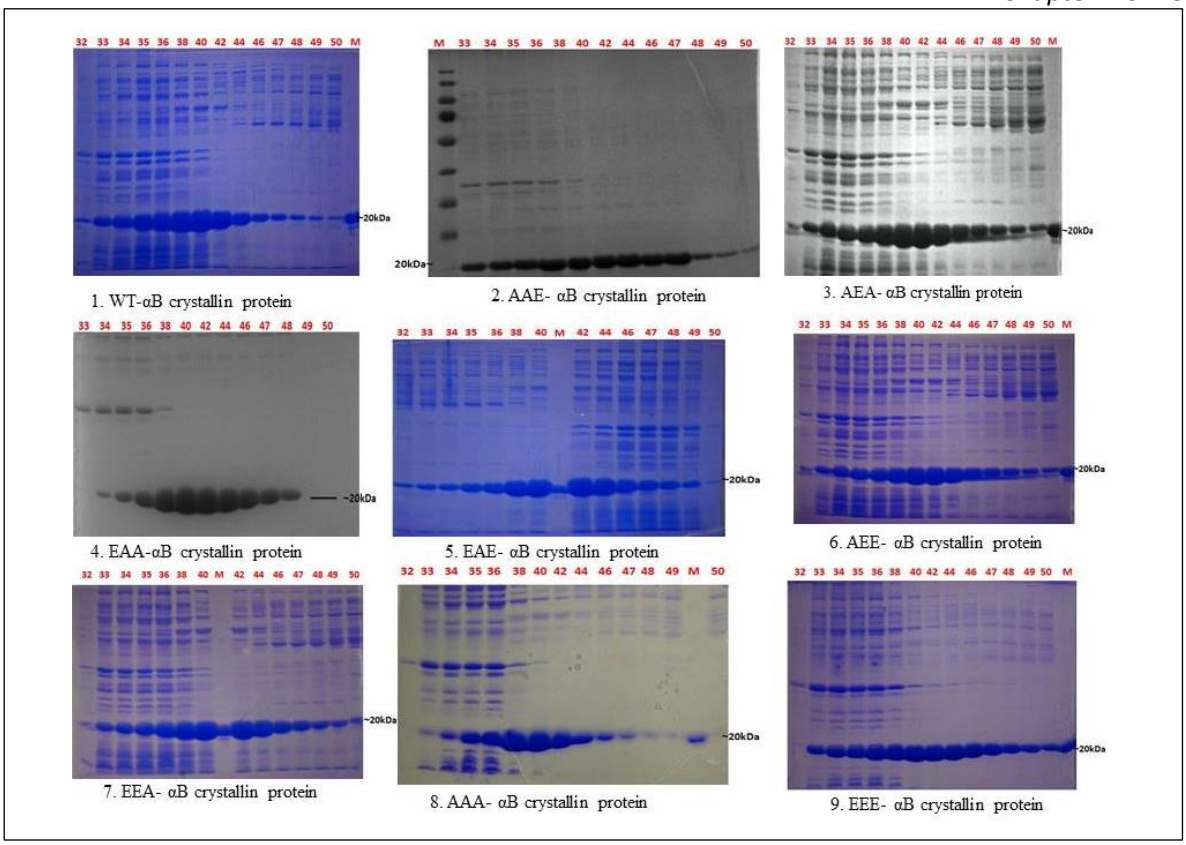

Figure 8: The SDS-PAGE of Gel-filtration fractions of αB-crystallin protein and its Phospho-mimicking single mutants (AAE, AEA & EAA), double mutants (AEE, EAE & EEA) and triple mutants (AAA & EEE).

The higher OD protein fractions collected from αB-crystallin protein and its phosphorylation-mimicking mutants at around ~20 kDa corresponded to the proteins of our interest (Fig 8). Based on the gel picture, the fractions that showed less contamination and higher expression of the desired protein were pooled and centrifuged at 20,000 rpm for 30 min at 4^{o}C. The supernatant was transferred into a fresh tube.

The supernatant was then passed through a Q-Sepharose column (Bed volume: 20 ml), an anion exchange chromatography column. The protein purification procedure used was already standardized in the laboratory. We obtained αB-crystallin protein and the mutant proteins in the flow through.

The purity of proteins was checked again by running the fractions on a 12%SDS-polyacrylamide gel. In most instances, the proteins thus obtained were found to be pure

(Fig 9 and 10). However, if contamination was found in the protein preparations, they were subjected to another round of Ion-Exchange Chromatography.

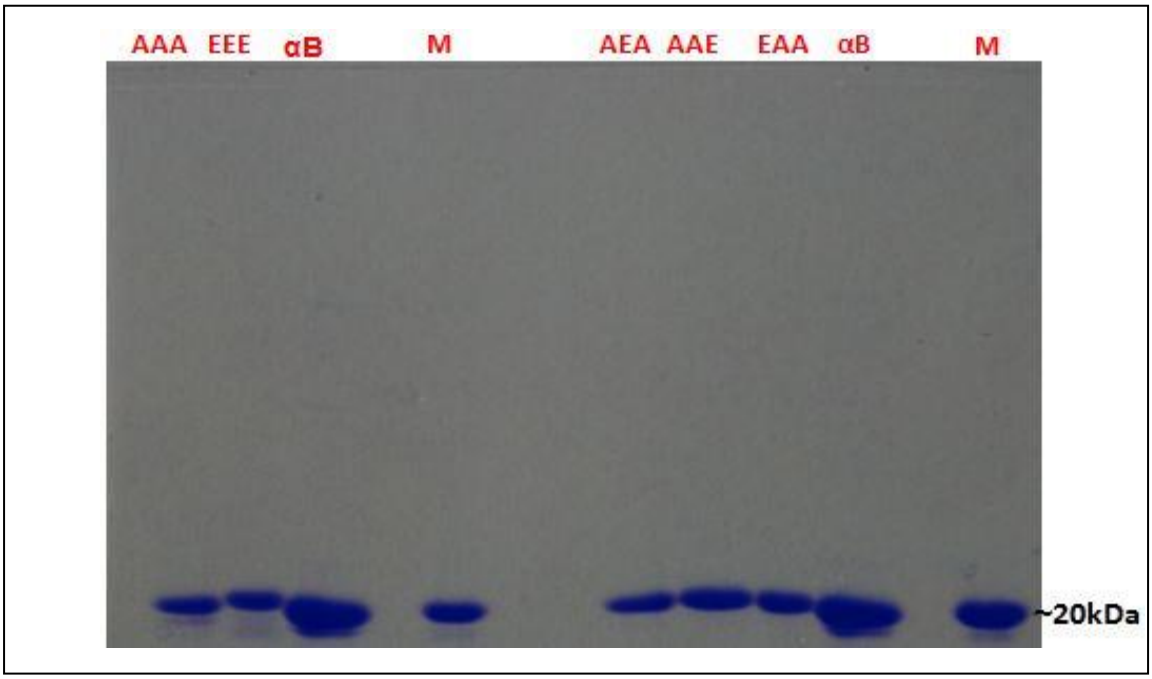

Figure 9: SDS-PAGE of Q-Sepharose column flow through for AAA, EEE, and AEA, AAE, EAA, αB. M represents pure αB-crystallin protein that serves as a Protein Marker.

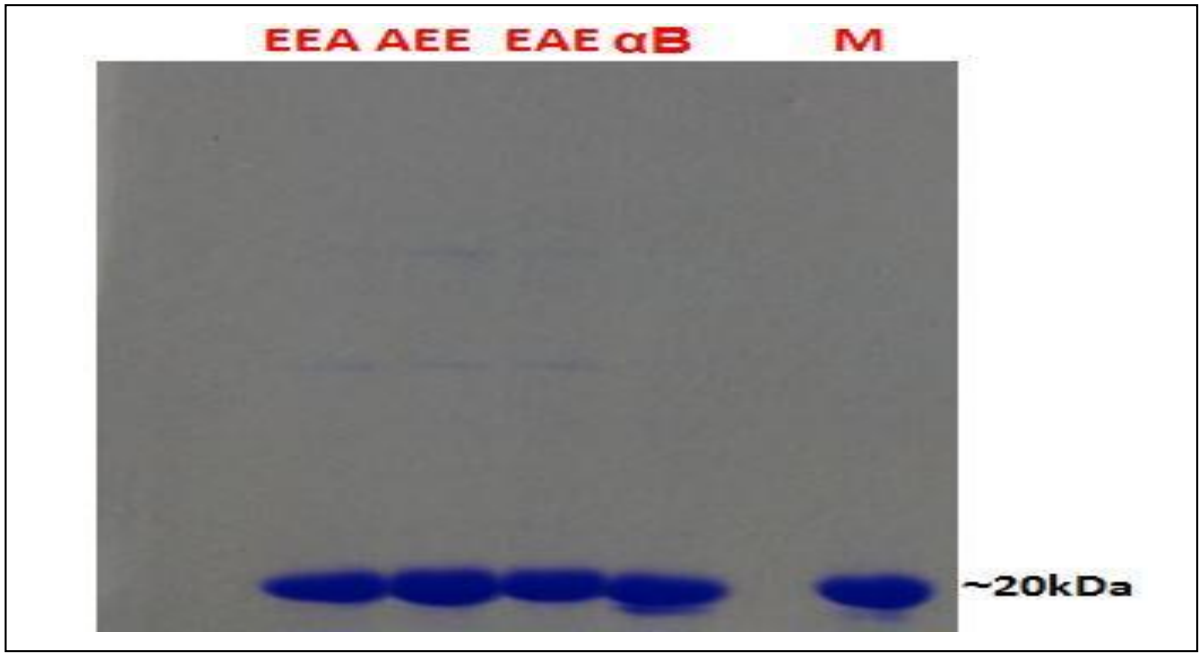

Figure 10: SDS-PAGE of Q-Sepharose column flow throughfor EEA, AEE, EAE and αB. M represents pure αB-crystallin protein that serves as a Protein marker.

From the gel pictures, it is evident that we could purify proteins to homogeneity. The proteins were then concentrated using Amicon Ultra-15 centrifugal filter units/ concentrators fitted with 30 kDa membrane filter. These centrifugal concentrator filters allow for protein concentration without compromising the yields.

The concentrated proteins in 1X TNE were filtered to remove any particulate matter and then were passed through a phosphate buffer equilibrated HiPrep 26/10 Desalting column fitted onto an FPLC machine (ÄKTA purifier 10) to achieve buffer exchange into Phosphate buffer.

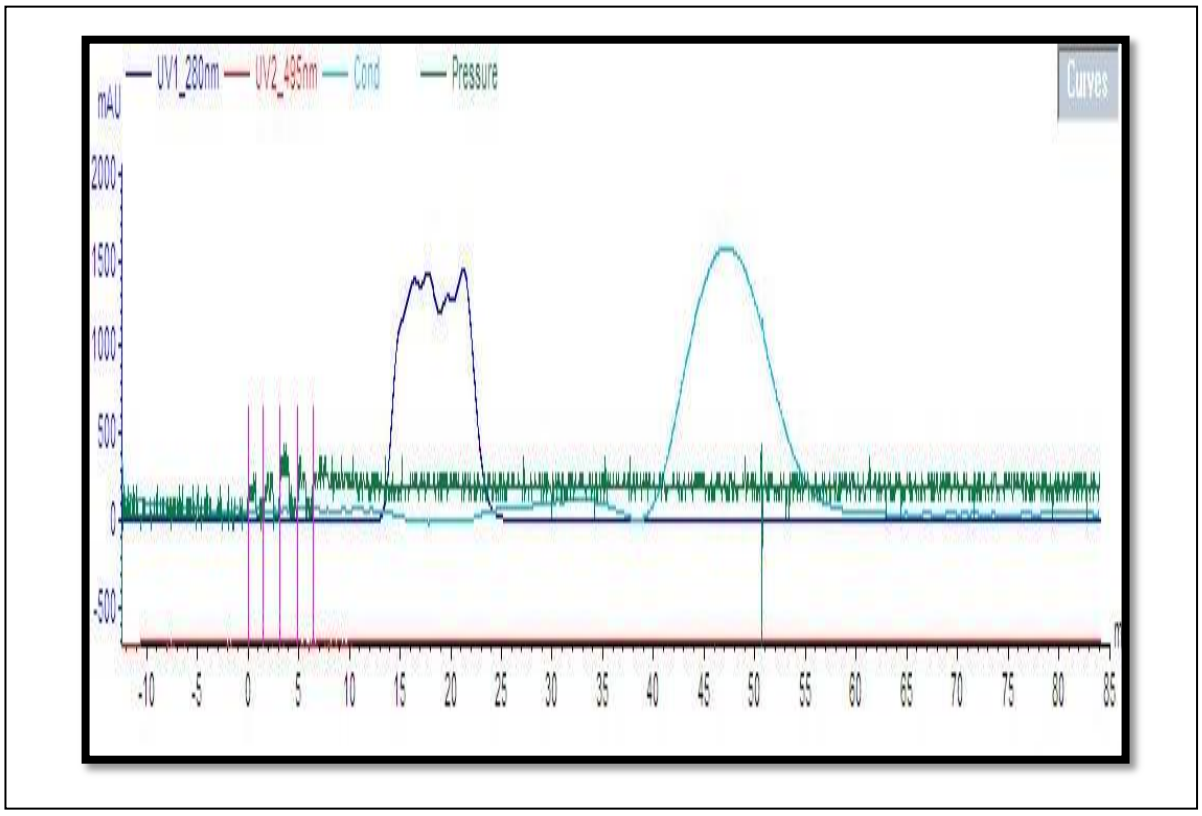

Figure 11: The above image shows a screen shot of the buffer exchange run. The initial blue peak is of the protein at Abs280 that elutes in the phosphate buffer and the later peak is the conductivity peak showing Tris-EDTA buffer.

The αB-crystallin protein and its phosphorylation-mimicking mutants were purified to their homogeneity employing different protein purification techniques.

1. As the first step of purification, the bacterial pellet (obtained from protein expression - induced transformed-BL21 culture) was lysed using lysozyme and ultrasonication. This step separated the proteins based on their solubility in a buffer at physiological pH.

2. The lysed sample was spun and the clear supernatant having the soluble proteins was subjected to "salting out" using ammonium sulfate. This step separated the proteins by their solubility in ammonium sulfate.

3. The ammonium sulfate pellets were resuspended in 1XTNE, and the filtered solution was subjected to gel filtration chromatography using S-300 column. This step separated the proteins based on their size. The fractions having the desired protein are pooled in a tube.

4. The gel filtration subjected sample was then passed through a Q-Sepharose column that removed the protein contaminants and also some amounts of DNA. This step separated proteins by their overall charge at the physiological pH.

The flow through from Q-Sepharose yielded a pure protein with negligible amounts of contaminants. Then, the proteins were concentrated, and the buffer was exchanged to PBS (20mM $Na.PO_4^-$ and 100mM NaCl).

4.2. Protein estimation

The protein in 20mM phosphate buffer (pH 7.2) containing 100mM NaCl was mixed in 10M urea solution such that the total concentration of urea becomes 8M urea and the absorbance at 280nm was measured. The proteins were thus estimated using a method described by Pace et al. (1995).

Table 1: Amount of protein in milligrams obtained from 1liter cell culture:

Protein	***Total yield of protein per litre of cell culture (mg/liter)***
αB-crystallin protein	12
AAE	10
AEA	11
EAA	12
AEE	8
EAE	9
EEA	7
AAA	18
EEE	16

4.3 FITC-tagging of proteins

FITC stock solution (1mg/ml) was made in DMSO and stored in an aluminium foil-wrapped 1.5 ml micro centrifuge tube to prevent exposure to light. FITC (50 µl) stock solution was added to 1 ml of 1.5mg/ml protein and the tube was incubated overnight on a rotating disc in the cold room (4^{o}C). The following day, the FITC-tagged protein solution was loaded onto a HiPrep^{TM} 26/10 desalting column to get rid of the unbound FITC. Absorbance was recorded at A280 and A495 for the entire run (Fig 12). The absorbance of FITC-tagged protein was measured in a Shimadzu Spectrophotometer (UV2600) at 495 nm for FITC and 280 nm for protein.

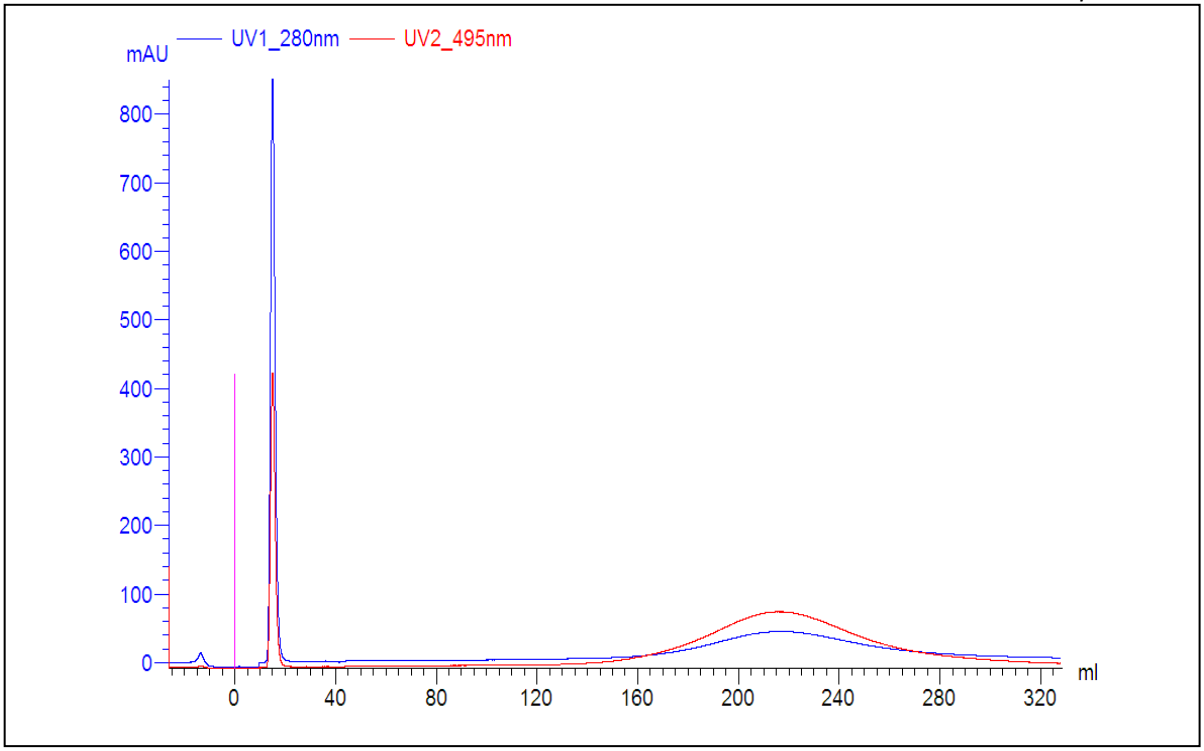

Figure 12: Screen shot image of the separation of FITC tagged αB-crystallin protein from unbound FITC using a desalting FPLC (fast protein liquid chromatography) column. The sharp initial overlapping peaks indicate that the protein is tagged with FITC and the later peaks indicate that the protein is tagged with FITC and the later peak shows unbound FITC.

4.4 Biophysical characterization of proteins

4.4.1 Dynamic light scattering (DLS):

This technique is one of the most popular methods used to determine the size of particles. Shining a monochromatic light beam, such as a laser, onto a solution with spherical particles in Brownian motion causes a Doppler Shift when the light hits the moving particle, changing the wavelength of the incoming light. This change is related to the size of the particle. It is possible to compute the size distribution and give a description of the particle's motion in the medium, measuring the diffusion coefficient of the particle and using the autocorrelation function.

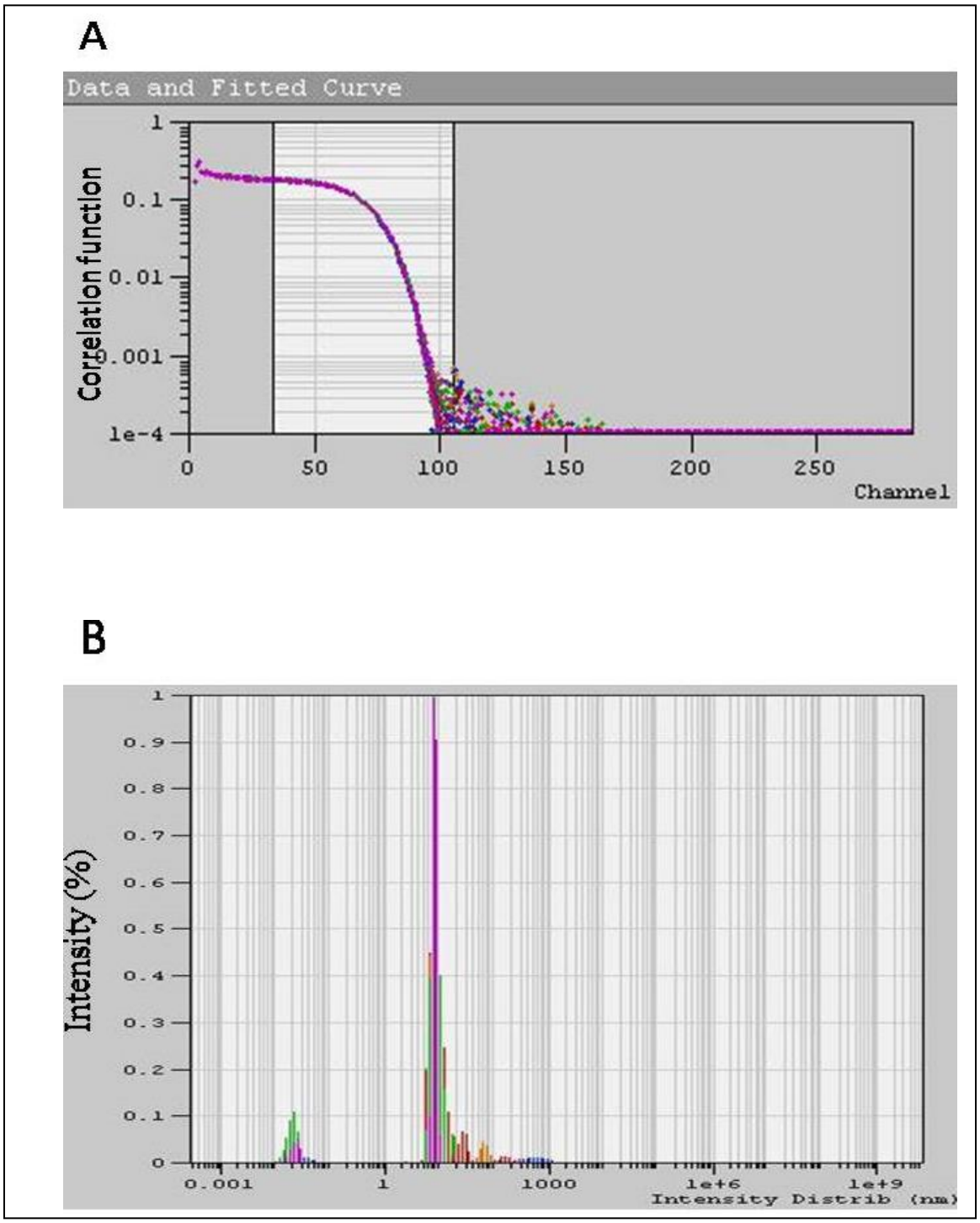

Figure 13: (A) Autocorrelation function (B) Size distribution graph of αB-crystallin protein using DLS

Table 2: The Hydrodynamic radii of αB-crystallin protein αB-crystallin protein wild type, triple mutants (EEE &AAA), double mutants (EEA, EAE & AEE) and single mutants (AAE, AEA & EAA).

protein	***mean hydrodynamic radius (r_{HYD}) in nm of all protein in phosphate buffer solution***
αB-crystallin protein	8.2
AAE	6.8
AEA	7.2
EAA	7.1
AEE	6.2
EAE	7.1
EEA	7.7
AAA	10.5
EEE	9.6

Descending order of the hydrodynamic radii of αB-crystallin protein and its phosphorylation-mimicking mutants is as follows: **AAA>EEE> αB> EEA> AAE> EAE>EAA>AEA>AEE**

The Hydrodynamic radius (R_h) for wild-type αB-crystallin protein was found to be 8.2 nm. This is agreement with previously reported Rh values of αB-crystallin protein. $R_h$values of phospho-mimics of αB-crystallin protein protein were found to range from 6-11nm.The 3A mutant of αB-crystallin protein exhibited a higher size (~11nm). The hydrodynamic radii of the AEA, EAA, EAE and EEA mutants were almost the same (i.e ~7nm).

4.4.2 Sedimentation velocity

The sedimentation coefficients of αB-crystallin protein and its phosphorylation-mimicking mutants, AAE, AEA, EAA, AEE, EAE, EEA, AAA, and EEE were obtained by performing sedimentation velocity experiments on a Beckman Coulter Proteome Lab XL-I Protein Characterisation System at 28000 rpm. The sedimentation coefficient of wild-type αB-crystallin protein was 17.835 S, while that of the mutant proteins was found to be lower as expected (Table 3), indicating that the oligomeric size of the mutant protein is low as a consequence of phosphorylation. Several other studies have also indicated that phosphorylation of αB-crystallin protein, as well as that of other sHsps such as Hsp27, leads

to a reduction in the oligomeric size. The sedimentation coefficients and the respective molecular weights of the species were derived using "sedfit" software.

The sedimentation coefficient distribution c(s) vs Sedimentation coefficient [S] plots for αB crystallin and its various phospho-mimicking mutants are shown in Fig 14 and 15.

Table 3: Sedimentation coefficients, Molecular weights and the oligomer sizes of αB-crystallin protein wild type, triple mutants (EEE &AAA), double mutants (EEA, EAE & AEE) and single mutants (AAE, AEA & EAA). – Represents undefined.

Protein	**Sedimentation coefficient $S_{20,w}$**	**Molecular weight (kDa)**	**Oligomeric size (Approx.Number of subunits)**
αB-crystallin protein	17.835 S	457.230	22
AAE	16.393 S	402.942	20
AEA	15.859 S	383.397	18-20
EAA	-	-	-
AEE	12.546 S	350.386	18
EAE	11.851 S	334.434	16-18
EEA	12.375 S	341.983	16-18
AAA	16.154 S	394.154	20
EEE	9.830 S	187.104	8-10

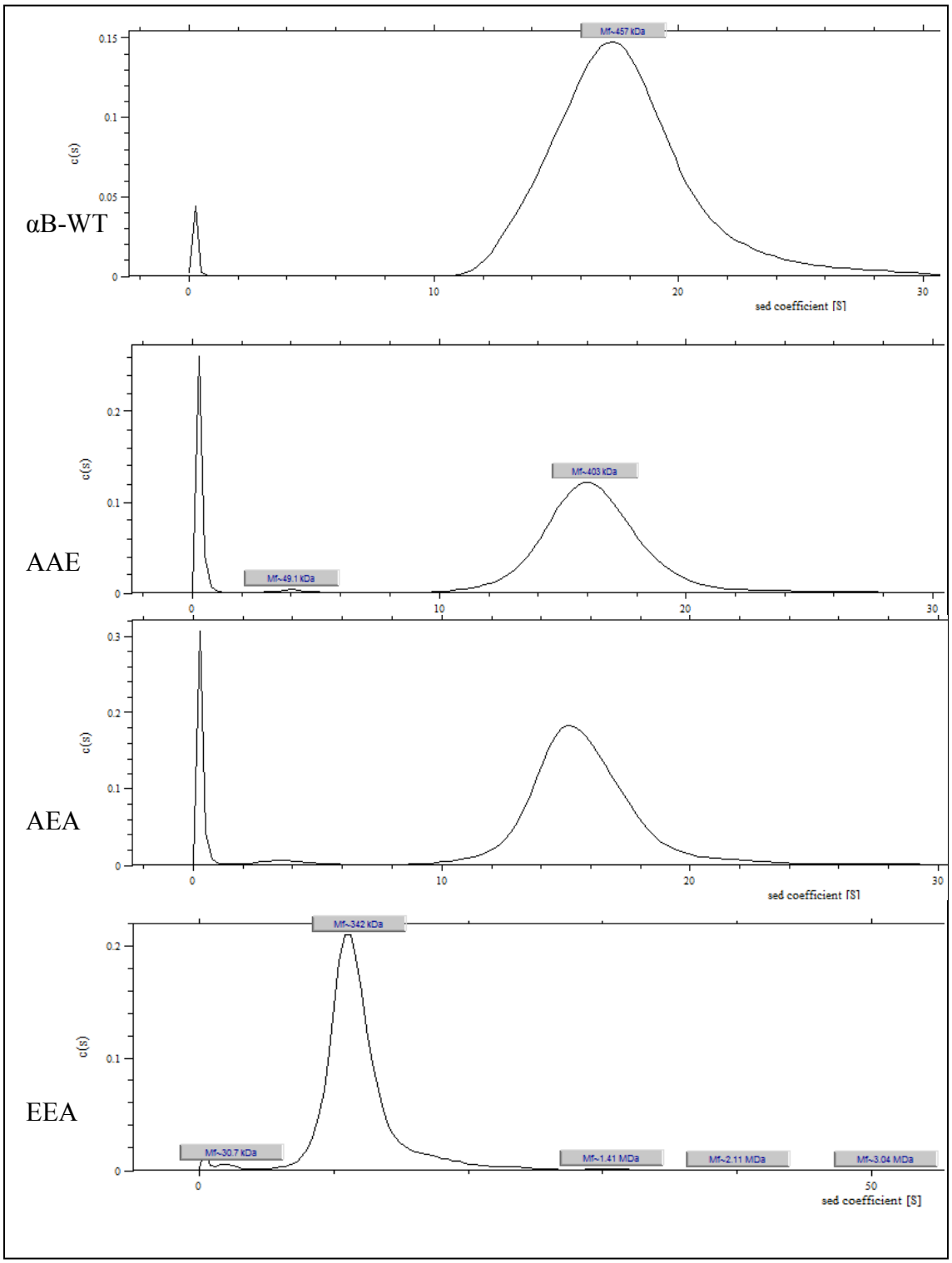

Figure 14: Sedimentation coefficient distribution c(s) graphs of aB-Crystallin αB-crystallin protein wild type, double mutants (EEA) and single mutants (AAE & AEA).after Sedimentation velocity Analysis using Sedfit.

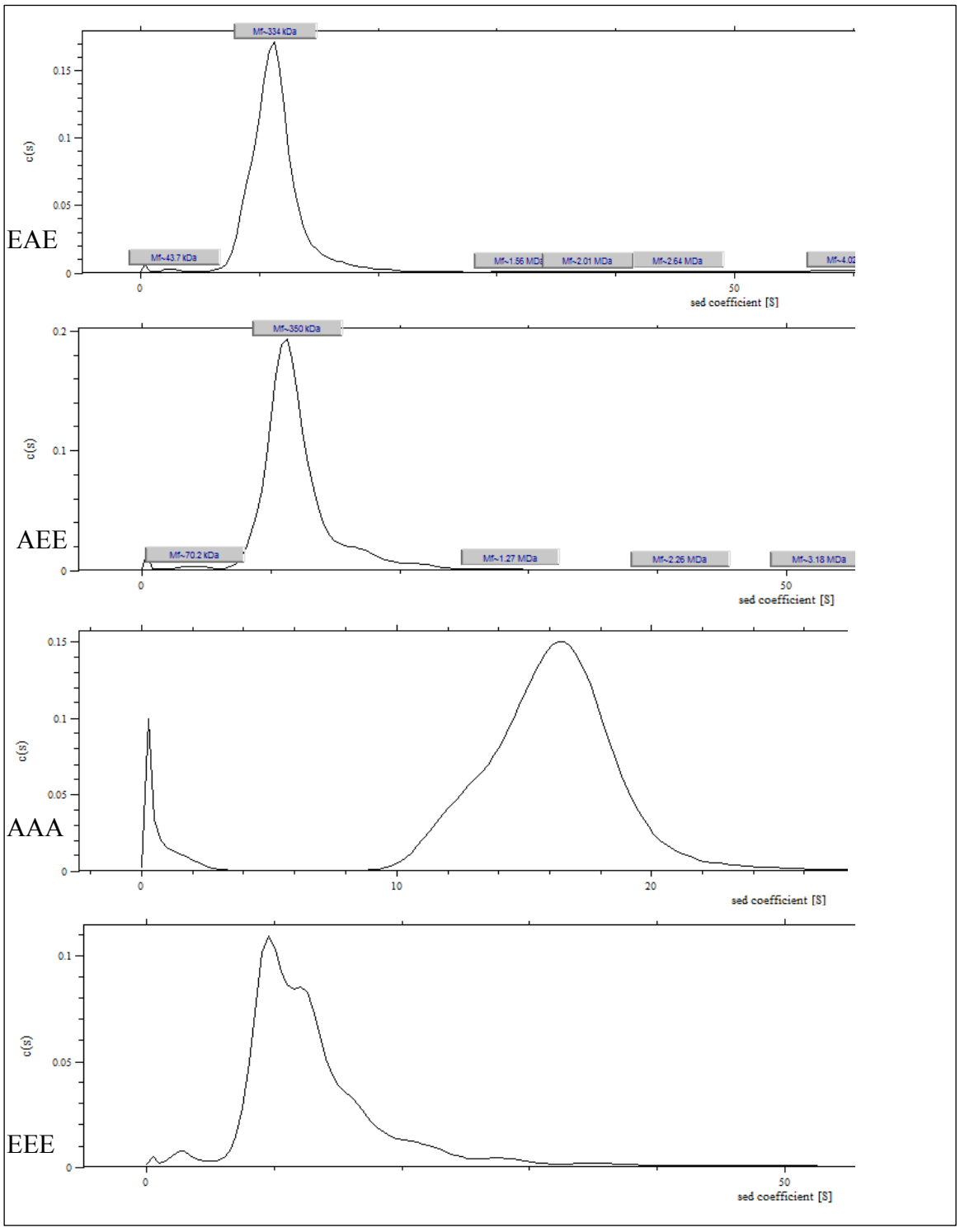

Figure 15.Sedimentation coefficient distribution c(s) graphs of double mutants (EAE & AEE) and triple mutants (AAA and EEE), after Sedimentation velocity Analysis using Sedfit.

The descending order of sedimentation coefficient of αB-crystallin protein and its phospho-mimicking mutants are as follows: **EAE>AEE>EEA> αB>AAE>AAA>AEA>EEE**

As shown from table 3, there is a significant decrease in the oligomeric size of the phospho-mimicking mutants compared to the wild-type αB-crystallin protein.

4.5. **Chick-embryo chorio allantoic membrane assay (CAM) to study angiogenesis**

The role of αB-crystallin protein and its S-59 phosphorylated form in angiogenesis is one of the recent highlights of the physiological effect of sHSPs. There is previous evidence that phosphorylated forms of αB-crystallin protein co-localize with EGF-2/VEGF-A and phosphorylation of αB-crystallin protein increases during hypoxic conditions along with VEGF-A/EGF-2. However, the exact biochemical mechanism of how αB-crystallin protein and its phosphorylated forms promote angiogenesis is unknown. To study the effect of phosphorylation on angiogenesis and correlate it with the chaperone-like activity of αB-crystallin protein, we chose to work on an in-ovo model using chicken eggs (as mentioned in Materials and methods).

For this study “0” day fertilized eggs were procured from Directorate of Poultry Research, Rajendranagar, Hyderabad. After 72hr incubation in Hatchery incubator, the developing eggs were used for CAM assay for checking the effect of αB-crystallin protein and its different phospho-mimicking mutants (1µg/mL) on angiogenesis. VEGF-A protein (20ng/mL) was used as a positive control, and the negative control was maintained with phosphate buffer. Images of the selected fields at 0hr and 4 hrs were taken through the NIKON SMZ75T stereo microscope attached with a camera at 2X. The images were later analyzed for various parameters such as the change in length, junctions (branching points) and size (diameter) of the blood vessels in both treated and control samples using, AngioQuant Software. The graph was plotted with respect to time using the GraphPad Prism v5.01 (California USA) software (www.graphpad.com).

Single mutants of αB-crystallin protein in CAM assay:

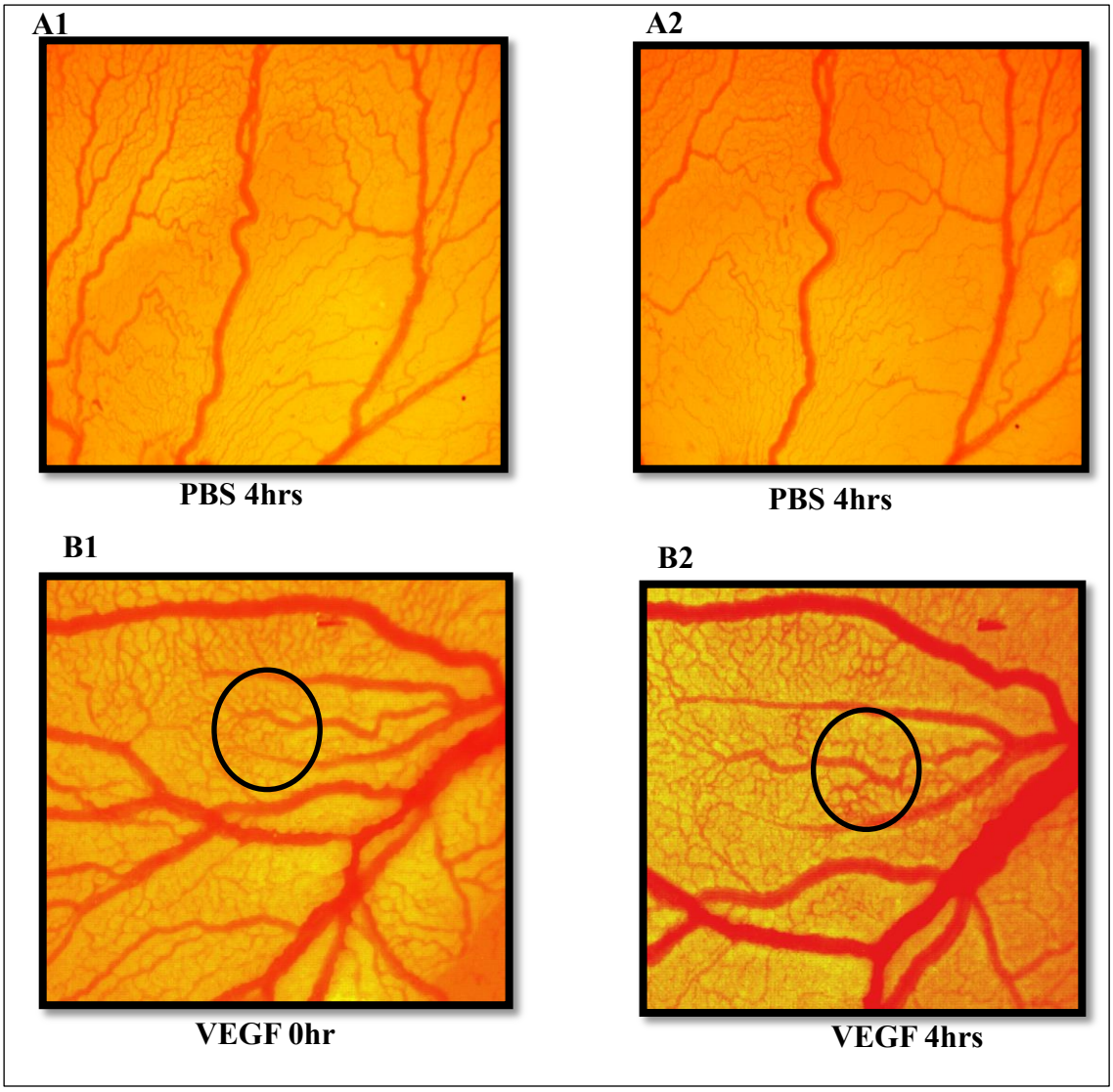

Figure 16: CAM assay images A1 (0hr) & A2 (4hrs) with treatment of negative control PBS and B1 (0hr) & B2 (4hrs) after treatment of protein (VEGF (20 ng) in the localized area (circle) for the measurement of size, length and junction. These pictures are best representative among nine observations of each experiment.

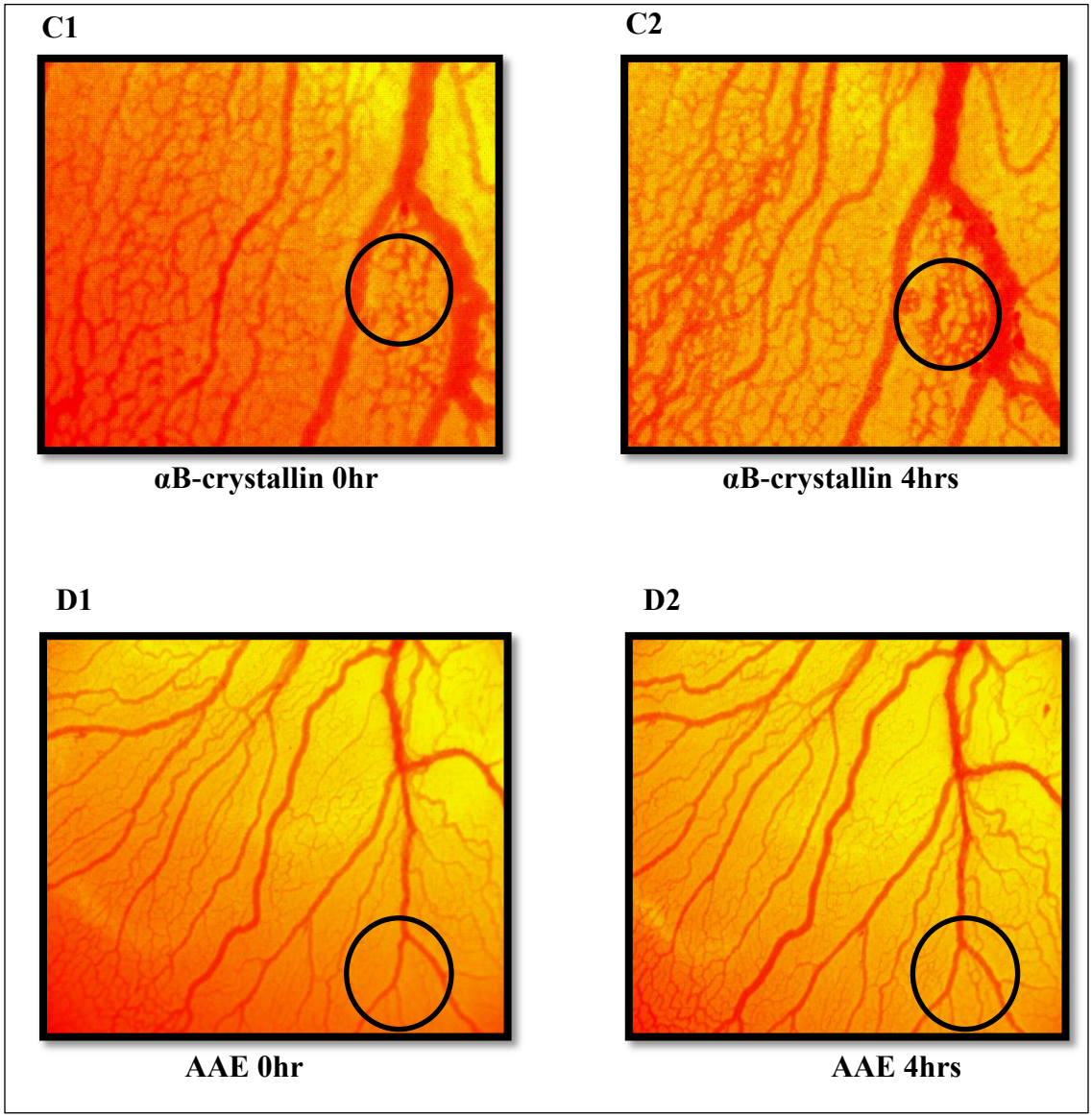

Figure 17: CAM assay images C1 (0hr) & C2 (4hrs) of wild type αB-crystallin protein and D1 (0hr) & D2 (4hrs) of single mutants (AAE- αB-crystallin protein) using only 1 µg each protein in the localized area (circle) for the measurement of size, length and junction. These pictures are best representative among nine observations of each experiment.

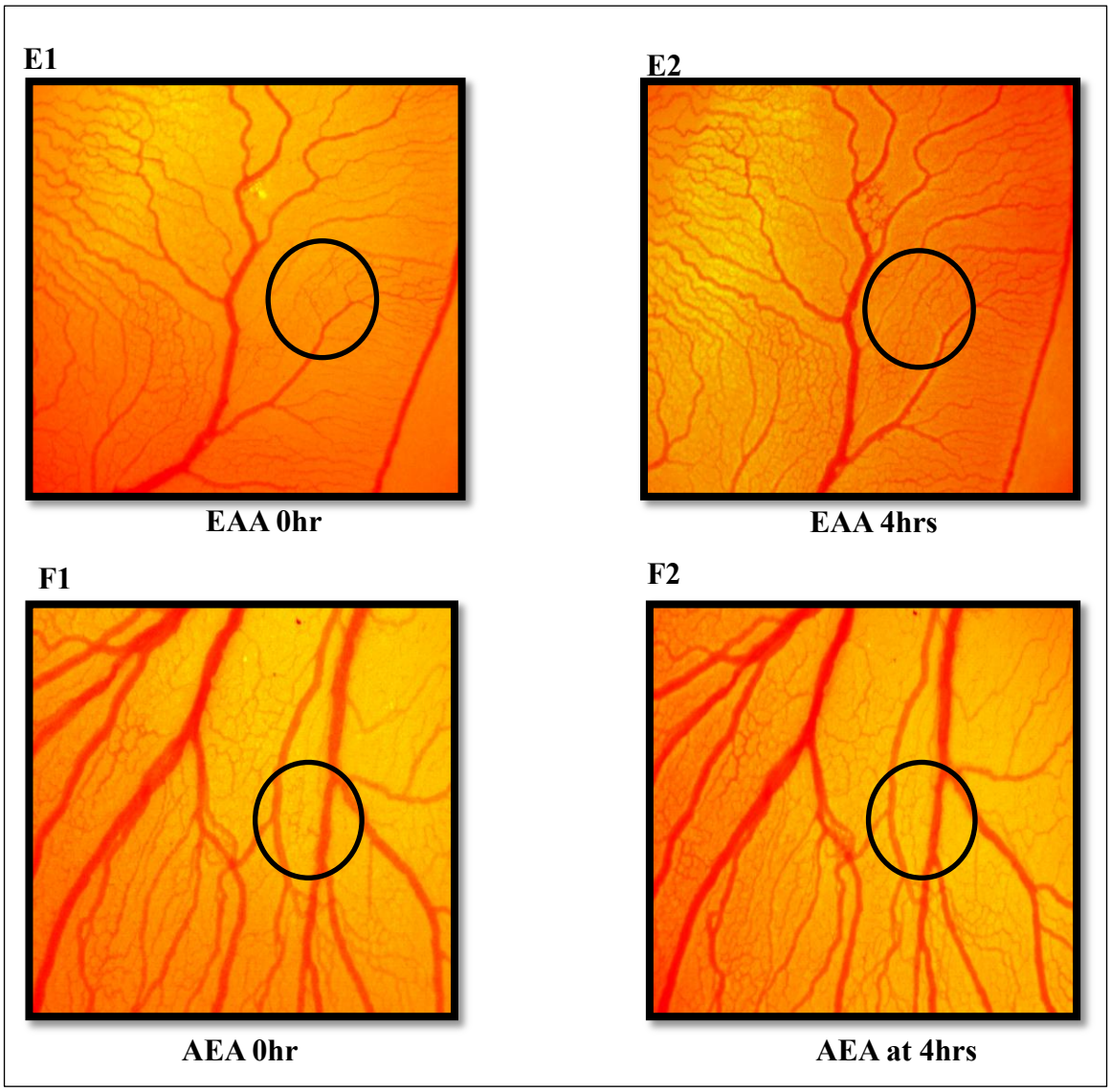

Figure 18: CAM assay images E1 (0hr) & E2 (4hrs) of single mutant EAA-αB-crystallin and F1 (0hr) & F2 (4hrs) of single mutants AEA- αB-crystallin using only 1 µg each protein in the localized area (circle) for the measurement of size, length, and junction. These pictures are best representative among nine observations of each experiment.

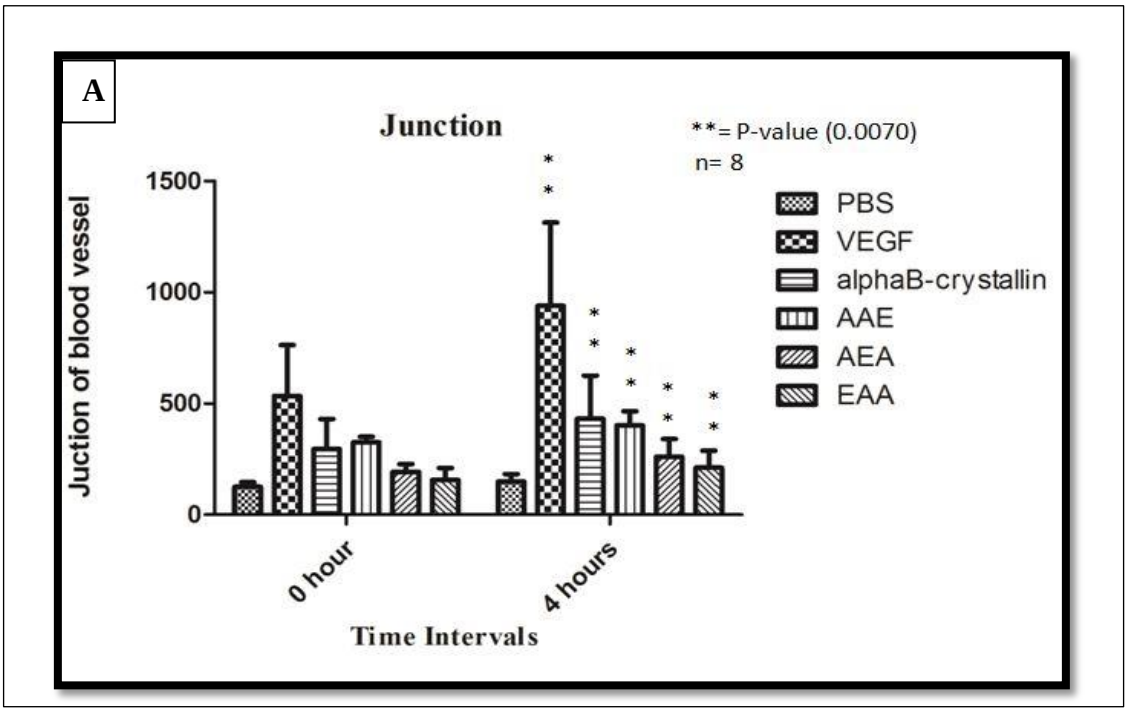
A
Junction
**= P-value (0.0070)
n= 8
Juction of blood vessel
1500
1000
500
0
0 hour
4 hours
Time Intervals
PBS
VEGF
alphaB-crystallin
AAE
AEA
EAA

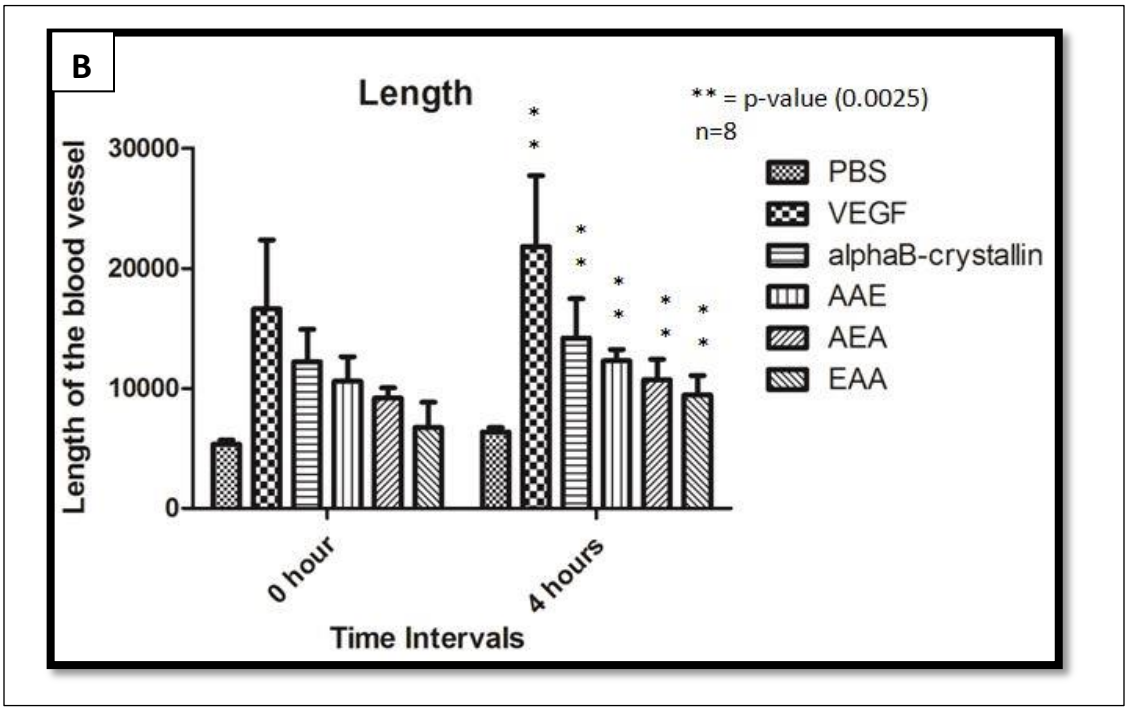
B
Length
** = p-value (0.0025)
n=8
Length of the blood vessel
30000
20000
10000
0
0 hour
4 hours
Time Intervals
PBS
VEGF
alphaB-crystallin
AAE
AEA
EAA

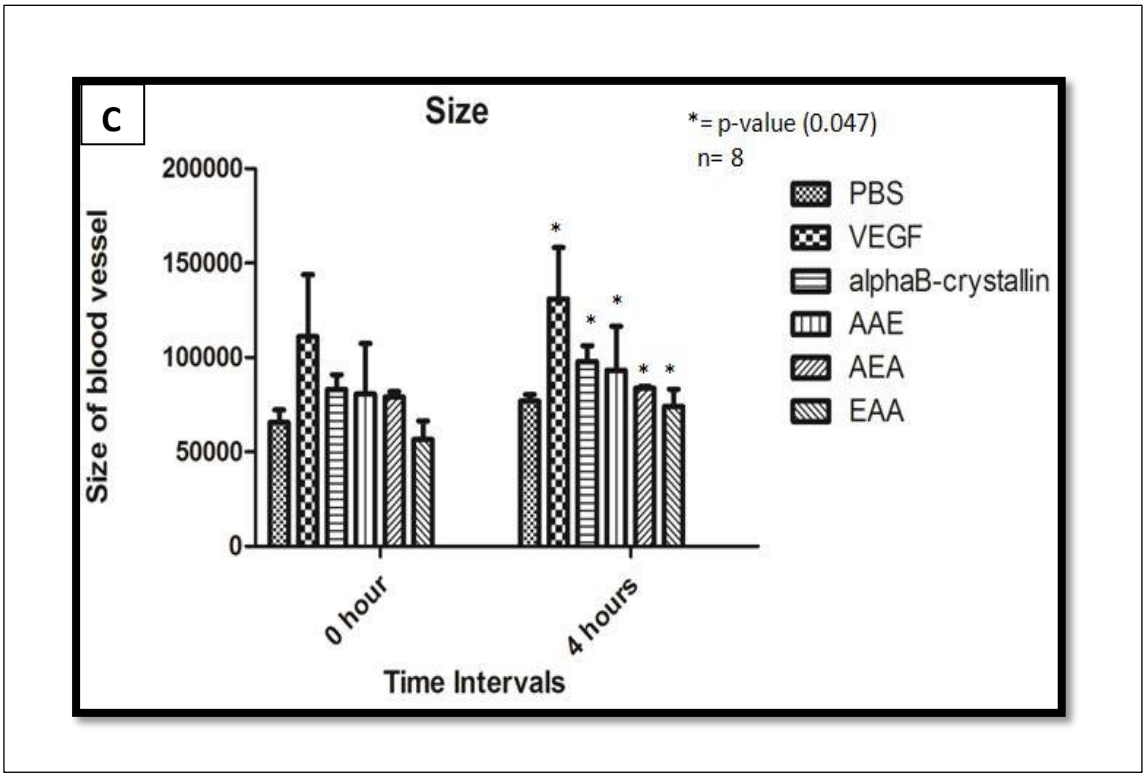

Figure 19: Graphs showing (A) junctions (B) length and (C) size of blood vessels at 0 hrs and 4hrs after treatment with αB-crystallin protein and its single phosphomimicking mutants. The X- and Y-axis represent time intervals and the arbitrary units given by the Angioquant software v1.33 2005 respectively. The data is given in appendix 5.1.

CAM assay results analyzed from the AngioQuant software indicated that treatment of αB-crystallin protein and its single phosphomimicking mutants (AAE-S59E, AEA-S45E and EAA-S19E) showed a significant increase in angiogenesis as evaluated by the increase in length (0.0025), size (p value 0.047) and junctions (p value 0.007) of blood vessels compared with the PBS-treated control (Fig 16, 17 and 18). VEGFs used as positive control gave highest angiogenesis in reference with the wt-αB crystallin and all single mutants of wild type. Among the three single phosphomimics, AAE brought about the highest increase in size, length, and junctions, which, however was less than that exhibited by αB-crystallin protein.

Double mutants of αB-crystallin protein in CAM assay:

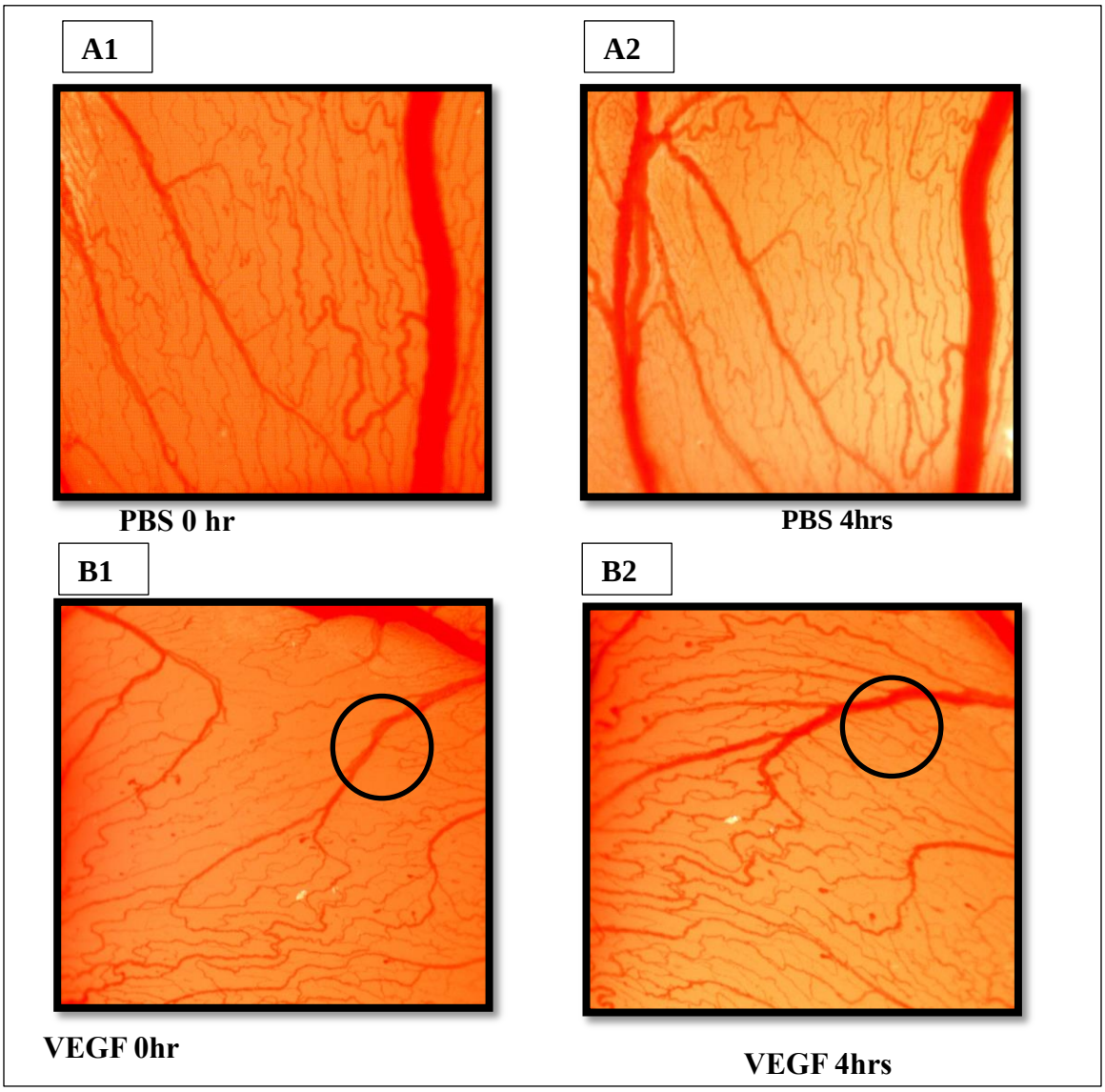

Figure 20: CAM assay images A1 (0hr) & A2 (4hrs) of negative control PBS (1µl) and B1 (0hr) & B2 (4hrs) of positive control VEGF (20µg) protein in localized area (circle) for the measurement of size, length and junction. These pictures are best representative among nine observations of each experiment.

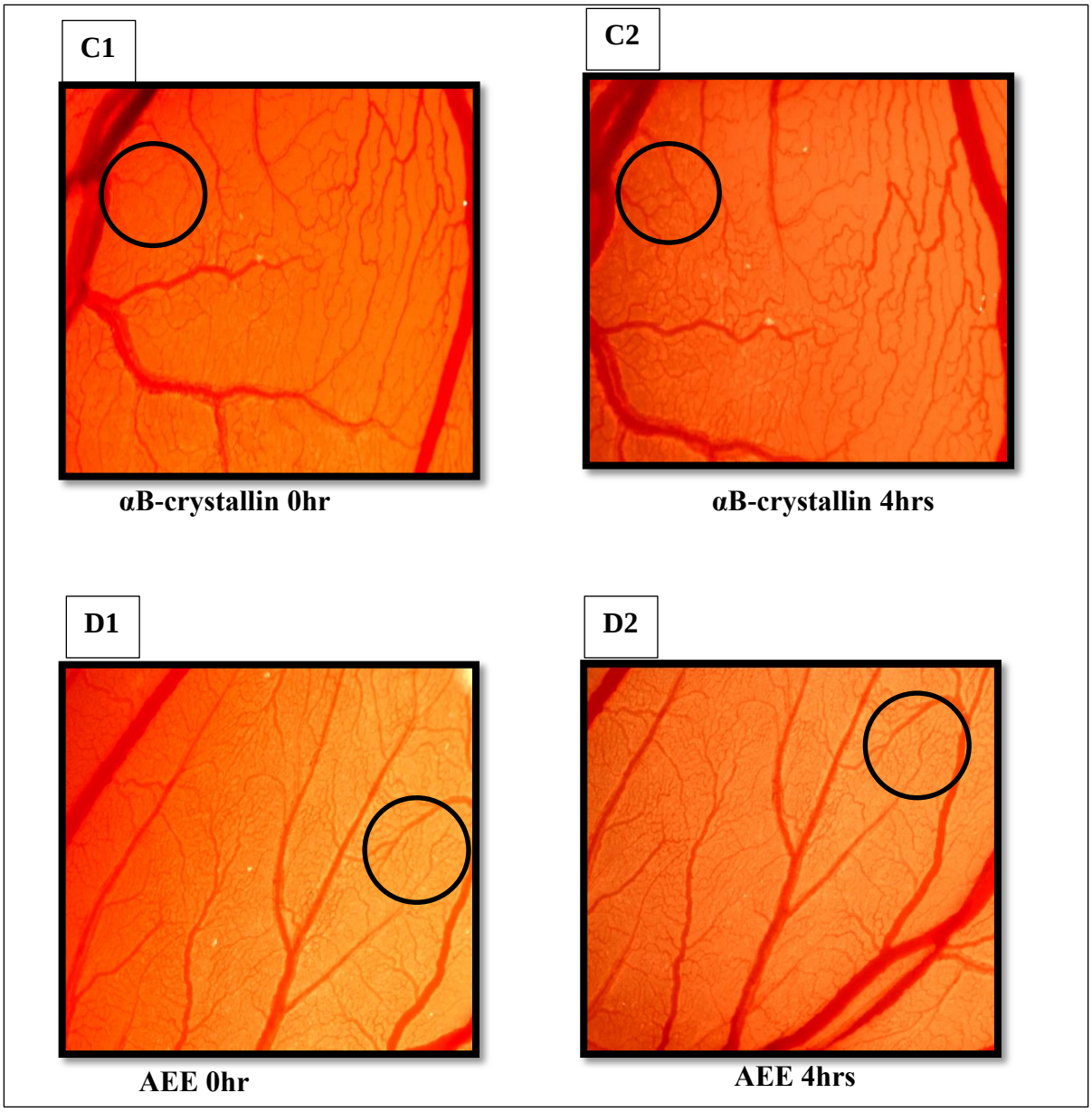

Figure 21: CAM assay images C1 (0hr) & C2 (4hrs) of wild type αB-crystallin and D1 (0hr) & D2 (4hrs) of double mutants (AEE- αB-crystallin) using only 1 µg each protein in localized area (circle) for the measurement of size, length and junction. These pictures are best representative among nine observations of each experiment.

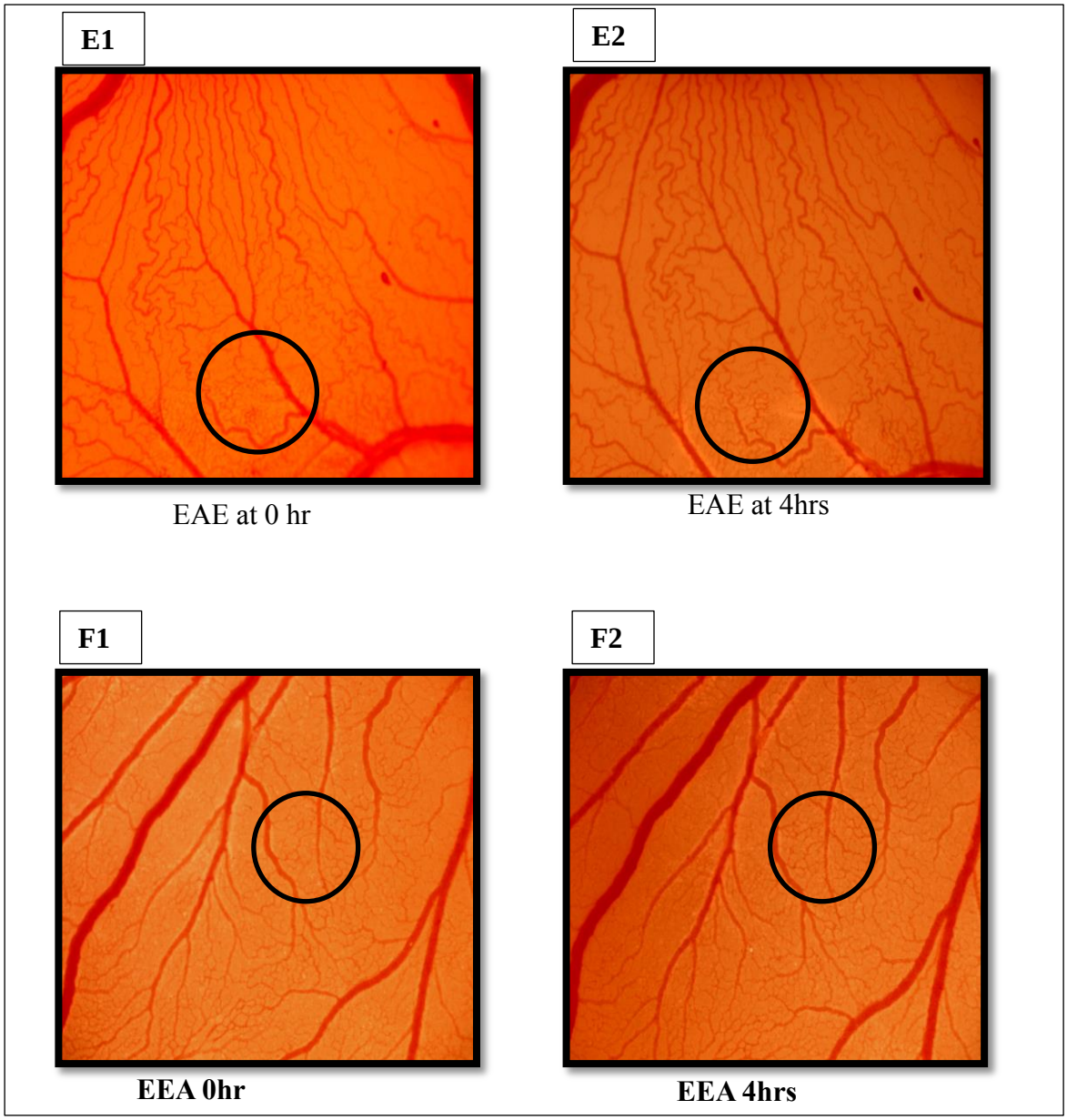

Figure 22: CAM assay images E1 (0hr) & E2 (4hrs) of double mutant EAE αB-crystallin and F1 (0hr) & F2 (4hrs) of double mutants EEA- αB-crystallin using only 1 µg each protein in localized area (circle) for the measurement of size, length and junction. These pictures are best representative among nine observations of each experiment.

.

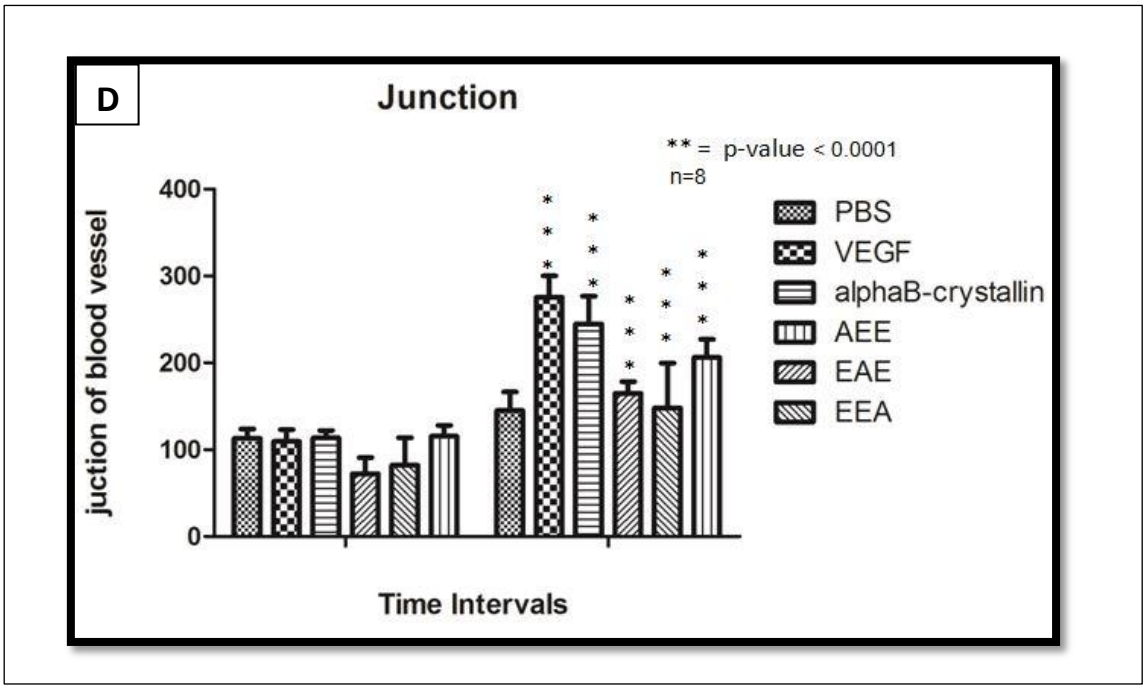
D
Junction
** = p-value < 0.0001
n=8
juction of blood vessel
400
300
200
100
0
Time Intervals
PBS
VEGF
alphaB-crystallin
AEE
EAE
EEA

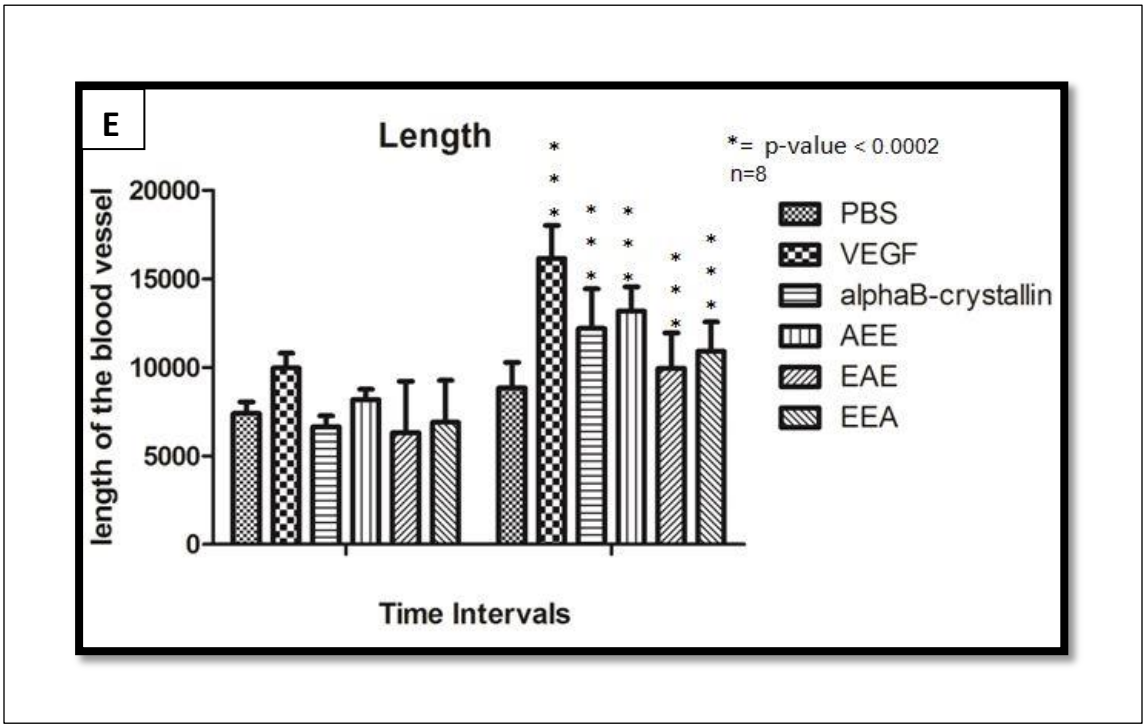
E
Length
*= p-value < 0.0002
n=8
length of the blood vessel
20000
15000
10000
5000
0
Time Intervals
PBS
VEGF
alphaB-crystallin
AEE
EAE
EEA

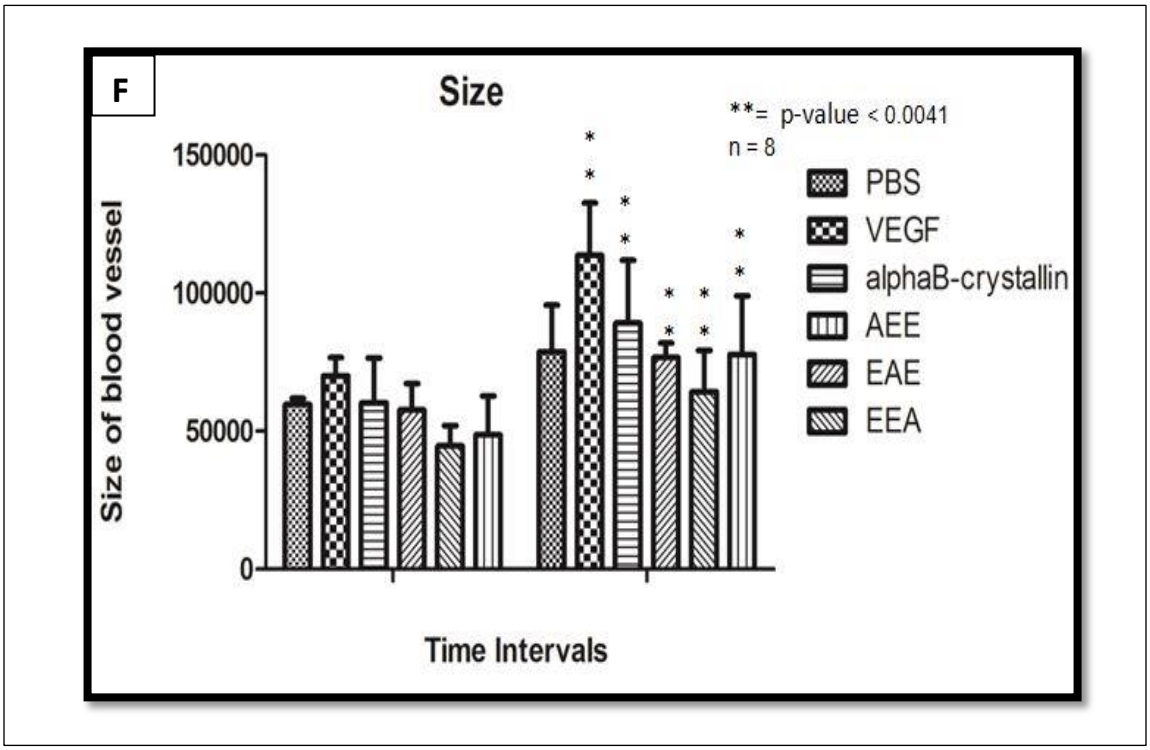

Figure 23: Graphs showing (D) junctions (E) length and (F) size of blood vessels at 0 hrs and 4hrs after treatment with αB-crystallin protein and its single phosphomimicking mutants. The X- and Y-axis represent time intervals and the arbitrary units given by the Angioquant v1.33 2005 software respectively. The data are given in appendix 5.2.

As observed earlier, αB-crystallin protein showed a significant increase in the junctions, size, and length of the blood vessels compared with the control (PBS treated) with single mutats of αB-crystallin. The double mutants (AEE-S45E & S59E, EAE-S19E & S59E and EEA-S19E & S45E) also showed a significant increase in all the parameters indicating angiogenesis, suggesting that treatment of αB-crystallin protein and its double phospho-mimicking mutants induces angiogenesis (Fig 20, 21 and 22). VEGF is positive control, significantly helped in formation of new blood vessel in mammalian cell increasing length (p value 0.0002), size (p value 0.0041) and junction (p value 0.0001) of blood vessels (Fig 22). Wt-αB-crystallin showed significant increase in angiogenesis (length, size and junction) compare with respective control PBS and other three double mutants but less than VEGF (Fig 22).

Among the three (EEA, EAE and AEE) mutants, AEE induced significant increase in angiogenesis where as EAE and EEA comparatively with other double mutants indicated moderate effect on angiogenesis.

Triple mutants of αB-crystallin in CAM assay:

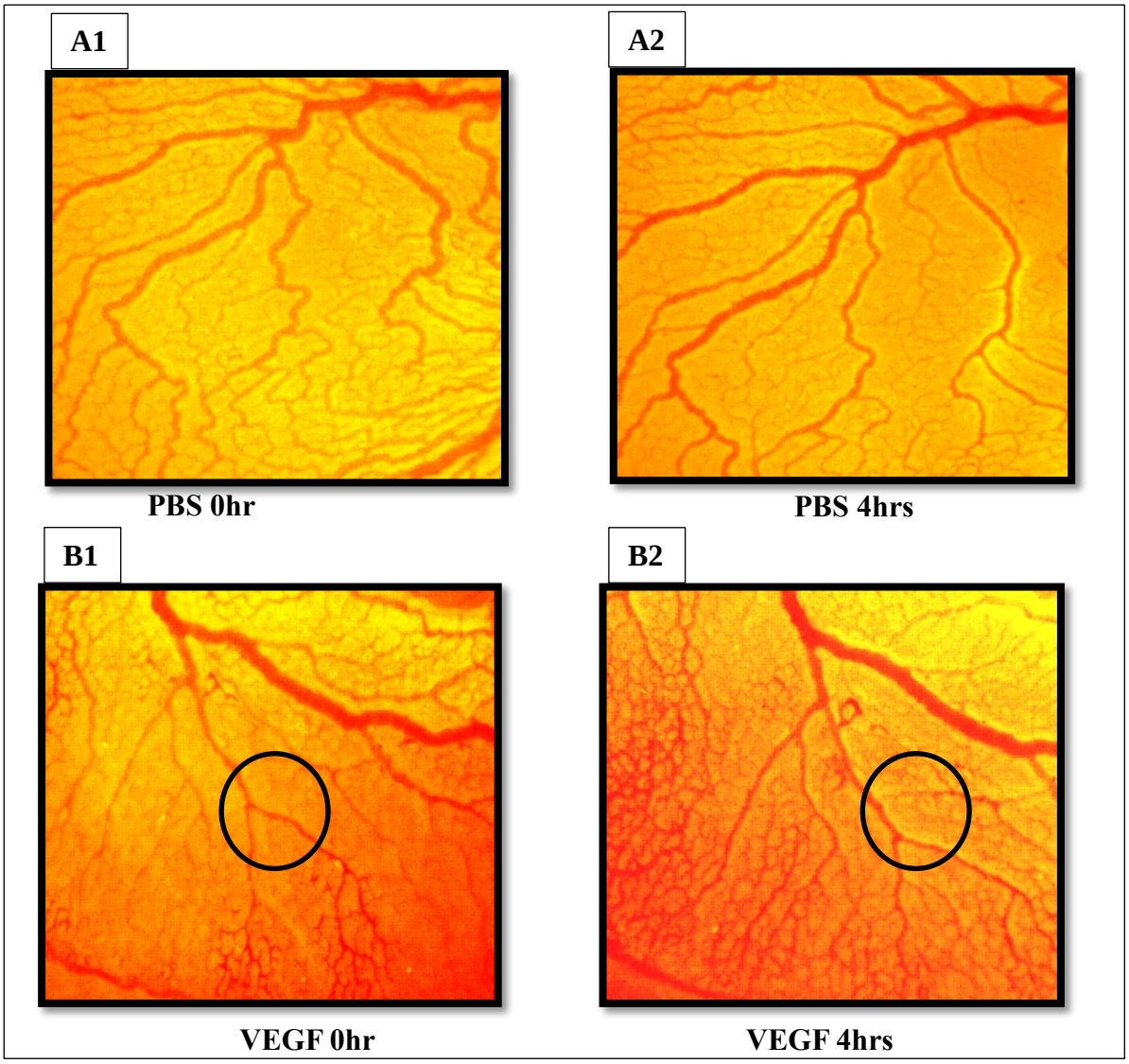

Figure 24: CAM assay images A1 (0hr) & A2 (4hrs) of negative control PBS and B1 (0hr) & B2 (4hrs) of positive control VEGF (20ng) protein in localized area (circle) for the measurement of size, length and junction. These pictures are best representative among nine observations of each experiment.

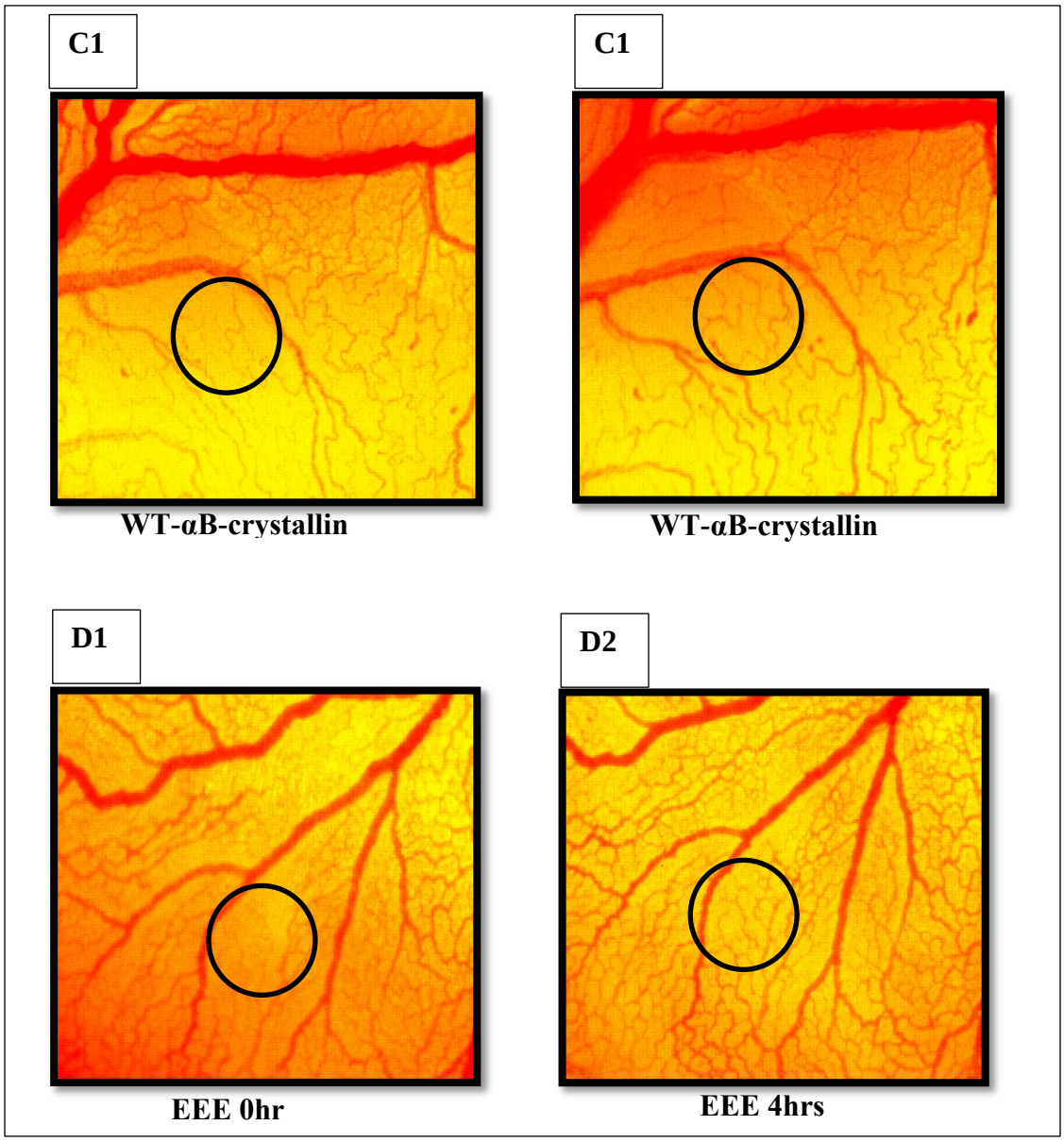

Figure 25: CAM assay images C1 (0hr) & C2 (4hrs) of WT-αB-crystallin and D1 (0hr) & D2 (4hrs) of triple mutant (EEE) protein each with 1µg in localized area (circle) for the measurement of size, length and junction. These pictures are best representative among nine observations of each experiment.

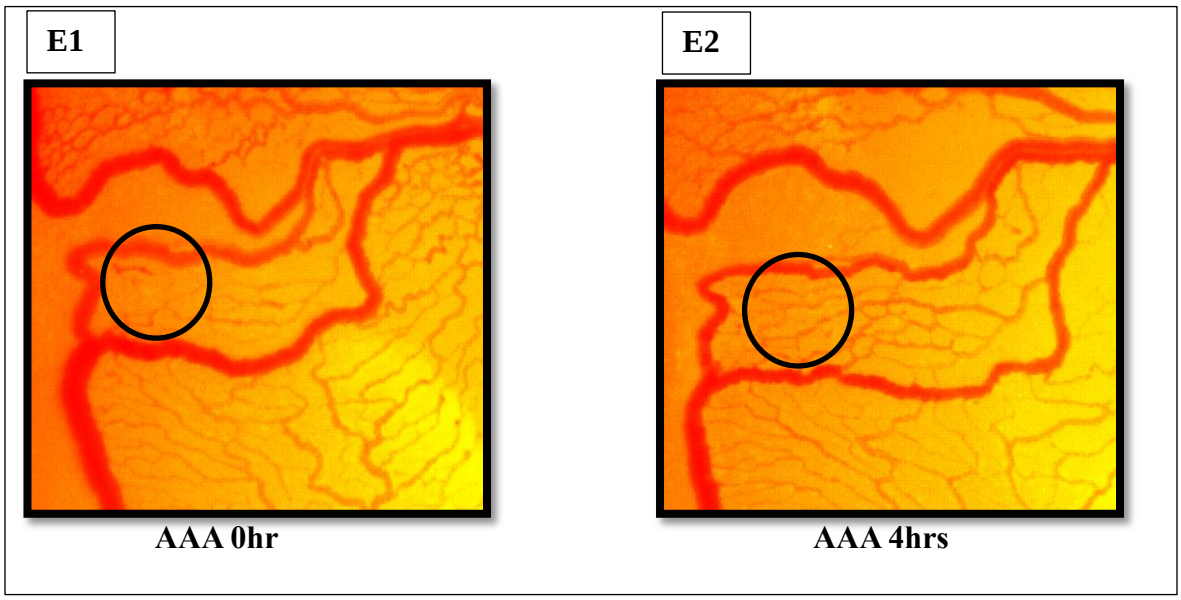

Figure 26: CAM assay images E1 (0hr) & E2 (4hrs) of triple mutant (AAA-αB-crystallin) protein with 1µg in the localized area (circle) for the measurement of size, length and junction. These pictures are best representative among nine observations of each experiment.

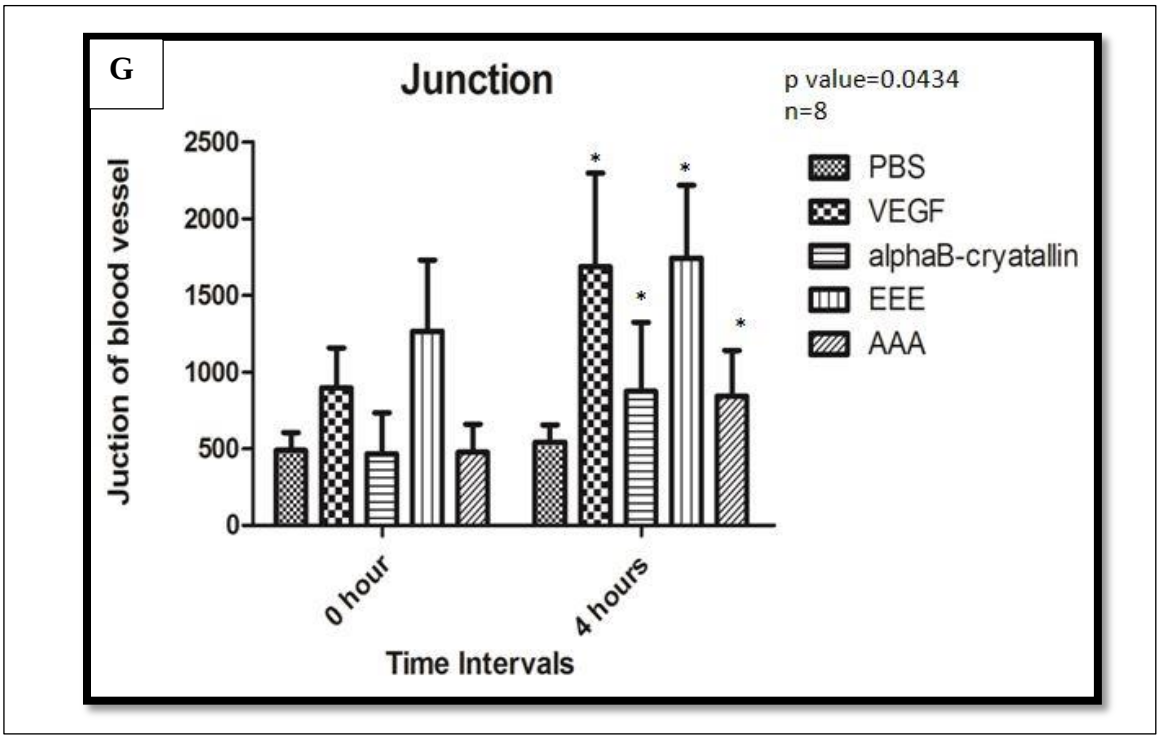

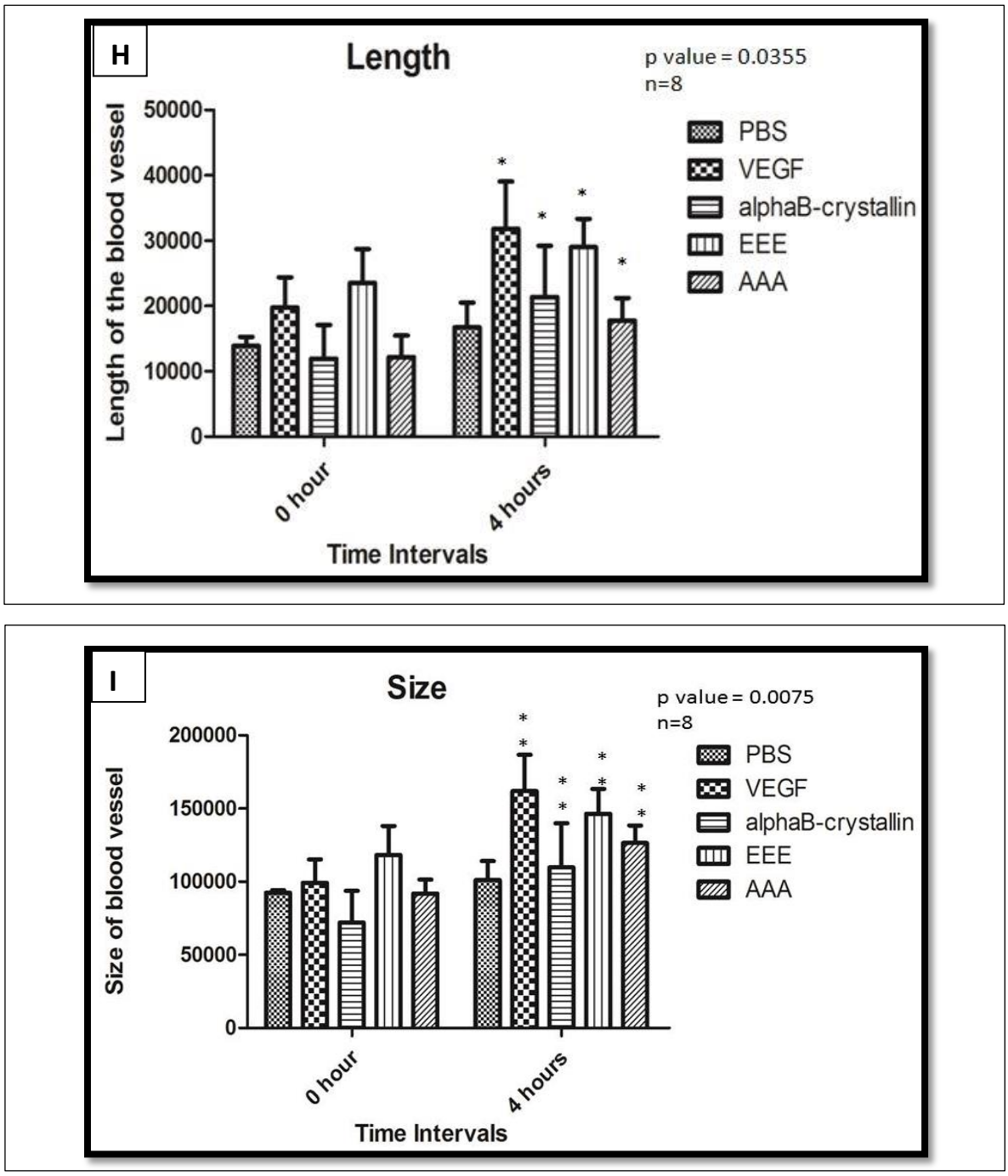

Figure 27: Graphs showing (G) junctions (H) length and (I) size of blood vessels at 0 hrs and 4hrs after treatment with αB-crystallin and its triple mutants. The X- and Y-axis represent time intervals and the arbitrary units given by the angioquant V1.33 2005 software respectively. The data are given in appendix 5.3.

From the above graph, it is evident that αB-crystallin protein, and its triple mutants (EEE-S19E, S45E & S59E, and AAA-S19A, S45A & S59A) showed a significant increase in the junctions (p value 0.0434), size (p value 0.0075 and length (p value 0.0355) of the blood vessels in the CAM assay compared with the respective PBS-treated control group. Although VEGF a positive control gave contributed more in formation of vascular in Chick chorio allantoic membrane, EEE also gave competitive effect on membrane with VEGF than all other used. However, the EEE mutant showed slightly higher junction formation compared to αB-crystallin protein. The triple mutant AAA showed less junction formation than all other protein but high compared to PBS.

The above analysis suggests that αB-crystallin protein and its single, double, and triple phospho-mimicking mutants show a significant increase in the junctions, size, and length of the blood vessels compared with the control group suggesting their role in inducing angiogenesis during CAM assay (Fig 19, 23 and 27).

The descending order of αB-crystallin protein and its single, double and triple phospho-mimicking mutants regarding junctions, length, and size of the blood vessels is outlined as follows.

1. Descending order of number **junctions** of blood vessel found during CAM assays: **EEE>αB-crystallin protein>AAA>AEE>EAE>AAE>EAA>AEA>EAA**
2. Descending order of **length** of blood vessel found during CAM assays: **αB-crystallin protein>AEE>AAA>EEE>EEA>EAE>EAA>AEA>AAE**
3. Descending order of **size** of blood vessel found during CAM assays: **αB-crystallin protein>AAA>EEE>EEA>AAE>EAA>AEE>EAE>AEA**

Figure 28: Above flow charts compares mutants (Single mutants (AAE, AEA & EAA), double mutants (EEA, AEE & EAE) and triple mutants (AAA & EEE)) data with the data wild type αB-crystallin results of CAM assay.

The significance of data was calculated using two-way ANOVA. The concentration at which angiogenesis was observed with recombinant human αB-crystallin protein was chosen and compared with the other phosphorylation-mimicking mutants at the same concentration (1µg). Significant angiogenesis was observed with αB-crystallin protein and all the phosphorylation-mimicking mutants compared to untreated eggs after 4hrs of incubation.

Although performing CAM assay is labor-intensive, it is cheaper and is a frequently used technique to investigate angiogenesis. Both *in-vitro* and *in-vivo* angiogenesis assays can be carried out to determine the angiogenic potential of a given sample (Auerbach *et al.,* 2003). The *in-vitro* test can be done using cell culture study and is valuable but expensive. It is used to provide initial information, subject to confirmation by the *in-vivo* assay. CAM assay is an *in-ovo* assay. After treatment with the sample compound/protein, pictures lend themselves to quantification, but interpretation should be carried out with extreme caution. CAM assay test is time-consuming and more difficult to perform; thereby we limited the number of the test sample at one time. Quantification is usually more difficult, and one should optimize the threshold level of images obtained.

CAM assay may limit the utility of the assay, and there is always the underlying concern that the CAM itself is undergoing rapid changes both morphologically and in terms of the gradual change in the rate of endothelial cell proliferation during the course of embryonic development (Auerbach *et al.,* 2003).

The effect of phosphorylation of αB-crystallin protein on angiogenesis is clearly understood from CAM assay. However, a basic inference can be drawn that when pure protein (1µg) is added on the chorio allantoic membrane, αB-crystallin protein, and its phosphorylation-mimicking mutants promote angiogenesis. The effect of human recombinant αB-crystallin protein is almost comparable to that of VEGF-A in all parameters in the CAM assay, but the amount of protein that has been added in the case of wild-type recombinant αB-crystallin protein to see significant change was 1µg, whereas only 20ng of VEGF-A was added to see significant change. Whether the mode of action is through the added αB-crystallin protein gaining entry into the cell, chaperoning VEGF-A and thereby promoting angiogenesis or αB-crystallin protein itself interacts with some membrane proteins of the endothelial cells and

inducing their proliferation is not clear. Therefore, the scheme of targeting αB-crystallin protein for therapy should be executed with extreme precaution.

4.6. Human retinal microvascular endothelial cells uptake studies of FITC tagged proteins

CAM assay showed a significant increase in angiogenesis upon adding αB-crystallin protein and its phosphomimicking mutants compared to the PBS-treated group. To further confirm whether externally added αB-crystallin protein and its phospho-mimicking mutant proteins enter the cells to have a functional effect, we chose to perform cell uptake studies using primary human retinal microvascular endothelial cells (HRMVECs). To localize the externally added protein within the cells, we tagged the proteins with Fluorescein isothiocyanate (FITC) for easy detection of protein within the cells.

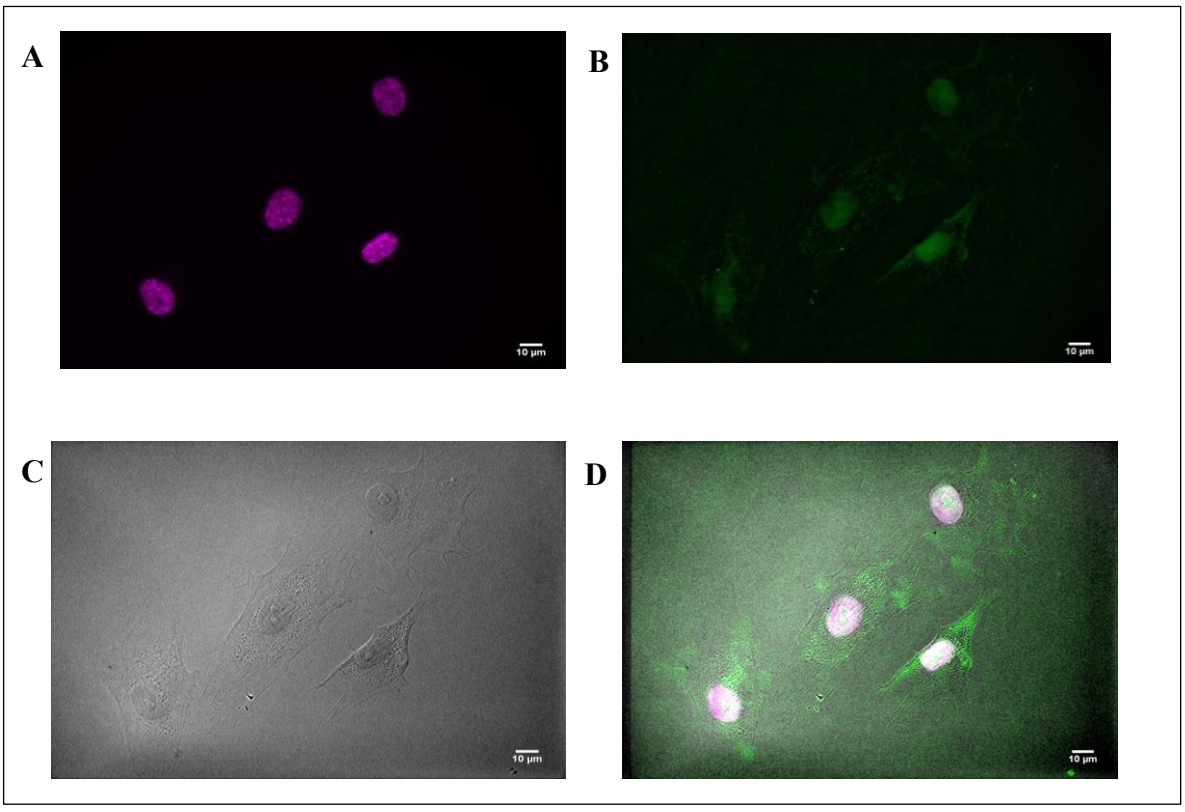

Figure 29: (A) Fluorescence microscope image of nucleus of HRMVE cells stained with Hoechst stain (Magenta). (B) A fluorescence image of FITC labeled αB-crystallin (Green) localized inside the cell. (C) A bright field (DIC) image of HRMVE cells. (D) An overlay of images shown A, B & C. All images were taken with a 40X objectives lens in oil immersion. Scale bar (10µM) is shown at the bottom right. Violet and green color indicates nucleus of HRMVCs cells and αB-crystallin protein present inside of cytoplasm respectively.

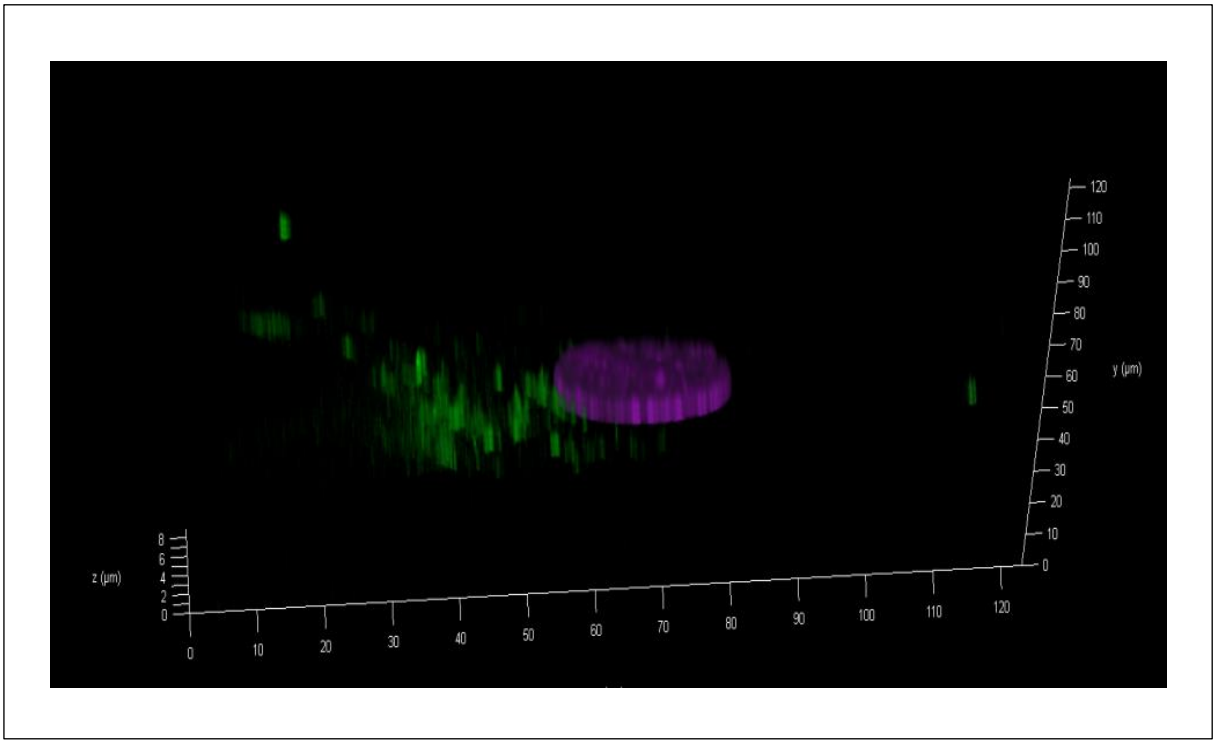

Figure 30: 3-Dimensional view (Confocal Imaging) of αB Crystallin (green) in HRMVECs. The violet and green color indicates nucleus of The HRMVC cell and αB-crystallin protein present inside of cytoplasm respectively.

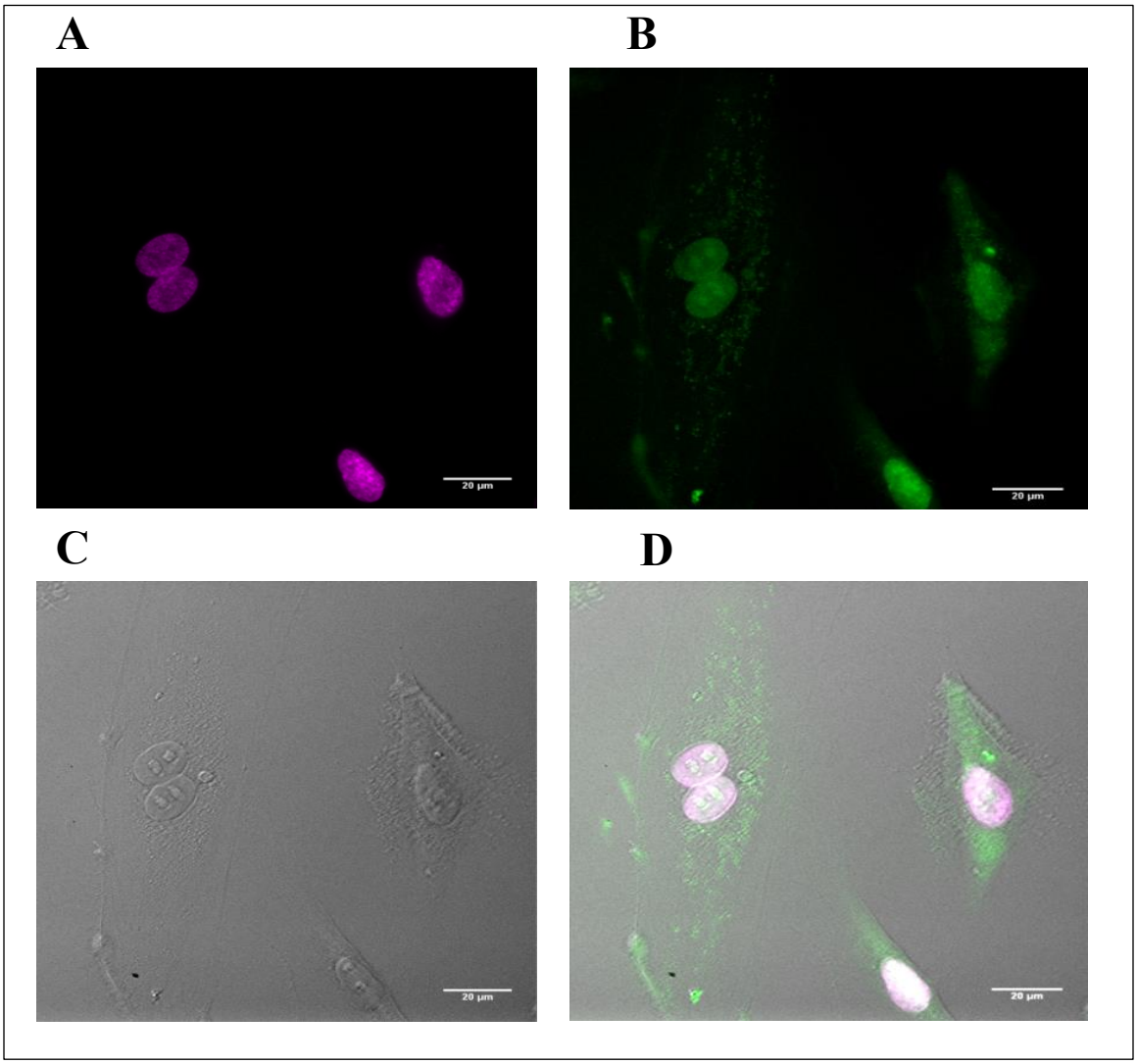

Figure 31: (A) A wide angle microscope image of nucleus of HRMVE cells stained with Hoechst stain (Magenta). (B) A wide angle microscope image of FITC labeled AEE- (green) localized inside the cell. (C) A bright field differential interference contrast (DIC) image of HRMVE cells. D) An overlay of images shown in A, B, & C. All images were taken with 40X objective lens. Scale bar (10µM) is shown at the bottom right. The violet and green color indicates nucleus of HRMVCs cell and AEE (double mutant) protein present inside the cytoplasm respectively.

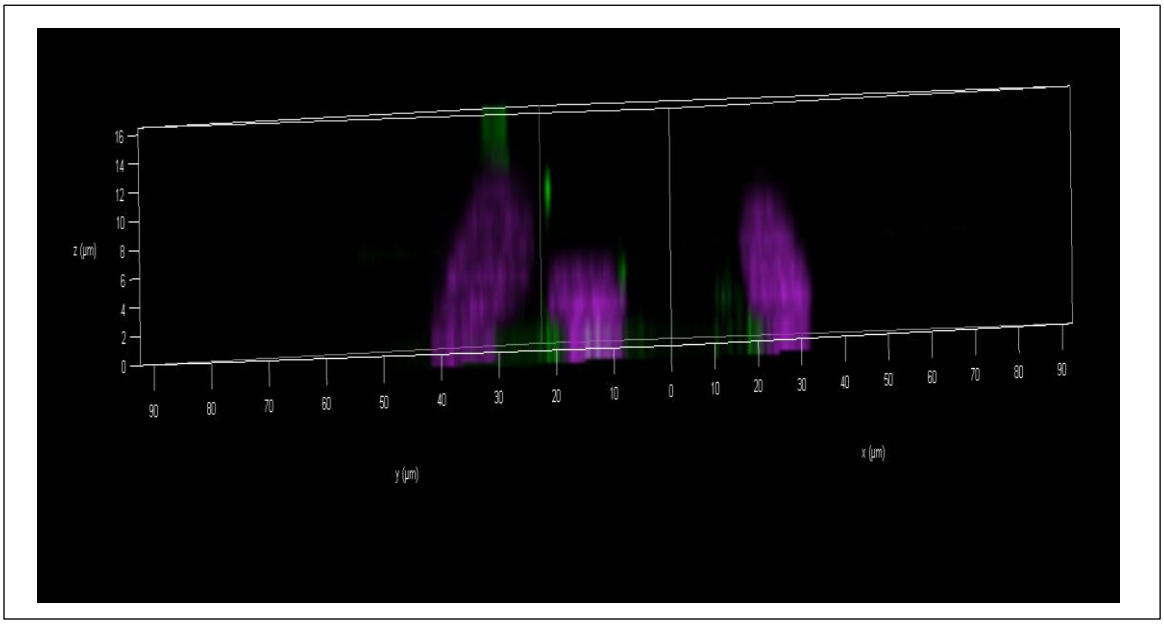

Figure 32: 3-Dimensional view (confocal image) of AEE in HRMVECs. The violet and green color indicates nucleus of the HRMVC cell and AEE protein present inside the cytoplasm respectively.

The fluorescence images confirmed that HRMVEC cells incubated with FITC-tagged αB-crystallin protein and phospho-mimicking mutant, AEA, was localized inside HRMVEC cells around the nucleus within the cytoplasm and the distribution was found to be diffused and speckled. We have performed the experiments with single, double and triple phospho-mimicking mutant proteins. The fluorescence images were obtained from Zeiss Axioplan fluorescent microscope, and the 3-D images were taken from Leica Sp8 confocal microscope (Fig 29-32).

The CAM assay results and HRMVE cell uptake study gave us logical idea about role of alphaB-crystallin and its phosphor-mimicking mutants protein in angiogenesis and goes inside retinal cells. And we can use these purely purified proteins for treatment along with existing one for angiogenesis related diseases hence our finding could be one of great approach for pharmaceuticals.

CHAPTER 5.0: DISCUSSION

The formation of new blood vessels from pre-existing vascular blood vessels is called as Angiogenesis and is essential for embryonic development as well as many pathophysiological processes in adult life, including wound healing, diabetic retinopathy (Vicart *et al.,* 1998), tumor growth, and metastasis. The αB-crystallin protein induces the intraocular neovascularization caused by retinopathies, such as retinopathy of prematurity, diabetic retinopathy, or age-related macular degeneration (AMD), typically occur from and initial stress (Penn *et al.,* 2008). Kase *et al* demonstrate a role for αB-crystallin protein and VEGF in intraocular neovascularization process in 2010.

5.1 Purification of αB-crystallin protein and it's phosphomimics mutants (single, double and triple).

The αB-crystallin protein represents half of the lens protein content, is expressed in the retinal tissue and protects cells from thermal and metabolic stress thereby maintaining the lens transparency. The αB-crystallin protein gene is located on chromosome 11 of the human genome and consists of 528 nucleotides and 175 amino acids (Jaenecke and Slingsby, 2001). The gene sequence was further taken into site-directed mutagenesis (SDMS) using overlapping PCR (polymerase chain reaction) using two 5' to 3' oligos primer. These mutants were produced causing point mutation in the coding site of three serine residue (19, 45 and 59). The point mutation was introduced in oligo primers in between the coding sequence of N-terminal region of wild-type gene. The mutation was done in three specific sites 19, 45 and 59. Those resultant products was cloned into pET-21a(+) vector between Nde I and Hind III restriction sites. Both Glutamic acid and Aspartic acid can be used for the mutation in making all phosphomimicking mutants. Both have equal negative charge and somehow equal molecular weight in mutated phosphomimicking mutants.

The $DH_{5\alpha}$ strain of *E. coli* is generally used for plasmid extraction purpose because; it increases the plasmid number, high efficiency with ease of transform. This plasmid has endA mutation which inactivates the intracellular endonuclease activity and also it avoids the homologous recombination in plasmid. And BL21 (DE3) strain of *E. coli* is used for the

expression of protein. BL21 (DE3) is suitable for expression from a T7 or T7-lac promoter or promoters. IPTG is required to maximally induce expression for this plasmid.

Wild-type αB-crystallin protein and its phosphorylation-mimicking mutants were purified to their homogeneity employing different protein purification techniques. As the first step of purification, the bacterial pellet (obtained from protein expression -induced transformed-BL21 culture) was lysed using lysozyme and ultrasonication. This step separated the proteins based on their solubility in a buffer at physiological pH.The lysed sample was spun and the clear supernatant having the soluble proteins was subjected to "salting out" using ammonium sulfate. This step separated the proteins by their solubility in ammonium sulfate. The ammonium sulfate pellets were resuspended in 1XTNE, and the filtered solution was subjected to gel filtration chromatography using S-300 column. This step separated the proteins based on their size. The fractions having the desired protein are pooled in a tube. The gel filtration subjected sample was then passed through a Q-Sepharose column that removed the protein contaminants and also some amounts of DNA. This step separated proteins by their overall charge at the physiological pH.

The hydrodynamic radii of the recombinant αB-crystallin protein and its phosphorylation-mimicking mutants were determined by using DLS. The Hydrodynamic radius (Rh) for wild-type αB-crystallin protein was found to be 8.2 nm. This is agreement with previously reported Rh values of αB-crystallin protein. Rh values of phospho-mimics of αB-crystallin proteins were found to range from 6-11nm.The 3A mutant of αB-crystallin protein exhibited a higher size (~11nm). The hydrodynamic radii of the AEA, EAA, EAE and EEA mutants were almost the same (i.e ~7nm).There is a significant decrease in the oligomeric size of the phospho-mimicking mutants compared to the wild-type αB-crystallin protein as shown by sedimentation velocity results by means of analytical ultra-centrifuge machine (AUC).

5.2 Chick chorioallantoic membrane assay of all purified protein including αB-crysallin and its phosphomimics mutants (single, double and triple).

Most studies of angiogenesis inducers and inhibitors rely on various models, both in vitro and in vivo, as indicators of efficacy such as the in vivo Matrigel plug and corneal neovascularization assays, the in vivo/in vitro chick chorioallantoic membrane (CAM) assay (Brooks *et al*.,1999), and the in vitro cellular (proliferation, migration, tube formation) (Auerbach & Auerbach, 1994) and organotypic (aortic ring) essays the chick aortic arch and the Matrigel sponge assays (Obeso *et al.,* 1990). In this report, we describe the principal methods now in use: the in vivo chick chorioallantoic membrane (CAM) assay and the in vitro HRMVE cellular uptake assay. In HRMVE cell we could study proliferation, migration, and tube formation assays. But we could not do proliferation, migration and tube formation assay in this study.

First of all the 3days incubated egg is opened and looked for less vessel formation in microscope and that particular area is marked for CAM assay process. The purified protein is placed in that area and picture is taken with help of camera attached to microscope then labeled as 0hr after that the egg is taken for incubation for 4hrs. When 4hrs is done, egg is carried out and picture is taken and labeled as 4hrs. The best pictures are separated out .Those pictures are used for quantification using AngioQuant v1.33, 2005(http://www.cs.tut.fi/sgn/csb/angioquant/) software.

CAM assay results analyzed from the AngioQuant V1.33 2005 software indicated that treatment of αB-crystallin protein and its phosphomimicking mutants showed a significant increase in angiogenesis as evaluated by the increase in length, size and junctions of blood vessels compared with the PBS-treated control (Fig 28). Among the three single phosphomimics (AAE, AEA and EAA), AAE brought about the highest increase in size, length, and number of junctions (Fig 16, 17, 18 and 19), which, however, was less than that exhibited by αB-crystallin protein. The double mutants also showed a significant increase in all the parameters indicating angiogenesis, suggesting that treatment of αB-crystallin protein and its double phospho-mimicing mutants (AEE, EAE and EEA) induce angiogenesis

(Fig 20, 21, 22 and 23). From our results, it is evident that αB-crystallin protein and its triple mutants (EEE, AAA) showed a significant increase in the junctions, size, and length of the blood vessels in the CAM assay compared with the respective PBS-treated control group (Fig 24, 25 , 26 and 27). However, the EEE mutant showed slightly higher junction formation compared to αB-crystallin protein.

This experiment suggests that αB-crystallin protein and its single, double, and triple phospho-mimicking mutants show a significant increase in the junctions, size, and length of the blood vessels compared with the control group suggesting their role in inducing angiogenesis during CAM assay.

It is found that triple phosphomimicking mutant (EEE) shows formation of higher number of junction so that we can conclude that EEE makes the endothelial cell somehow active in new branches formation. To find out why this mutant is active than others mutants will be another topic for research. In other hand why αB-crystallin is showing more active in making size and length of blood vessels, can be another topic for research.

However, a basic inference can be drawn that when pure protein (1µg) is added on the chorioallantoic membrane, αB-crystallin protein, and its phosphorylation-mimicking mutants promote angiogenesis. The effect of human recombinant αB-crystallin protein is almost comparable to that of VEGF-A in all parameters in the CAM assay, but the amount of protein that has been added in the case of wild-type recombinant αB-crystallin protein to see significant change was 1µg, whereas only 20ng of VEGF-A was added to see significant change. Whether the mode of action is through the added αB-crystallin protein gaining entry into the cell, chaperoning VEGF-A and thereby promoting angiogenesis or αB-crystallin protein itself interacts with some membrane proteins of the endothelial cells and inducing their proliferation is not clear. Therefore, the scheme of targeting αB-crystallin protein for therapy should be executed with extreme precaution.

5.3 Human Retinal Microvascular Cell (HRMVC) uptake study of all purified proteins including wild type αB-crystallin and its phosphomimics mutants (single, double and triple)

Our microscopy results confirmed that HRMVEC cells incubated with FITC-tagged αB-crystallin protein and phospho-mimicking mutant, AEA, was localized inside HRMVEC cells around the nucleus within the cytoplasm and the distribution was found to be diffused and speckled. We have performed the experiments with single, double and triple phospho-mimicking mutant proteins. This is the proof of concept. This is the proof of concept that the endothelial cells take up the externally added alpha-crystallin proteins. The fluorescence images were obtained from Zeiss Axioplan fluorescent microscope, and the 3-D images were taken from Leica Sp8 confocal microscopy (Fig 29-32).

Ghose *et al*., 2007 has shown tha αB-crystallin protein function as chaperone activity preventing aggregation of various proteins under a wide range of stress condition and also contribute to the transparency and refractive index of the lens. The stability of VEGF is also depends on the αB-crystallin protein. The inner retinal vascular density was slightly low in αB-crystallin knockout mice, which imply that αB-crystallin also plays role in formation of retinal vasculature (Kase *et al*., 2010).

The important post-translational modification of αB-crystallin is phosphorylation. Phosphorylation is carried out in response to variety of stimuli from physiological changes or cellular environmental changes (Hoover *et al*., 2000). The αB-crystallin undergoes three sites phosphorylation; 19^{th}, 45^{th} and 59^{th} (Smith *et al*., 1992). Phosphorylation is carried out by different kinases, p44/42 MAP Kinase and MAPKAP kinase-2 phosphorylates Ser-45 and Ser-59 respectively (Kato *et al*., 1998). The method how Ser-19 position gets phosphorylated is still unknown. Ito *et al* studied using phosphorylated mimics resulted with the increase of phosphorylation leads to decrease in oligomeric size of protein in 2001. The phosphorylation at 19^{th} serine does not affect the cell protection. However phosphorylation at Ser-45, Ser-59 position either alone or combine protects the cell. Phosphorylated αB-crystallin at Ser-59 position increase the neovaculature in retinal and choroidal (Kase *et al*., 2010) suggesting that phosphorylation increases the angiogenesis activity.

The main first hypothesis of our study was whether αB-crystallin and it's phosphomimics induces angiogenesis and second not. Our findings support second hypothesis; the αB-crystallin and its phosphomimicking mutants (single (AAE-S59E, AEA-S45E & EAA-S19E) double (AEE-S45E-S59E, EAE- S19E-S59E & EEA-S19E-S45E)and triple (EEE-S19E-S45E-S59E & AAA-S19A-S45A-S59A) promote/induces angiogenesis. Another hypothesis was that whether these proteins could enter inside the cell or not. Our cell uptake study showed these proteins can go inside the cell.

All the function of αB-crystallin described has distinct role in pathogenesis of angiogenesis related diseases. The neovascularization related disease like Age related-macular degeneration disease where angiogenesis, retinopathy, cancer tissue where problem is formation of uncontrolled formation of new blood vessels and expression of αB-crystallin is increased (De *et al*., 2007; Kase *et al*., 2010). Increase in expression of αB-crystallin in retinal pigmented endothelium is taken as biomarker of age related macular degeneration (AMD) disease (De *et al*., 2007). These problems persist since long and this kind of disease VEGF acts main role to promote angiogenesis although there is αB-crystallin helps in angiogenesis. There is already available treatment like anti-VEGF antibodies (Avastin drug) to suppress the angiogenesis and many pharmaceutical companies producing this antibody. The current therapies for angiogenesis related diseases (AMD, diabetic retinopathy and other neuroinflammatory) may be less effective thus need for new therapies is rising up. This has been proved that αB-crystallin also helps in angiogenesis. Now, we can use a molecular strategy which controls the expression of αB-crystallin. In other hand diseases like Ischemia; heart condition where blood supply is the problem. So here we need more blood vessels to supply blood to heart.

The αB-crystallin has shown to have pluripotent functions stemming from cell protection through preventing inflammation. Recombinant αB-crystallin therapy was shown to be effective in multiple disease models such as experimental autoimmune (Sreekumar *et al*., 2012a) encephalomyelitis, stroke, cardiac ischemia-reperfusion, optic neuropathy, experimental autoimmune uveitis, and other inflammation-induced toxicity models. The route of administration of a-crystallin in these studies was intravenous, intravitreous or

intraperitoneal and irrespective of the route of administration, crystallin showed anti-inflammatory and neuroprotective functions and rescued the phenotype in all the models studied.

It is clear that αB-crystallin and it's phosphomimicking mutants can induces angiogenesis and can use αB-crystallin protein and it's phosphomimicking mutants in angiogenesis or use molecular strategies to reduce αB-crystallin protein expression in neovascularization related diseases. Direct injection of Ser-59E αB-crystallin protein rescued the mice from ischemia. The specific inhibitors for αB-crystallin and VEGF interaction can be explored so that increase in VEGF secretion in angiogenesis needed tissue area. We can use αB-crystallin protein and it's phosphomimics to promote angiogenesis or use molecules or strategies to reduce αB-crystallin in neovascular related diseases. Hence the proteins are important enough in clinical view or pharmacogenomics.

CHAPTER 6.0: SUMMARY

The development of new blood vessels (Angiogenesis) is an integral part of both normal processes and numerous pathologies, ranging from tumor growth and metastasis to inflammation and ocular (Eye) disease (Auerbach and Auerbach, 1994). The αB-crystallin represents half of the lens protein content, is expressed in the retinal tissue and protects cells from thermal and metabolic stress thereby maintaining the lens transparency. In this study, we described two methods: the in vivo chick chorioallantoic membrane (CAM) assay, and the in vitro cellular uptake study.

Wild-type αB-crystallin coding sequence was used to make mutant by site-directed mutagenesis and cloned into pET21a(+) vector in between Nde I and Hind III and pure and homogenous protein was isolated using various previously standardized protocol and also DLS and AUC.

To check the whether those proteins induce or suppress angiogenesis or not we used basic technique; chick chorio allantoic membrane (CAM) assay. In this assay, we used our proteins as a sample and VEGF as the positive control and PBS (Phosphate buffer saline) as a negative control. We found that our sample protein showed inducing blood vessel formation (Angiogenesis). The triple mutant EEE-αB crystalline protein showed the higher number of blood vessels junction formation than WT-αB crystalline protein in CAM assay. CAM assay only gave the basic idea about angiogenesis to check further we use human retinal microvascular endothelial (HRMVE) cells in media. After incubating the HRMVE cells in media with FITC labelled WT-αB-crystallin and other six mutated (AAE, AEA, EAA, AEE, EAE, EEA, AAA and EEE) for 4hrs, the cells were thoroughly washed with phosphate buffer saline, stained with Hoechst stain and microscopy was done, which results the presence of all sample protein inside the HRMVE cells under florescence microscopy. Further investigation needs to be done for the tube formation, cell migration and proliferation of HRMVE cells with samples proteins.

These experiments (CAM assay and HRMVE cells) result αB-crystallin and its phosphomimics helped in angiogenesis. Thus we can use these proteins in pharmacology industries to make drugs for angiogenesis diseases such as retinopathy, diabetic retinopathy, pre-mature retinopathy, age related macular degeneration where expression of αB-crystallin increased in retina of human and ischemia where expression is decreased. Both anti-angiogenesis and angiogenesis promoting agent can be made. Anti-angiogenesis drug which means to supress the expression of αB-crystallin and reducing phosphorylation of αB-crystallin in cancer tissue. Tissue specific administration αB-crystallin can be used in patient suffering from ischemia disease.

CHAPTER 7.0: CONCLUSION AND RECOMMENDATION

7.1 CONCLUSION

This study is the first evidence to report αB-crystallin protein and phospho-mimicking mutants (single, double and triple) in inducing angiogenesis during CAM assays. Moreover, this study results showed that externally added FITC labeled αB-crystallin protein and phospho-mimicking mutants entered the HRMVE cells and showed their distribution within the cytoplasm (Fig 29-32). The localization studies in HRMVE cells open up a new direction to study the function of αB-crystallin protein and its phospho-mimicking mutants in more refined manner. Further studies are being carried to study the ability of these proteins in inducing angiogenesis by performing tube formation assays, migration assays, and proliferation assays to establish the role of αB-crystallin protein and phospho-mimicking mutants in angiogenesis. The application of this study is in pharmacogenomics. The αB-crystallin and phosphomimics can be purified and used as drugs for angiogenesis related diseases such as Ischemia. Other anti-αB crystallin and its phosphomimics can be produced and used in neovasculature disease like retinopathy, diabetic retinopathy, choroidal neovascularizatio etc.

7.2 RECOMMENDATION

1. Present study focused on the angiogenesis of alphaB-crystallin and its phosphorylation mimicking mutant proteins *in vivo* and endothelial cell uptake of these proteins *in vitro*. The next tenable approach would be how endothelial cell uptake these proteins.
2. With HRMVECs exposed to various phosphomimic mutant proteins in *in-vitro* condition; Tubule formation, Migration and Proliferation assays can be studied.
3. Study of Proteomic profile of HRMVECs exposed to various phosphomimic mutant proteins can also be done.
4. The natural compounds which are anti-angiogenic can be used in cell cultures and the effect of then on αB-crystallin expression can be studied.

BCHAPTER 8.0: BIBLIOGRAPHY

Adamis, A. P., Miller, J. W., Bernal, M. T., D'Amico, D. J., Folkman, J., Yeo, T. K., & Yeo, K. T. (1994). Increased vascular endothelial growth factor levels in the vitreous of eyes with proliferative diabetic retinopathy. *American journal of ophthalmology*, *118*(4), 445-450.

Ahmad, M. F., Raman, B., Ramakrishna, T., & Rao, C. M. (2008). Effect of phosphorylation on αB-crystallin: Differences in stability, subunit exchange and chaperone activity of homo and mixed oligomers of αB-crystallin and its phosphorylation-mimicking mutant. Journal of molecular biology, 375(4), 1040-1051..

Aquilina, J. A., Benesch, J. L., Ding, L. L., Yaron, O., Horwitz, J., & Robinson, C. V. (2004). Phosphorylation of αB-crystallin alters chaperone function through loss of dimeric substructure. *Journal of Biological Chemistry*, *279*(27), 28675-28680.

Asahara, T., Murohara, T., Sullivan, A., Silver, M., van der Zee, R., Li, T., Witzenbichler, B., Schatteman, G. & Isner, J.M. (1997). Isolation of putative progenitor endothelial cells for angiogenesis. *Science*, *275*(5302), pp.964-966.

Auerbach, W., & Auerbach, R. (1994). Angiogenesis inhibition: a review. Pharmacology & therapeutics, 63(3), 265-311.

Bakthisaran, R., Tangirala, R., & Rao, C. M. (2015). Small heat shock proteins: role in cellular functions and pathology. *Biochimica et Biophysica Acta (BBA)-Proteins and Proteomics*, *1854*(4), 291-319.

Bhat, S. P., & Nagineni, C. N. (1989). αB-subunit of lens-specific protein α-crystallin is present in other ocular and non-ocular tissues. *Biochemical and biophysical research communications*, *158*(1), 319-325.

Bhat, S. P., Horwitz, J., Srinivasan, A., & Ding, L. (1991). αB-crystallin exists as an independent protein in the heart and in the lens. *The FEBS Journal*, *202*(3), 775-781.

Brooks, P. C., Montgomery, A. M., & Cheresh, D. A. (1999). Use of the 10-day-old chick embryo model for studying angiogenesis. *Integrin protocols*, 257-269.

Charan, R., Dogra, M. R., Gupta, A., & Narang, A. (1995).The incidence of retinopathy of prematurity in a neonatal care unit. *Indian journal of ophthalmology*, *43*(3), 123.

Cimpean, A. M., Ribatti, D., & Raica, M. (2008).The chick embryo chorioallantoic membrane as a model to study tumormetastasis.*Angiogenesis*, *11*(4), 311-319.

Crabb, J.W., Miyagi, M., Gu, X., Shadrach, K., West, K.A., Sakaguchi, H., Kamei, M., Hasan, A., Yan, L., Rayborn, M.E. & Salomon, R.G. (2002. Drusen proteome analysis: an approach to the etiology of age-related macular degeneration. *Proceedings of the National Academy of Sciences*, *99*(23), pp.14682-14687.

Davison, T. F. (2003). The immunologists' debt to the chicken. *British poultry science*, *44*(1), 6-21.

De Jong, W. W., Leunissen, J. A., & Voorter, C. E. (1993).Evolution of the alpha-crystallin/small heat-shock protein family. *Molecular Biology and Evolution*, *10*(1), 103-126.

De, S., Rabin, D. M., Salero, E., Lederman, P. L., Temple, S., & Stern, J. H. (2007). Human retinal pigment epithelium cell changes and expression of αB-crystallin protein: a biomarker for retinal pigment epithelium cell change in age-related macular degeneration. *Archives of Ophthalmology*, *125*(5), 641-645.

Delaye, M., & Tardieu, A. (1983). Short-range order of crystallin proteins accounts for eye lens transparency. *Nature*, *302*(5907), 415-417.

denEngelsman, J., Gerrits, D., de Jong, W. W., Robbins, J., Kato, K., & Boelens, W. C. (2005). Nuclear import of αB-crystallin protein is phosphorylation-dependent and hampered by hyperphosphorylation of the myopathy-related mutant R120G. *Journal of Biological Chemistry*, *280*(44), 37139-37148.

Deryugina, E. I., & Quigley, J. P. (2008). Chick embryo chorioallantoic membrane model systems to study and visualize human tumor cell metastasis. *Histochemistry and cell biology*, *130*(6), 1119-1130.

Dimberg A, Rylova S, Dieterich LC, Olsson AK, Schiller P, Wikner C, Bohman S, Botling J, Lukinius A, Wawrousek EF, & Claesson-Welsh L.(2008).αB-crystallin protein promotes tumor angiogenesis by increasing vascular survival during tube morphogenesis. *Blood*;111(4):2015-2023.

Duh, E., & Aiello, L. P. (1999). Vascular endothelial growth factor and diabetes: the agonist versus antagonist paradox. *Diabetes*, *48*(10), 1899-1906.

Eaton, P., Fuller, W., Bell, J. R., & Shattock, M. J. (2001). αB-Crystallin Translocation and Phosphorylation: Signal Transduction Pathways and Preconditioning in the Isolated Rat Heart. *Journal of molecular and cellular cardiology*, *33*(9), 1659-1671.

Ecroyd, H., Meehan, S., Horwitz, J., Aquilina, J.A., Benesch, J.L., Robinson, C.V., Macphee, C.E. & Carver, J.A. (2007). Mimicking phosphorylation of αB-crystallin affects its chaperone activity. *Biochemical Journal*, *401*(1), pp.129-141.Ecroyd,

Ferrara, N. (1999). Molecular and biological properties of vascular endothelial growth factor. *Journal of Molecular Medicine*, *77*(7), 527-543.

Ferrara, N. (2001). Role of vascular endothelial growth factor in regulation of physiological angiogenesis. *American Journal of Physiology-Cell Physiology*,*280*(6), C1358-C1366.

Ferrara, N. (2010). Vascular endothelial growth factor and age-related macular degeneration: from basic science to therapy. *Nature medicine*,*16*(10), 1107-1111.

Folkman, J. (1971). Tumor angiogenesis: therapeutic implications. *New england journal of medicine*, *285*(21), 1182-1186.

Fort, P. E., Freeman, W. M., Losiewicz, M. K., Singh, R. S., & Gardner, T. W. (2009). The Retinal Proteome in Experimental Diabetic Retinopathy Up-regulation of Crystallins and Reversal by Systemic and Periocular Insulin.*Molecular& Cellular Proteomics*, *8*(4), 767-779.

Funk, P. E., & Thompson, C. B. (1996).Current concepts in chicken B cell development. In *Immunology and Developmental Biology of the Chicken* (pp. 17-28). Springer Berlin Heidelberg.

Ghosh, J. G., Shenoy, A. K., & Clark, J. I. (2007). Interactions between important regulatory proteins and human αB crystallin. Biochemistry, 46(21), 6308-6317.

Guthrie, S. M., Curtis, L. M., Mames, R. N., Simonko, G. G., Grant, M. B., & Scott, E. W. (2005). The nitric oxide pathway modulates hemangioblast activity of adult hematopoietic stem cells. *Blood*, *105*(5), 1916-1922.

Hagedorn, M., Javerzat, S., Gilges, D., Meyre, A., de Lafarge, B., Eichmann, A., & Bikfalvi, A. (2005).Accessing key steps of human tumor progression in vivo by using an avian embryo model. *Proceedings of the National Academy of Sciences of the United States of America*, *102*(5), 1643-1648.

Hobbs, S. K., Monsky, W. L., Yuan, F., Roberts, W. G., Griffith, L., Torchilin, V. P., & Jain, R. K. (1998). Regulation of transport pathways in tumor vessels: role of tumor type and microenvironment. *Proceedings of the National Academy of Sciences*, *95*(8), 4607-4612.

Hoeben, A., Landuyt, B., Highley, M. S., Wildiers, H., Van Oosterom, A. T., & De Bruijn, E. A. (2004). Vascular endothelial growth factor and angiogenesis. *Pharmacological reviews*, *56*(4), 549-580.

Horwitz, J. (1992). Alpha-crystallin can function as a molecular chaperone.*Proceedings of the National Academy of Sciences*, *89*(21), 10449-10453.

Horwitz, J. (1993). Proctor Lecture. The function of alpha-crystallin. *Investigative ophthalmology & visual science*, *34*(1), 10-22.

Horwitz, J. (2000, February). The function of alpha-crystallin in vision.In*Seminars in cell & developmental biology* (Vol. 11, No. 1, pp. 53-60).Academic Press.

Horwitz, J. (2003). Alpha-crystallin. *Experimental eye research*, *76*(2), 145-153.

Horwitz, J., Bova, M. P., Ding, L. L., Haley, D. A., & Stewart, P. L. (1999). Lens α-crystallin: function and structure. *Eye*, *13*, 403-408.

Hunter, J. (1840). *A treatise on the blood, inflammation, and gunshot wounds*(Vol. 945). Haswell, Barrington, and Haswell.

Ide A, G. Baker N H., & Warren, SL**.** (1939).Vascularization of the Brown Pearce rabbit epithelioma transplant as seen in the transparent ear chamber.*Am J Roentgenol*, pp. 42; 891–899.

Inaguma, Y., Hasegawa, K., Goto, S., Ito, H., & Kato, K. (1995). Induction of the synthesis of hsp27 and αB crystallin in tissues of heat-stressed rats and its suppression by ethanol or an α1-adrenergic antagonist. *Journal of biochemistry*, *117*(6), 1238-1243.

Ito, H., Kamei, K., Iwamoto, I., Inaguma, Y., Nohara, D., & Kato, K. (2001). Phosphorylation-induced change of the oligomerization state of αB-crystallin protein.*Journal of Biological Chemistry*, *276*(7), 5346-5352.

Iwaki, T. O. R. U., Kume-Iwaki, A. K. I. K. O., & Goldman, J. E. (1990). Cellular distribution of alpha B-crystallin in non-lenticular tissues. *Journal of Histochemistry&Cytochemistry*, *38*(1), 31-39.

Iwaki, T., Kume-Iwaki, A., Liem, R. K., & Goldman, J. E. (1989). αB-crystallin protein is expressed in non-lenticular tissues and accumulates in Alexander's disease brain. *Cell*, *57*(1), 71-78.

Jaenicke, R., & Slingsby, C. (2001). Lens crystallins and their microbial homologs: structure, stability, and function. Critical Reviews in Biochemistry and Molecular Biology, 36(5), 435-499.

Jakob, U., Gaestel, M., Engel, K., & Buchner, J. (1993). Small heat shock proteins are molecular chaperones. *Journal of Biological Chemistry*, *268*(3), 1517-1520.

Janković, B. D., Isaković, K., Lukić, M. L., Vujanović, N. L., Petrović, S., & Marković, B. M. (1975). Immunological capacity of the chicken embryo. I. Relationship between the maturation of lymphoid tissues and the occurrence of cell-mediated immunity in the developing chicken embryo. *Immunology*,*29*(3), 497..

Janse, E. M., & Jeurissen, S. H. (1991). Ontogeny and function of two non-lymphoid cell populations in the chicken embryo. *Immunobiology*, *182*(5), 472-481.

Kandpal, R.P., Rajasimha, H.K., Brooks, M.J., Nellissery, J., Wan, J., Qian, J., Kern, T.S. & Swaroop, A. (2012). Transcriptome analysis using next generation sequencing reveals molecular signatures of diabetic retinopathy and efficacy of candidate drugs.

Kannan R., Sreekumar P. G., & Hinton D. R. (2012). Novel roles for a-crystallins in retinal function and disease. Progress in Retinal and Eye Research 31 (2012) 576e604

Kappé, G., Franck, E., Verschuure, P., Boelens, W. C., Leunissen, J. A., & de Jong, W. W. (2003). The human genome encodes 10 α-crystallin–related small heat shock proteins: HspB1–10. *Cell stress & chaperones*, *8*(1), 53-61.

Kappé, G., Leunissen, J.A., de Jong, W.W. (2002). Evolution and diversity of prokaryotic small heat shock proteins. Prog. Mol. Subcell. Biol. 28, 1e17.

Kase, S., He, S., Sonoda, S., Kitamura, M., Spee, C., Wawrousek, E., Ryan, S.J., Kannan, R. & Hinton, D.R. (2010). αB-crystallin regulation of angiogenesis by modulation of VEGF. *Blood*, *115*(16), pp.3398-3406.

Kase, S., Ishida, S., Rao, N.A. (2011). Increased expression of aA-crystallin in human diabetic eye. Int. J. Mol. Med. 28, 505e511.

Kato, K., Ito, H., Kamei, K., & Iwamoto, I. (1999). Selective stimulation of Hsp27 and αB-crystallin protein but not Hsp70 expression by p38 MAP kinase activation. *Cell stress & chaperones*, *4*(2), 94.

Kelly, D. J., Zhang, Y., Gow, R. M., Itescu, S., & Gilbert, R. E. (2005). Cells expressing the stem cell factor receptor, c-kit, contribute to neoangiogenesis in diabetes. *Diabetes and Vascular Disease Research*, *2*(2), 76-80.

Kim, J.H., Auerbach, J.M., Rodríguez-Gómez, J.A., Velasco, I., Gavin, D., Lumelsky, N., Lee, S.H., Nguyen, J., Sánchez-Pernaute, R., Bankiewicz, K. & McKay, R. (2002). Dopamine neurons derived from embryonic stem cells function in an animal model of Parkinson's disease. *Nature*, *418*(6893), pp.50-56.

Koteiche, H. A., & Mchaourab, H. S. (2003). Mechanism of Chaperone Function in Small Heat-shock Proteins phosphorylation-induced activation of two-mode binding in αb-crystallin. Journal of Biological chemistry, 278(12), 10361-10367.

Kumar, P. A., Haseeb, A., Suryanarayana, P., Ehtesham, N. Z., & Reddy, G. B. (2005). Elevated expression of αA-and αB-crystallin proteins in streptozotocin-induced diabetic rat. *Archives of biochemistry and biophysics*, *444*(2), 77-83.

Lewis, W. H. (1922). Endothelium in tissue cultures. *American Journal of Anatomy*, *30*(1), 39-59.

Lowe, J., McDermott, H., Pike, I., Spendlove, I., Landon, M., & Mayer, R. J. (1992). αB-crystallin expression in nonlenticular tissues and selective presence in ubiquitinated inclusion bodies in human disease. *The Journal of pathology*, *166*(1), 61-68.

Matsuoka, M., Ogata, N., Otsuji, T., Nishimura, T., Takahashi, K., & Matsumura, M. (2004). Expression of pigment epithelium derived factor and vascular endothelial growth factor in choroidal neovascular membranes and polypoidal choroidal vasculopathy. *British Journal of Ophthalmology*, *88*(6), 809-815.

Maulik, N., Sato, M., Price, B. D., & Das, D. K. (1998). An essential role of NFκB in tyrosine kinase signaling of p38 MAP kinase regulation of myocardial adaptation to ischemia. *FEBS letters*, *429*(3), 365-369.

Mehlen, P., Kretz-Remy, C., Briolay, J., Fostan, P., Mirault, M. E., & Arrigo, A. P. (1995). Intracellular reactive oxygen species as apparent modulators of heat-shock protein 27 (hsp27) structural organization and phosphorylation in basal and tumour necrosis factor α-treated T47D human carcinoma cells.*Biochemical Journal*, *312*(2), 367-375.

Michaelson, I. C. (1948). The mode of development of the vascular system of the retina, with some observations on its significance for certain retinal diseases. *Trans Ophthalmol Vis Sci*, *68*, 137-180.

Michels, S., Schmidt-Erfurth, U., & Rosenfeld, P. J. (2006). Promising new treatments for neovascular age-related macular degeneration. *Expert opinion on investigational drugs*, *15*(7), 779-793.

Mizutani, M., Kern, T. S., & Lorenzi, M. (1996). Accelerated death of retinal microvascular cells in human and experimental diabetic retinopathy. *Journal of Clinical Investigation*, *97*(12), 2883.

Monsky, W.L., Fukumura, D., Gohongi, T., Ancukiewcz, M., Weich, H.A., Torchilin, V.P., Yuan, F. & Jain, R.K., 1999. Augmentation of transvascular transport of macromolecules and nanoparticles in tumors using vascular endothelial growth factor. *Cancer Research*, *59*(16), pp.4129-4135.

Nakano, A., Baines, C. P., Kim, S. O., Pelech, S. L., Downey, J. M., Cohen, M. V., & Critz, S. D. (2000). Ischemic preconditioning activates MAPKAPK2 in the isolated rabbit heart. *Circulation Research*, *86*(2), 144-151.

Nakata, K., Crabb, J. W., & Hollyfield, J. G. (2005). Crystallin distribution in Bruch's membrane–choroid complex from AMD and age-matched donor eyes. *Experimental eye research*, *80*(6), 821-826.

Nishijima, K., Ng, Y.S., Zhong, L., Bradley, J., Schubert, W., Jo, N., Akita, J., Samuelsson, S.J., Robinson, G.S., Adamis, A.P. & Shima, D.T. (2007). Vascular endothelial growth factor-A is a survival factor for retinal neurons and a critical neuroprotectant during the adaptive response to ischemic injury. *The American journal of pathology*, *171*(1), pp.53-67.

Obeso, J., Weber, J., & Auerbach, R. (1990). A hemangioendothelioma-derived cell line: its use as a model for the study of endothelial cell biology. *Laboratory*

O'Reilly, M.S., Boehm, T., Shing, Y., Fukai, N., Vasios, G., Lane, W.S., Flynn, E., Birkhead, J.R., Olsen, B.R. & Folkman, J. (1997). Endostatin: an endogenous inhibitor of angiogenesis and tumor growth. *cell*, *88*(2), pp.277-285.

Ousman, S.S., Tomooka, B.H., Van Noort, J.M., Wawrousek, E.F., O'Conner, K., Hafler, D.A., Sobel, R.A., Robinson, W.H. & Steinman, L. (2007). Protective and therapeutic role for αB-crystallin in autoimmune demyelination. *Nature*, *448*(7152), pp.474-479.

Patel, J. I., Tombran-Tink, J., Hykin, P. G., Gregor, Z. J., & Cree, I. A. (2006). Vitreous and aqueous concentrations of proangiogenic, antiangiogenic factors and other cytokines in diabetic retinopathy patients with macular edema:

Implications for structural differences in macular profiles. *Experimental eye research*, *82*(5), 798-806.

Pathak, R.K., Middeldorp, M.E., Meredith, M., Mehta, A.B., Mahajan, R., Wong, C.X., Twomey, D., Elliott, A.D., Kalman, J.M., Abhayaratna, W.P. & Lau, D.H. (2015). Long-term effect of goal-directed weight management in an atrial fibrillation cohort: a long-term follow-up study (LEGACY). *Journal of the American College of Cardiology*, *65*(20), pp.2159-2169.

Pinter, E., Barreuther, M., Lu, T., Imhof, B. A., & Madri, J. A. (1997). Platelet-endothelial cell adhesion molecule-1 (PECAM-1/CD31) tyrosine phosphorylation state changes during vasculogenesis in the murine conceptus. *The American journal of pathology*, *150*(5), 1523.

Resnikoff, S., Pascolini, D., Etya'ale, D., Kocur, I., Pararajasegaram, R., Pokharel, G. P., & Mariotti, S. P. (2004). Global data on visual impairment in the year 2002. *Bulletin of the world health organization*, *82*(11), 844-851.

Ribatti, D. (2008). Chick embryo chorioallantoic membrane as a useful tool to study angiogenesis. *International review of cell and molecular biology*, *270*, 181-224.

Richardson, M., & Singh, G. (2003). Observations on the use of the avian chorioallantoic membrane (CAM) model in investigations into angiogenesis.*Current Drug Targets-Cardiovascular &Hematological Disorders*, *3*(2), 155-185.

Risau, W. (1997). Mechanisms of angiogenesis. *Nature*, *386*(6626), 671.

Robinson, M. L., & Overbeek, P. A. (1996). Differential expression of alpha A-and alpha B-crystallin during murine ocular development. *Investigative ophthalmology & visual science*, *37*(11), 2276-2284.

Romanoff, A. L. (1960). The avian embryo.Structural and functional development. *The avian embryo.Structural and functional development.*

Roskoski, R. (2007). Vascular endothelial growth factor (VEGF) signaling in tumor progression. *Critical reviews in oncology/hematology*, *62*(3), 179-213.

Rothbard, J.,B., Kurnellas, M.,P., Brownell, S., Adams, C.,M., Su, L., Axtell, R.,C., Chen. R., Fathman, C.,G., Robinson, W.,H., & Steinman, L. (2012). Therapeutic effects of systemic administration of the chaperone alpha B crystallin associated with binding proinflammatory plasma proteins. *Journal of Biological Chemistry*, *287*(13), 9708-9721.

Ruan, Q., Han, S., Jiang, W. G., Boulton, M. E., Chen, Z. J., Law, B. K., & Cai, J. (2011). αB-crystallin protein, an effector of unfolded protein response, confers anti-VEGF resistance to breast cancer via maintenance of intracrine VEGF in endothelial cells. *Molecular Cancer Research*, *9*(12), 1632-1643.

Rudolf, M., Winkler, B., Aherrahou, Z., Doehring, L. C., Kaczmarek, P., & Schmidt-Erfurth, U. (2005). Increased expression of vascular endothelial growth factor associated with accumulation of lipids in Bruch's membrane of LDL receptor knockout mice. *British journal of ophthalmology*, *89*(12), 1627-1630.

Schmidt, A., Brixius, K., & Bloch, W. (2007). Endothelial precursor cell migration during vasculogenesis. *Circulation research*, *101*(2), 125-136.

Sheikpranbabu, S., Kalishwaralal, K., Venkataraman, D., Eom, S. H., Park, J., & Gurunathan, S. (2009). Silver nanoparticles inhibit VEGF-and IL-1β-induced vascular permeability via Src dependent pathway in porcine retinal endothelial cells. *Journal of nanobiotechnology*, *7*(1), 1.

Smith, J. B., Sun, Y., Smith, D. L., & Green, B. (1992). Identification of the posttranslational modifications of bovine lens αB-crystallins by mass spectrometry. Protein Science, 1(5), 601-608.

Sreekumar, P. G., Kannan, R., Kitamura, M., Spee, C., Barron, E., Ryan, S. J., & Hinton, D. R. (2010). αBcrystallin is apically secreted within exosomes by polarized human retinal pigment epithelium and provides neuroprotection to adjacent cells. *PloS one*, *5*(10), e12578.

Sreekumar, P.G., Spee C., Ryan, s.j., Cole, S.P.C., Kannan, R., & Hinton, D.R. (2012a). Mechanism of RPE cell death in α-crystallin deficient mice: a novel and critical role for MRP1-mediated GSH efflux. PLoS One 7 (3). e33420

Srinivasan, A. N., Nagineni, C. N., & Bhat, S. P. (1992). alpha A-crystallin is expressed in non-ocular tissues. *Journal of Biological Chemistry*, *267*(32), 23337-23341.

Tardieu, A., & Delaye, M. (1988). Eye lens proteins and transparency: from light transmission theory to solution X-ray structural analysis. *Annual review of biophysics and biophysical chemistry*, *17*(1), 47-70.

Tufan, A. C., & Satiroglu-Tufan, N. L. (2005). The chick embryo chorioallantoic membrane as a model system for the study of tumor angiogenesis, invasion and development of anti-angiogenic agents. *Current cancer drug targets*, *5*(4), 249-266.

Ueda, T., Tsuji, K., Yoshino, H., Ebihara, Y., Yagasaki, H., Hisakawa, H., Mitsui, T., Manabe, A., Tanaka, R., Kobayashi, K. and Ito, M. (2000). Expansion of human NOD/SCID-repopulating cells by stem cell factor, Flk2/Flt3 ligand, thrombopoietin, IL-6, and soluble IL-6 receptor. *Journal of Clinical Investigation*, *105*(7), p.1013.

Ueda, Y., Duncan, M. K., & David, L. L. (2002). Lens proteomics: the accumulation of crystallin modifications in the mouse lens with age.*Investigative ophthalmology & visual science*, *43*(1), 205-215.

Valdes, T. I., Kreutzer, D., & Moussy, F. (2002). The chick chorioallantoic membrane as a novel in vivo model for the testing of biomaterials. *Journal of biomedical materials research*, *62*(2), 273-282.

van de Schootbrugge, C., Bussink, J., Span, P.N., Sweep, F.C., Grénman, R., Stegeman, H., Pruijn, G.J., Kaanders, J.H. & Boelens, W.C. (2013). αB-crystallin stimulates VEGF secretion and tumor cell migration and correlates with enhanced distant metastasis in head and neck squamous cell carcinoma. *BMC cancer*, *13*(1), p.128.

van den IJssel, P. R., Overkamp, P., Bloemendal, H., & de Jong, W. W. (1998). Phosphorylation of αB-crystallin and HSP27 is induced by similar stressors in HeLa cells. *Biochemical and biophysical research communications*, *247*(2), 518-523.

Van Guilder, H. D., Bixler, G. V., Kutzler, L., Brucklacher, R. M., Bronson, S. K., Kimball, S. R., & Freeman, W. M. (2011). Multi-modal proteomic analysis of retinal protein expression alterations in a rat model of diabetic retinopathy.*PLoS One*, *6*(1), e16271.

van Noort, J. M., Bsibsi, M., Nacken, P. J., Verbeek, R., & Venneker, E. H. (2015). Therapeutic intervention in multiple sclerosis with alpha B-crystallin: A randomized controlled phase IIa trial. *PloS one*, *10*(11), e0143366.

Verschuure, P., Croes, Y., van den IJssel, P. R., Quinlan, R. A., de Jong, W. W., & Boelens, W. C. (2002). Translocation of small heat shock proteins to the actin cytoskeleton upon proteasomal inhibition. *Journal of molecular and cellular cardiology*, *34*(2), 117-128.

Vicart, P., Caron, A., Guicheney, P., Li, Z., Prévost, M.C., Faure, A., Chateau, D., Chapon, F., Tomé, F., Dupret, J.M. & Paulin, D. (1998). A missense mutation in the αB-crystallin chaperone gene causes a desmin-related myopathy. *Nature genetics*, *20*(1), pp.92-95.

Wang, A.L., Lukas, T.J., Yuan, M., Du, N., Tso, M.O., & Neufeld, A.H. (2009a). Autophagy and exosomes in the aged retinal pigment epithelium: possible relevance to drusen formation and age-related macular degeneration. PLoS One 4, e4160.

Wang, K., Gawinowicz, M. A., & Spector, A. (2000). The effect of stress on the pattern of phosphorylation of αA and αB crystallin in the rat lens.*Experimental eye research*, *71*(4), 385-393.

Weber, W. T., & Mausner, R. (1977). Migration patterns of avian embryonic bone marrow cells and their differentiation to functional T and B cells. In*Avian immunology* (pp. 47-59).Springer US.

Witmer, A. N., Vrensen, G. F. J. M., Van Noorden, C. J. F., & Schlingemann, R. O. (2003). Vascular endothelial growth factors and angiogenesis in eye disease. *Progress in retinal and eye research*, *22*(1), 1-29.

Yaung, J., Jin, M., Barron, E., Spee, C., Wawrousek, E. F., Kannan, R., & Hinton, D. R. (2007). alpha-Crystallin distribution in retinal pigment epithelium and effect of gene knockouts on sensitivity to oxidative stress. *Mol Vis*,*13*(57-61), 565-577.

Yu, J., Feng, L., Wu, Y., Wang, H., Ba, J., Zhu, W., & Xie, C. (2014). Vitreous proteomic analysis of idiopathic epiretinal membranes. *Molecular BioSystems*, *10*(10), 2558-2566.

Yu, J., Liu, F., Cui, S.J., Liu, Y., Song, Z.Y., Cao, H., Chen, F.E., Wang, W.J., Sun, T. & Wang, F. (2008). Vitreous proteomic analysis of proliferative vitreoretinopathy. *Proteomics*, *8*(17), pp.3667-3678.

Zhou, L., Liu, X., Koh, S. K., Li, X., & Beuerman, R. W. (2011). Quantitative proteomic analysis of retina in oxygen-induced retinopathy mice using iTRAQ with 2D nanoLC-nanoESI-MS/MS. *Journal of Integrated OMICS*, *1*(2), 226-235.

Zijlstra, A., Aimes, R.T., Zhu, D., Regazzoni, K., Kupriyanova, T., Seandel, M., Deryugina, E.I. & Quigley, J.P. (2004). Collagenolysis-dependent angiogenesis mediated by matrix metalloproteinase-13 (collagenase-3). *Journal of Biological Chemistry*, *279*(26), pp.27633-27645.

APPENDIX

Appendix 1:0 Preparation of buffers

1.1 50X TAE buffer:

Dissolve 242g of Tris base in Milli-Q water, add 57.1ml of glacial acetic acid and 100ml of 500mM EDTA (pH 8.0), and adjust the pH to 7.4 using concentrated HCl. Make up the volume to 1 litre. This stock solution can be diluted to 50:1 with Milli-Q water to make a 1X working solution. This 1X working solution contains 50mM Tris, 20mM acetic acid of 1mM EDTA. Store at 4^{o}C.

1.2 10X Tris-NaCl EDTA (TNE) buffer

Weigh 121.1g of Tris and 5.8g of EDTA and add them to 800ml Milli-Q water. Adjust the pH to 7.2 using concentrated HCl while stirring the solution on a magnetic stirrer. After adjusting the pH make up the volume to 1000ml and filter (0.22µm). Sodium azide is added to avoid contamination.

1.3 1X TNE buffer:

Measure 100ml of 10XTE from stock in a 1000ml measuring cylinder. Add 20ml of 5M NaCl solution from stock and makeup to 1 litre solution and use as working solution.

1.4 Phosphate Buffered Saline (PBS): 20mM PO_4^{--}, 100mM NaCl, pH 7.2-7.4

i. Prepare one liter of 1molar (1M) monobasic (NaH_2PO_4/K H_2PO_4)
ii. Prepare one liter of 1molar (1M) di-basic (Na_2HPO4/K_2 HPO_4)
iii. 1M phosphate buffer: Monobasic phosphate is added to the stirring dibasic solution while the pH of the solution is adjusted to 7.2 using NaOH/KOH.
iv. 1M phosphate buffer is filtered; 50ml aliquots should be made and stored at -20^{o}C.
v. 5M NaCl is prepared and stored for further use.
vi. 20ml of each 1M phosphate buffer and 5M NaCl stocks were mixed and the volume is made up to 1L with MQ water. 20mM PO_4^{--}, 100mM NaCl is made. Filter the Buffer Solution and store it at 4 ^{o}C. Do not add sodium azide to this solution.

1.5 Lysis buffer (For 500ml culture)

i. 5ml 1XTNE
ii. 300µl of PMSF
iii. 150 µl Lysozyme (1mg/ml)

These chemicals are added in subsequent way

Appendix 2.0 Preparation of Reagents

2.1 500mM EDTA solution:

Dissolve 93.05g of EDTA in 500ml of Milli-Q water, while stirring adjust the pH to 8.0 with 1N NaOH or by directly adding NaOH pellets. Store at room temperature.

2.2 Destaining solution (1000ml) used for SDS-PAGE:

To prepare one liter of Destaining solution add 400 ml of methanol and 100 ml of acetic acid to 500 ml of Milli-Q water. Store at room temperature.

2.3 Staining solution (1liter) used for SDS-PAGE:

To the destaining solution, add 0.25% (w/v) Coomassie Brilliant Blue dye and stir the contents for 4 hrs, filter the solution using a Whatman filter paper. Store at room temperature.

2.4 SDS-PAGE Loading dye (4x)

20mM Tris base pH 6.8, 400mM DTT, 8% SDS, 0.4% Bromophenol blue, 40% Glycerol is the composition of a 4X SDS-PAGE Loading dye. The above solution is stored either at room temperature or 4^{o}C. Whenever the dye is needed, take 900 µl of the above mixture and add 100ul of 14M β-mercapto ethanol.

2.5 PMSF (Phenyl methyl sulphonyl chloride) (100mM)

174.2 mg of PMSF (Sigma, India) is dissolved in 5ml of isopropanol, and the volume is made up to 10 ml. Make aliquots of 1 ml each and store at -20^{o}C.

2.6 Lysozyme (10mg/ml)
Dissolve 10mg of Chick-lysozyme in 1ml of autoclaved Milli-Q water. Store it at -20^{o}C.

2.7 Ampicillin (100mg/ml)

1g of ampicillin powder was dissolved in 10 ml of autoclaved Milli-Q water and was liquated in to 1ml vials and stored at -20^{0}C.

2.8 1M IPTG (Isopropyl thio-β-D galactose**)**

Dissolve 2.383gm of IPTG in 8ml of Milli-Q water and make up the volume to 10ml. Filters sterilize the solution and make aliquots of 1ml each and store at -20^{0}C.

2.9 NaCl (5M)

Weigh 292.2g of NaCl and dissolve in 800ml of MQ water, make up the volume to 1liter. Filter the solution with 0.22µm filter using vacuum pump and store at room temperature.

2.10 SDS-PAGE components:

Components	**12% Resolving gel (10ml)**	**Stacking gel (5ml)**
Milli-Q	3.3ml	3.4ml
Tris-base	2.5ml (1.5M, pH 8.8)	0.63ml (1M, pH 6.8)
30% Acrylamide	4ml	0.83ml
10% SDS	100µl	50µl
10% Ammonium persulfate	100µl	50µl
TEMED	8 µl	5 µl

Appendix 3:0 Nucleotide sequence of wild type αB-crystallin

3.1. Target human αB-crystallin complete gene sequences were retrieved from National center for biotechnology information (NCBI), sequence id: KM220606.1. The gene sequences of target protein are shown below in FASTA format.

AGGAGGAGGAGGCACCAAACGGCCTGGGTGGATAGAAGGGGGACAAGGAGGCACACCCAGGCCGGCAAAGAGCAGGTATCAGCACTGCAAGC
ACCAAGTGTGTCTTGAGGTCAGCAGGAATGGGAAAGATCTCTGCTTGGAGGGGATGAGGGGTAGTCTGGGGTGGGGGGTGGCTGGTCCCAGGA
GATCAGTTAAGCCCAGAGTGGGGTGGAGGCCAGCAACGTTGGGAGGTCAGCCCAGAATTTCAGGGGGTGGGGGTGGGGGGCAAGGGGGTGGT
GTCTGTGCCATACCTTCTCCGAAGCGCTGCTCACCCAGGCGGCTCGGGTTGGCAAATTCGTACTCGGCGGTGGCCGGGTGGGCATGTGGCACTGA
GCGGCCCGACATGGCTGCAGATGCAGCAGAAGCCCTGGTCCGAGGTGCAGCCCCAACAGGCGCAGCGCGACCCCTCCAGCTGCCCGGAGAGCCA
GGGCTCGATAGGAGGTGGGGGCGGGGTCGACACCACCCAAAATAGTGCCGAGCCTCTTGGGGGGGGAGGGGCTGGGAGTGGGGGCCCTGAGT
GAGAGCAACGAGGGTGTGACCAGCGCCGCCCGGACCCCTAGTCCCCTCCCCCGCACACTCTTCAGCTGTCGCAGGGGGCCTGAGAGGACAGCTGA
GGGTCCTGGCTGGGAACGAGCTGGGGAGGGGGAGCTGGTGGTGCCTGGGGCATGAAGAGGCCTCGCTGAGACCCTCACAAACGGTTTGCACGT
TTCCACACCTCATTTTCTCCTCTTCGGTGGCAGGCACTGTGCACCCAATTCCTAAAGCACTCCTGGATTTAATGTTCTGAGAGCCACATAGAACGAAA
GATGCAAGAAATCTGTTTGCTCTTTTTTCAGGGGGTGGGGTCTTTCTGCCCAGATGTGGGATCCTCTCCTAAACCCAGGTCAACCCAGGGCACGAG
GCAGATGGCTGGTGCTGACATGTTGACCATCACTGCTCTCTTCCAAGGACTCACAAAGAGTTAATGTCCCTGGGGCTCAGCCTAGGAAGATTCCAG
TCCCTGCCCAGGCCCAAGATAGTTGCTGGCCTGATTCCCCTGGCATTCAGGACTGGAAAGGAGGAGGAGGGGCACACTACGCCGGCTCCCATCCT
*CCCCCCACCCCGCGTGCCTGCTTGGGATTCCTGACTCTGTACCAGCTTCAGAGAACAGGGGTGGGGGT*GGGTGCCATTGGGTGTGGACAGAAAGC
TAGTGAAACAAGACCATGACAAGTCACTGGCCGGCTCAGACGTGTTTGTGTCTCTCTTTTCTTAGCTCAGTGAGTACTGGGTATGTGTCACATTGC
CAAATCCCGGATCACAAGTCTCCATGAACTGCTGGTGAGCTAGGATAATAAAACCCCTGACATCACCATTCCAGAAGCTTCACAAGACTGCATATA
TAAGGGGCTGGCTGTAGCTGCAGCTGAAGGAGCTGACCAGCCAGCTGACCCCTCACACTCACCTAGCCACC**ATGGACATCGCCATCCACCACCCC**
TGGATCCGCCGCCCCTTCTTTCCTTTCCACTCCCCCAGCCGCCTCTTTGACCAGTTCTTCGGAGAGCACCTGTTGGAGTCTGATCTTTTCCCGACGT
CTACTTCCCTGAGTCCCTTCTACCTTCGGCCACCCTCCTTCCTGCGGGCACCCAGCTGGTTTGACACTGGACTCTCAGAGGTGAGTCTCCCCACAG
CTAGGACGGGAGAGTCCTTACTGGAACCTCCTGGAAACTTCTCCATCCATTTTCCTTTCCTACCCTGCCTAAACCATTTTAGGCACATGTGTGTCCAA
ATGTGAAGAAAAATGAGGAGGTTGCTAGTGCCTTCCTCCCCCATCACCTGTTTCTATTTGATAGTCCTCTGTATCCCATTTATTACATTTTTTCATGC
ACTGTCAAGTTTATCCTCCGTCCCCTAACTTCTCTACAGGATACCCCTTTCTGGTTTGGTTCATGACAATCTGCAGGGAAAGAGCTGCCTTCAAACTC
CTTTGCTTATCTCTTCCAACACCTTGGACTCTTGACCGATTTTACCATCTCAGGTTTCAGAGCCAGGAGAGAGCCCTGCCTCATCCTGAGCTGTTCAT
CCCCATGGGTATTTTCTGCCTTTCTATTCCCTCTTCTATGATTTTCTGGGTTTCTCAGGGCTACGACAGGGCGCTGGCCTGGGTCCAATCAAGCCCTA
CGAGGAAACAATATAGGGACGCCCATTTGTCCTAAGAGGGTGGAAGAACAGGGTGAACAAATAAGGTTGACAGAGCTGTCACAGATAACACTCT
GGTTTAAAAATATTCAAGTGTGAGTAAACAGGAGCTGAGTGGGCAAGGGCTTTGGAAGGACAAGCAGGACCAGCAGAACATTCCAGATTGGGT
GGGTGGAAAACTGGCAAAGAGACCTGAGCCAGAAGAAGAGGCCTTTGTCTCACAGACAAACCACAAAGCCAGGCATTGGAGTCAGAGAGGCAG
CAGATGCCAGGCTTGCACCCATCCTTGCGACTGGTCCCCTGGGTGATCTGTCTTCTTCTCTGTCCCTGTAAATAAAGTTTGGGTCTGATCACCATGA
GCCTTAGGTATCACTGTGGTGGCTCCCTGAAGCAGACAGCTATGTTTATTTAAAAAGGAGATTTTTTAAGCAGAGAAGAGAAGGATGAATTACCC
GGACAGAAAGCAGCTCTGCAGAATAAGACAGCACCTGTGTAATCAGTATTTTTGCCCTCTTTCTCCCATCCCATTCCCTTACCTTGCTATTTCTAG**AT**
GCGCCTGGAGAAGGACAGGTTCTCTGTCAACCTGGATGTGAAGCACTTCTCCCCAGAGGAACTCAAAGTTAAGGTGTTGGGAGATGTGATTGA
GGTGCATGGAAAACATGAAGAGCGCCAGGTATGTAGCTTGTTTTTTTGTTTTCTGCTCATTCATTCAGTGCATACTGTAATAGTCCAGGTAGTGCT
ATCAGCTTTGGAGGCTGGCTACATTCCAGTCCCAAGCCATAACAGTCGGGATCAGGGGTTACAAATCAATGTCTAGAAGACTAAGTTAGGATAGA
CATATTGCTGTTGTTACTATTATGGCCAGAGATGTGGCCTTTGATTTGATCGCCTTAGATGGGATGATGGGATGCTGATGCCCCATTTAAGCCAGT
GGTTCTGAATCTGGGCCACATTAGAATCACCAGGGGAACTTTCAAAAAACCTAATGCTCGGGCATACTCCAGACCAATTAGCATATGTGCTGCCGA
AGCGAGCACTACTCCAGACCAATTAAATCAGCATTTTTAAGGGTGGGACCCAGGCATCAGCAATTTTTAAGGTAATTCTAATCTACAGTCAAGGTT
GAGAACCACTGATTAGGTATAGGGCTGTCAGACACCTAGTTGCTTTGCATAATTACATTAACTACAGGTACCCTAAAAGCACTTGAGTTGTGACTT
CTCTTTTAGCTGTGCAAGAATCCGTGTCTCTTCTTTAGCCCATCTTAATGCTGAACTACTTGGTTTGTCTAAATTTCAGAGCTGTGCTCAGTCTTTAAT
CCCCTACAGCCCATGTGGTAATCAGTTAACGAGAGCCTGTTTGGCTACATGCTTGAGAGTCAGCAGGCATACGGGTTAAGGTCATCTACTCTTTGG
GGGAGTTCTGACAAATGGAACAGCTTGTTATGACTTTATAAGAGGGCTTTAAAATTGCTTCTCACCATTTAACGATAGCTCAGAACCTGTGCGTCA
ACCAGTACAGTTTGTCCTCAGTAATGTCCTCAGGCTGTTTCAATTTTGCTTATATGATTTAGGTTTGGGTCATAGTCTCCTTGGATGGAGTCATTTTT
TTTTTTTTTAATTTCAGCAGCAGTCCTATTGTTCTGGAACCTTCTGGGACATTCCTGAAGAGTCAGGACAATTTCAGGGCTTCCTCAGGGACTCAG
ATTCTAAATGAGATTCCAAATTCTGTAGGCCCAGCCAACATTGATCTAAACCTTTGGGAAATACCCCTAAACATATCTATGCCTCAGGGTTTGAAAA
ACAATGAAGTGTTGGACTGTTTCAGACTTCTCAGATTCTCACTGGTAGGAGTGACTACCTAGGCAATTTCATCTTAGCTGCAACCCTGAAACGAAG
CTCTATTTATTTTTCCTATGTTGTCATGGCATTTGGTCTCACCTAAGGGGAAATCAGGATGCCTGAGTTCTGGGCAGGTGATAATAGTTCCTGTTCT
TATCTCTCTGCCTCTTTCCTCATTCTTTTGGGTTAG**GATGAACATGGTTTCATCTCCAGGGAGTTCCACAGGAAATACCGGATCCCAGCTGATGTA**
GACCCTCTCACCATTACTTCATCCCTGTCATCTGATGGGGTCCTCACTGTGAATGGACCAAGGAAACAGGTCTCTGGCCCTGAGCGCACCATTCC
CATCACCCGTGAAGAGAAGCCTGCTGTCACCGCAGCCCCCAAGAAATAGATGCCCTTTCTTGAATTGCATTTTTTAAAACAAGAAAGTTTCCCCAC
CAGTGAATGAAAGTCTTGTGACTAGTGCTGAAGCTTATTAATGCTAAGGGCAGGCCCAAATTATCAAGCTAATAAAATATCATTCAGCAACAGATA
ACTGTCTTGTGTTTGAATATTCCACACACTTTTAAATAAATATACAGATACCACAG

Promoter sequence 1199 bp
5' UTR 290 bp
Exon 1 206 bp
Intron 1 1069 bp
Exon 2 123 bp
Intron 2 1359 bp
Exon 3 204 bp
3' UTR 199 bp

The complete gene length human αB-crystallin has 4,649 bases including promoter, 5'UTR and 3'UTR. Size of a) promotor 1199bp, b) 5'UTR 290bp, c) exon1: 206bp, d) intron1 1069bp, e) exon2 123bp, f) intron2 1359, g) exon3 204bp, h) 3'UTR 199bp

3.2 The table to show the mutation site and mutated codon in human αB-crystallin gene.

Mutation Sites	Initial Amino acid codon in mRNA	Mutated amino acid in wt-protein	Mutated Amino acid coden in mRNA	Final amino acid in protein
Ser 19,45,59	TCC,AGT, AGC	19th Serine	GAA,GCC GCC	Glu, Ala, Ala
Ser 19,45,59	TCC,AGT, AGC	45th Serine	GCC GAA, ,GCC	Ala, Glu, Ala
Ser 19,45,59	TCC,AGT, AGC	59th Serine	GCC,GCC,GAA,	Ala, Ala, Glu
Ser 19,45,59	TCC,AGT, AGC	19th, 45th , Ser	GAA,GAA, GCC	Glu, Glu, Ala
Ser 19,45,59	TCC,AGT, AGC	19th , 59th , Ser	GAA, GCC, GAA	Glu, Ala, Glu
Ser 19,45,59	TCC,AGT, AGC	45th , 59th , Ser	GCC, GAA, GAA	Ala ,Glu, Glu
Ser 19,45,59	TCC,AGT, AGC	19th, 45th, 59th Ser	GAA, GAA,GAA	Glu, Glu, Glu
Ser 19,45,59	TCC,AGT, AGC	19th, 45th, 59th Ser	GCC,GCC,GCC	Ala, Ala, Ala

Appendix 4:0 Figures

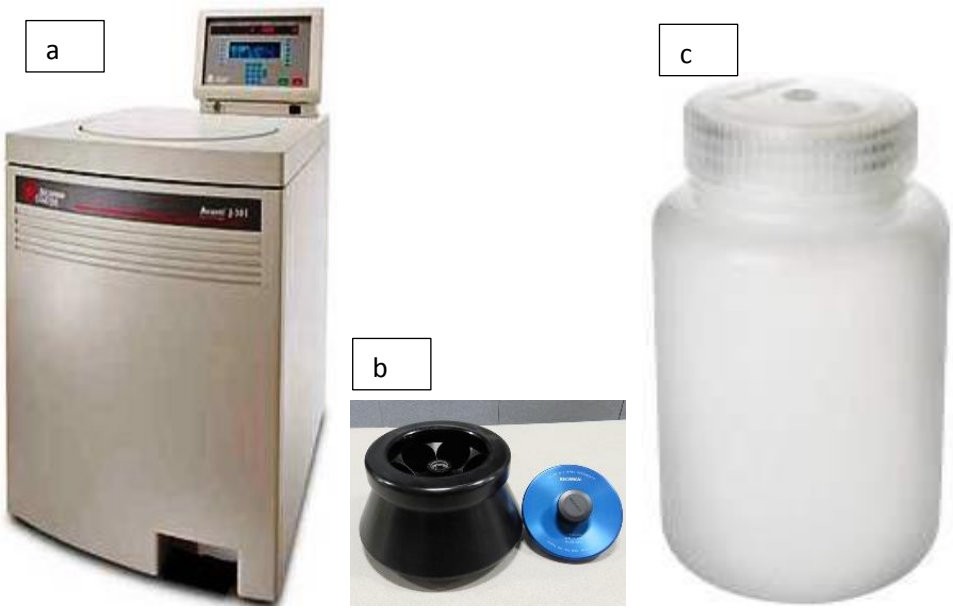

Figures 4.1: (a) Beckman coulter centrifuge (b) JLA-16.250 rotor and (c) Nalgene bottles (500ml) use for centrifugation: these instruments are used to purify desired protein from culture.

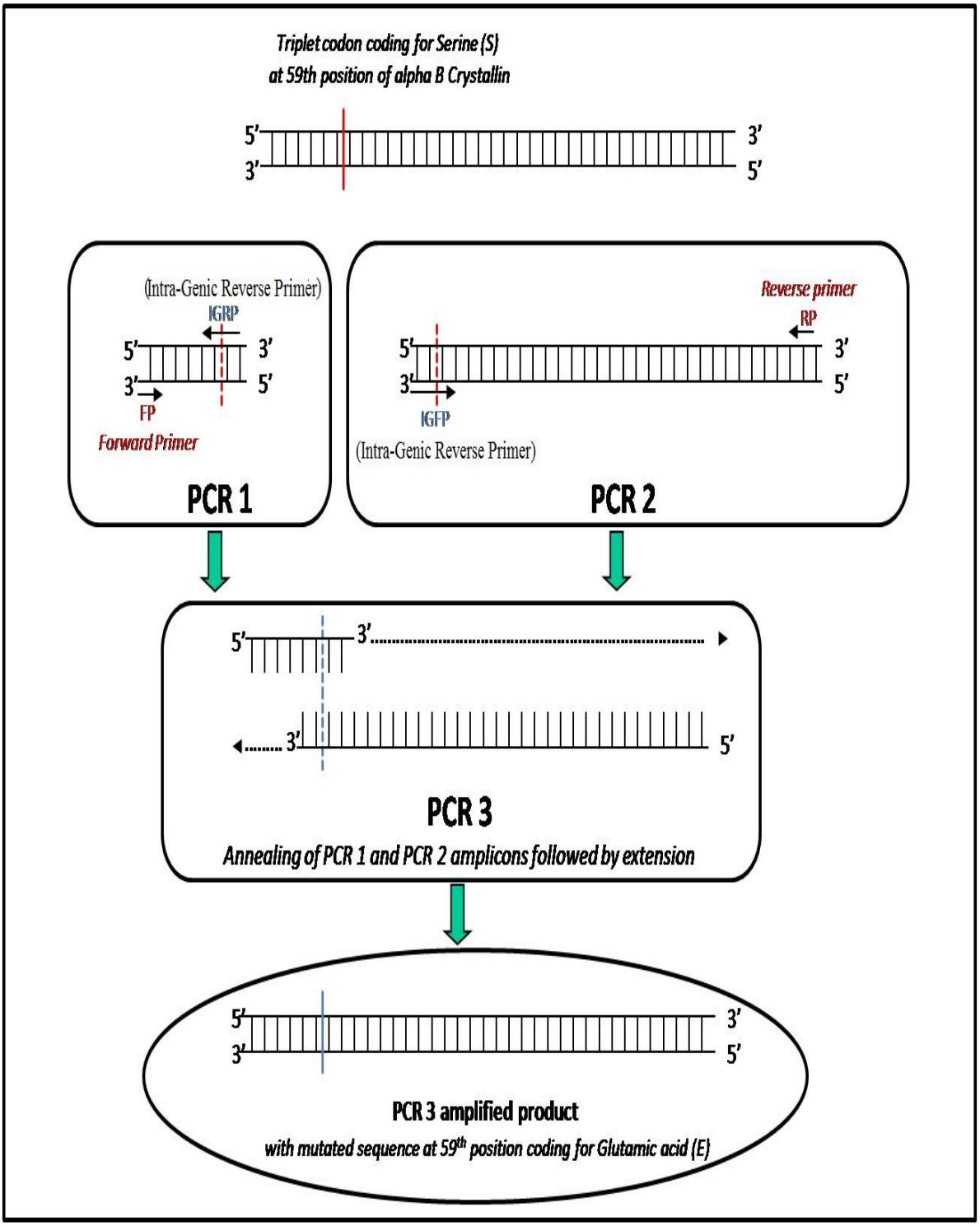

Figure 4.2: Schematic diagram of SDMS Overlapping PCR method. PCR1 and PCR2; amplification of two genes (amplicons) by two sets of primers, PCR3; Annealing of PCR1 and PCR2 amplicons leaving site of overhangs. Overhangs are filled by Taq polymerase used for PCR1 and PCR2 to give new amplicon of interest.

Appendix 5:0

Data of CAM assay images given by Angioquant software (ver. 1.3.2005, http://www.cs.tut.fi/sgn/csb/angioquant/)

5.1. Data given by picture using angioquant software of αB-crystallin and Single mutants (AAE, AEA & EAA)

Table 5.1.1 Average lengths of blood vessels

Name of protein	Time	Day 1	Day 2	Day 3
PBS	0hr	5039.85	4934.95	6051.70
	4hrs	5671.72	6368.41	7019.59
VEGF	0hr	27720.15	13654.35	8496.46
	4hrs	33453.57	17530.03	14485.56
αB-crysatllin	0hr	8120.34	11239.55	17289
	4hrs	9473.15	12548.08	20522.11
AAE-S59E	0hr	13732.51	11301.04	6697.34
	4hrs	13845.24	12488.45	10519.4
AEA-S45E	0hr	8748.48	8007.03	10825.42
	4hrs	9167.97	8923.55	14077.81
EAA-S19E	0hr	5465.08	3918.07	10825.42
	4hrs	9473.33	6603.15	12232.15

Table 5.1.2 Average sizes of blood vessels

Name of protein	Time	Day 1	Day 2	Day3
PBS	0hr	64429	54742	77651
	4hrs	72250	75039	83606
VEGF	0hr	175461	89725	67931
	4hrs	183673	116043	93633
αB-crysatllin	0hr	74722	75615	98777
	4hrs	88587	90611	114432
AAE-S59E	0hr	114843	99287	27895
	4hrs	125094	106878	47725
AEA-S45E	0hr	84706	77613	74846
	4hrs	85364	83857	82272
EAA-S19E	0hr	53581	41350	74846
	4hrs	84204	55743	82170

Table 5.1.3 Average junctions of blood vessels

Name of protein	Time	Day 1	Day 2	Day3
PBS	0hr	86	138	154
	4hrs	90	148	209
VEGF	0hr	979	407	218
	4hrs	1685	518	615
αB-crysatllin	0hr	129	192	564
	4hrs	223	254	818
AAE-S59E	0hr	344	275	357
	4hrs	378	306	523
AEA-S45E	0hr	151	167	263
	4hrs	176	186	420
EAA-S19E	0hr	117	89	263
	4hrs	192	90	352

5.2. Data given by picture using angioquant software of αB-crystallin and Double mutants (AEE, EAE & EEA)

Table 5.2.1 Average lengths of blood vessels

Name of protein	Time	Day 1	Day 2	Day3
PBS	0hr	6539.37	8653.58	6988.94
	4hrs	7505.6	11716.91	7282.9
VEGF	0hr	9109.74	11617.2	9171.72
	4hrs	17039.17	12569.15	18829.23
αB-crysatllin	0hr	7167.52	7351.55	5408.38
	4hrs	11242.64	16450.84	8868.82
AEE-S45E-S59E	0hr	7103.55	9098.73	8333.21
	4hrs	11240.08	15816	12471.44
EAE-S19E-S59E	0hr	12038.63	4089.58	2816.74
	4hrs	13935.72	7797.95	8075.63
EEA-S19E-S45E	0hr	2234.27	8488.21	9966.42
	4hrs	8075.63	10809.16	13829.63

Table 5.2.2 Average sizes of blood vessels

Name of protein	Time	Day 1	Day 2	Day 3
PBS	0hr	54972	62483	61421
	4hrs	56466	112015	67979
VEGF	0hr	56711	75978	77466
	4hrs	104061	86628	150370
αB-crysatllin	0hr	42801	92635	45658
	4hrs	70519	134462	62647
AEE-S45E-S59E	0hr	48117	73325	24779
	4hrs	63603	119654	50067
EAE-S19E-S59E	0hr	71500	39240	62419
	4hrs	83248	66136	80593
EEA-S19E-S45E	0hr	35651	39240	59294
	4hrs	37587	66136	89238

Table 5.2.3 Average junctions of blood vessels

Name of protein	Time	Day 1	Day 2	Day 3
PBS	0hr	99	134	106
	4hrs	108	183	144
VEGF	0hr	92	136	101
	4hrs	321	269	285
αB-crysatllin	0hr	110	130	100
	4hrs	285	268	181
AEE-S45E-S59E	0hr	109	140	98
	4hrs	195	247	176
EAE-S19E-S59E	0hr	99	81	38
	4hrs	188	140	166
EEA-S19E-S45E	0hr	99	122	105
	4hrs	48	222	174

5.3. Data given by picture using angioquant software of αB-crystallin and Triple mutants (EEE & AAA)

Table 5.3.1 Average lengths of blood vessels

Name of protein	Time	Day 1	Day 2	Day 3
PBS	0hr	13659.7	16408.74	11592.45
	4hrs	14488.32	24151.27	11495.17
VEGF	0hr	10580.5	23177.8	25520.13
	4hrs	19474.97	44567.71	31373.3
αB-crysatllin	0hr	10239.39	3981.54	21615.62
	4hrs	18735.63	9408.82	36099.01
EEE-S19E-S45E-S59E	0hr	32026.19	14017.07	24522.37
	4hrs	35795.67	20955.18	30325.8
AAA-S19AS45A--S59A	0hr	18567.37	7694.24	10305.32
	4hrs	24034.34	12105.44	17221.68

Table 5.3.2 Average sizes of blood vessels

Name of protein	Time	Day 1	Day 2	Day 3
PBS	0hr	91347	96110	89589
	4hrs	94182	126157	82960
VEGF	0hr	70720	100666	126117
	4hrs	114619	198602	172464
αB-crysatllin	0hr	71951	34544	109668
	4hrs	102098	61885	165407
EEE-S19E-S45E-S59E	0hr	140094	78427	136079
	4hrs	163755	112552	162988
AAA-S19AS45A--S59A	0hr	110865	83162	81874
	4hrs	134524	102435	142065

Table 5.3.3 Average junctions of blood vessels

Name of protein	Time	Day 1	Day 2	Day 3
PBS	0hr	396	720	352
	4hrs	446	765	420
VEGF	0hr	378	1093	1218
	4hrs	676	2785	1597
αB-crysatllin	0hr	300	109	990
	4hrs	582	280	1759
EEE-S19E-S45E-S59E	0hr	2120	522	1154
	4hrs	2654	1049	1525
AAA-S19AS45A--S59A	0hr	835	238	354
	4hrs	1432	481	618